Development and Testing of a PEM Fuel Cell System for an Electric Land Speed Vehicle

A Thesis

Presented in Partial Fulfillment of the Requirements for Graduation with Distinction in Mechanical Engineering at the Ohio State University College of Engineering

By

Carrington Bork

The Ohio State University

2009

Examination Committee:

Giorgio Rizzoni, Adivsor

Yann Guezennec

Abstract

Racing is truly the ultimate test for a vehicle technology. That is why students at the Ohio State University built the Buckeye Bullet 2, the world's first hydrogen fuel cell powered land speed car. In October 2007, the Buckeye Bullet became the world's fastest fuel cell powered vehicle reaching a top speed of 360.977 [km/h] (224.301 [mph]). Although this was a remarkable achievement it fell short of the vehicle's ultimate goal to contend with the original Buckeye Bullet's battery powered record of 508.485 [km/h] (315.958 [mph]). This thesis investigates the design improvements and testing methodology that the team used to improve on their initial success. The focus is on the fuel cell system and directly related systems. This paper reviews the following 2008 racing season as well as analyzes failures that occurred during the 2008 racing events. Suggestions for further investigation and improvement are also explained.

This thesis is dedicated to all the hard working individuals that have been a part of the Buckeye Bullet 2 team. Without their dedication and sleepless nights this project would not be possible.

Table of Contents

List of Figures

List of Tables

Chapter 1 :

Introduction to Electric and Hydrogen Land Speed Racing

This chapter gives information on the history of electric and hydrogen land speed racing as it directly pertains to this thesis. It discusses the history of land speed racing at Ohio State as well as previous Hydrogen powered land speed vehicles. It also discusses the motivation for performing this research and its relevance to today's automotive community.

1.1 Project Background

Almost immediately after the inception of the first automobiles, man has raced them. There is an inherent drive to push vehicles to their limits of performance and speed. One of the purest forms of motorsport is the all-out pursuit of top speed. Know as land speed racing, this motorsport has been populated by big money teams and backyard mechanics alike. In the past several years, a team of engineering students from the Ohio State University has joined the ranks of these speed-enthusiasts as part of the Buckeye Bullet racing program.

1.1.1 The Buckeye Bullet

The Buckeye Bullet program evolved from the Ohio State University Smokin' Buckeye team which raced in the Formula Lightning racing series during the 1990s. This series was an intercollegiate series that raced open wheeled battery electric race cars. The

series ended in the late 1990s, leaving a group of students with a significant amount of electric racing experience without a project to work on. This group of students eventually started what has become the Buckeye Bullet Land Speed Racing Team. The original Buckeye Bullet (BB1) was a battery powered electric streamliner. A streamliner is a purpose-built race car for land speed racing. It is characterized by a long narrow body with enclosed wheels. The Buckeye Bullet is pictured in Figure 1.1. The Buckeye Bullet was initially powered by 12,000 sub-C cell NiMH batteries. In later seasons the batteries were upgraded to prismatic NiMH batteries equivalent to that of almost 16 Toyota Prius battery packs. In August 2004 the BB1 became the first electric car to travel faster than 300 mph. The BB1 currently holds the record for the fastest electric car both internationally at 438.927 [km/h] (272.737 mph) (under FIA sanctioning) and nationally at 508.485 [km/h](315.958 mph)(under SCTA sanctioning).

Figure 1.1: The Battery Powered Buckeye Bullet

The Buckeye Bullet last raced in October 2004. At the end of the 2004 racing season it was determined that the Buckeye Bullet had achieved its top speed potential given the state of available battery technology at the time. Thus, a new generation of electric land speed vehicle was proposed.

1.1.2 The Buckeye Bullet 2

What was proposed had never been previously attempted. The next generation, the Buckeye Bullet 2 (BB2), is the world's first hydrogen fuel cell powered land speed race car. Like the BB1, the BB2 was designed and built by students at the Ohio State University with the help of industry supporters. The most notable of these supports would be Ford Motor Company and Ballard Power Systems. The Buckeye Bullet 2 is powered two Ballard P5 Fuel Cell Modules (FCMs). Fuel cells were used in the BB2 as opposed to batteries for several reasons. Fuel cell systems have been increasing in popularity in recent years and are a strong candidate for widespread use in transportation applications in the future. Working with fuel cells offers a whole new set of technical challenges for the Buckeye Bullet team to overcome. Additionally from a performance standpoint they offer several advantages over batteries in land speed racing. A batteries voltage and potential power output is dependent on the state of charge of the battery. During a run the power output decreases as the battery's state of charge depletes, meaning that the vehicle can expend less power just when it needs it the most: at high speed. For a fuel cell system the power output is constant as long there is fuel available. Therefore, the power output can be constant throughout the entire run. Additionally a battery takes time to recharge. The BB1 requires several hours of charging for a complete charge. The BB2 can refueled within approximately 20 minutes. This is important for international records. In order to obtain an international record the vehicle

must make two consecutive runs within an hour. The Buckeye Bullet team is currently attempting to break the record held by the battery powered BB1 with the fuel cell powered BB2.

Figure 1.2: The Buckeye Bullet 2 on the Bonneville Salt Flats in 2007

1.1.3 The Bonneville Salt Flats

The mecca for land speed racing is the Bonneville Salt Flats in Utah. The salt flats are a naturally occurring surface created by an ancient salt lake that has evaporated leaving behind miles of almost perfectly flat terrain. The salt flats stretch for over 30,000 acres. For most of the year the salt flats are covered by shallow water, making it not suitable for racing. However, during the late summer and early fall, the water dries and salt forms a hard surface ideal for land speed racing.

Before racing events, a strip of salt is compacted and groomed to form a track for racing. Under the Southern California Timing Association (SCTA) rules, the track consists of 7 total miles. The first two miles of the track are for acceleration. Miles three through

five are timed miles. The last two miles are for deceleration. A timed mile is used to determine a record. Therefore, the average speed through the fastest time mile is considered for a record rather than the fastest instantaneous speed. The actual record speed is the average of two consecutive runs over the same relative or physical mile[1]. Due to the performance characteristics of the BB2, the fastest mile on a good run is always the fifth mile. Figure 1.3 shows a depiction of the race course at Bonneville.

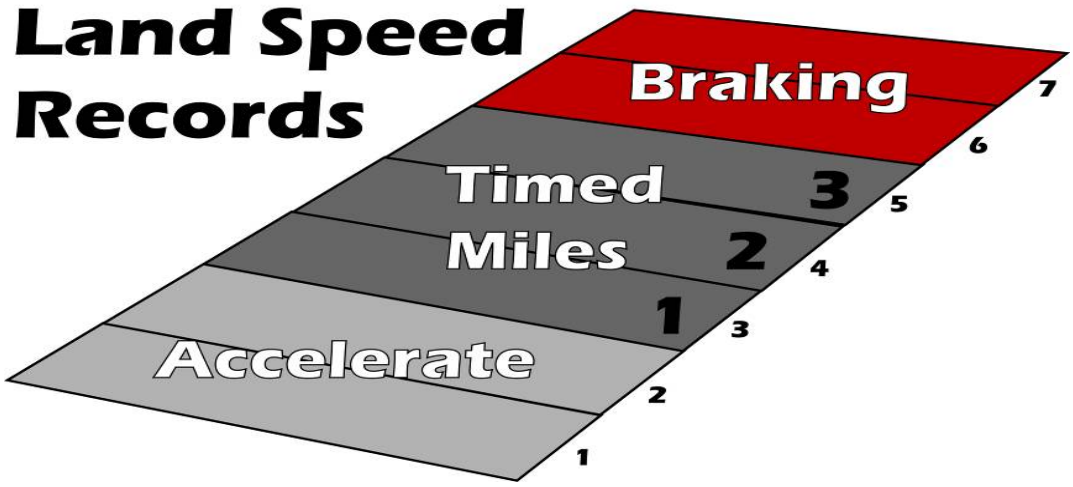

Figure 1.3: SCTA Bonneville Course Setup

1.2 Previous Hydrogen Land Speed Records

With many eyes on hydrogen as the world's answer to green mobility in the future, several attempts have been made to set land speed records with hydrogen powered vehicles.

1.2.1 The BMW H2R

The BMW H2R set the record for the world's fastest hydrogen powered car on September 19, 2004 at the Miramas Proving Grounds in France. The vehicle set nine records including the fastest flying kilometer for a hydrogen car at 301.95 [km/h] (187.62 [mph]) and the fastest flying mile at 292.66 [km/h] (181.85 [mph])[2]. Unlike the Buckeye Bullet 2, the H2R is powered by a 6.0-liter V-12 internal combustion (IC) engine. The engine was based

on the BMW 760i's gasoline powerplant and specially modified to run on hydrogen fuel. The BMW H2R is shown in Figure 1.4.

The fundamental difference between the H2R and the Buckeye Bullet 2 is that the H2R's IC engine burns the hydrogen similar to the way that gasoline is burned in most cars. The Buckeye Bullet 2 is powered by hydrogen fuel cells. The fuel cells combine hydrogen and oxygen molecules without combustion and create electric energy directly from the reaction. This electric energy is then transferred to kinetic energy by an electric motor. This means that the Buckeye Bullet 2 can develop maximum power with greater efficiency compared to the H2R.

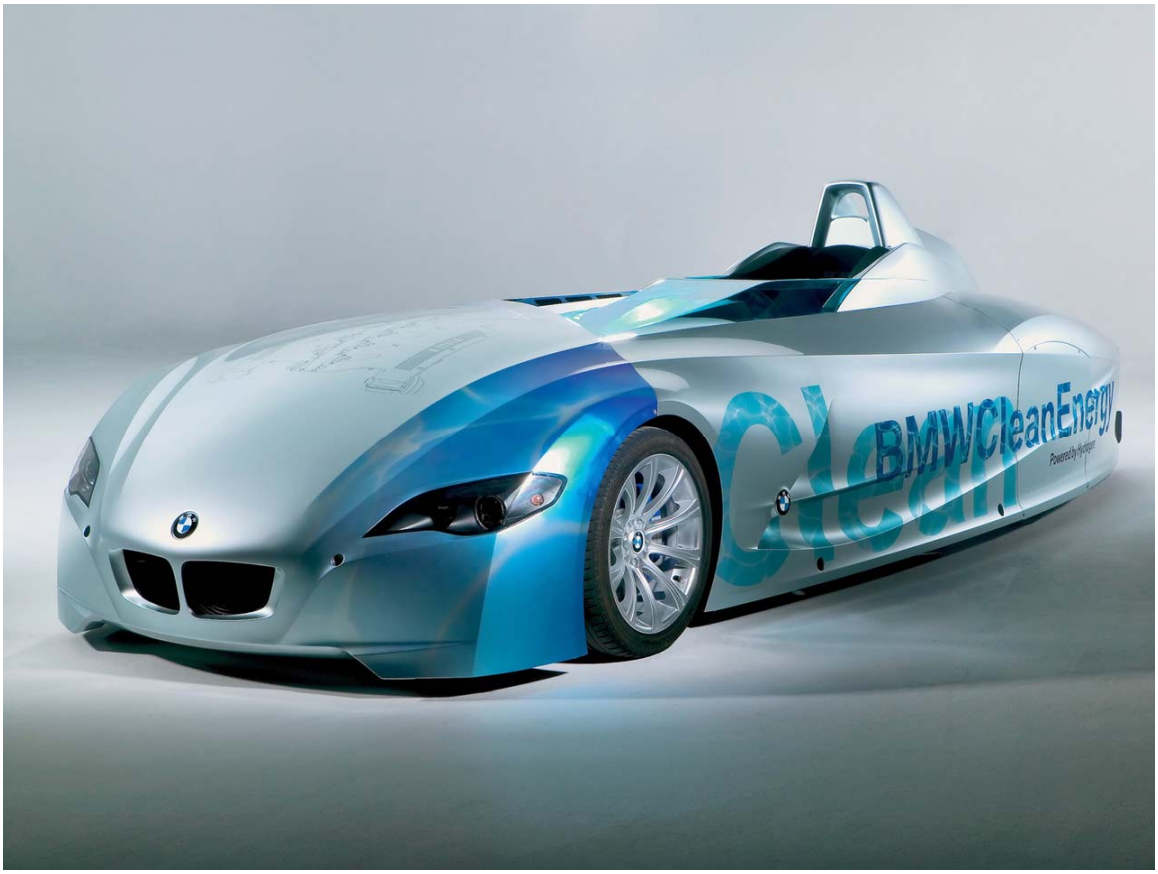

Figure 1.4: BMW H2R Hydrogen Car [3]

1.2.2 The Ford Fusion 999

The Buckeye Bullet 2 was developed with the help of Ford Motor Company. Ford built the Ford Fusion 999, a hydrogen fuel cell powered land speed car, concurrently with the Buckeye Bullet 2 project. Both vehicles were a result of the collaboration of the Ford fuel cell engineers and Ohio State University engineering students. The Ford 999 used the same motor and inverter as the Buckeye Bullet 2 and a similar fuel cell system. Both the BB2 and the Ford 999 fuel cell stacks were provided by Ballard Power Systems. The Ford 999 set the record for the world's fastest fuel cell vehicle at 333.612 [km/h] (207.297 [mph]) in August 2007 at the Bonneville Salt Flats, Utah [4]. The Ford Fusion 999 is shown in Figure 1.5.

The main difference between the 999 and the BB2 is that the Ford 999 was built to be a production based race vehicle while the BB2 is a streamliner. The Ford 999 was built on a Ford Fusion body heavily modified for land speed racing. Aside from the body the vehicle retained almost no components from the production Ford Fusion. The production body limits the 999's potential top speed due to the higher drag coefficient compared to the BB2.

Figure 1.5: The Ford Fusion 999 on the Bonneville Salt Flats 2007

1.3 Brief Review of the Buckeye Bullet 2 2007 Racing Season

In August 2007 the Buckeye Bullet 2 made its inaugural appearance on the Bonneville Salt Flats during Speedweek 2007. In its first appearance on the salt the vehicle reached a speed of 324.502 [km/h] (201.636 [mph]). In October 2007 the BB2 raced during the World Finals and during a private FIA sanctioned event. During the World Finals the car achieved a top speed of 360.977 [km/h] (224.301 [mph]). The BB2 went on to set a world record for the world's fastest fuel cell powered vehicle at 212.641 [km/h] (132.129 [mph]) during the FIA meet in October 2007. These speeds attained were fantastic achievements for the first season of racing. However, the vehicle had serious reliability issues during the 2007 racing season. The car was still far short of its intended goal of breaking 300 mph. Great advances were made during the 2008 season in terms of reliability, ease of service and performance. This thesis will document the progression of the BB2 from the 2007 season till

the 2008 season and explain the issues encountered, testing approach and methodology involved in advancing the future of land speed racing even farther.

1.4 Thesis Motivation

The world is in need of new forms of clean, renewable energy both for transportation and general public usage. This has been demonstrated by numerous publications and billions of dollars in alternative fuel research. For passenger vehicles a number of manufacturers are turning to fuel cell technology as a means of replacing the internal combustion engine. These manufacturers include major names in the industry including: Ford, Daimler, General Motors, Honda and Nissan. Indeed fuel cell technology holds a lot of potential for the future of transportation; however, researchers and engineers have many problems to overcome before fuel cell cars become mainstream. Also, fuel cell technology has many competitors from battery powered vehicles, to plug-in hybrids and biofuels.

The Buckeye Bullet 2 is a showcase for fuel cell technology. It is meant to show industry leaders and the general public what a fuel cell powered vehicle is capable of. The Buckeye Bullet 2 is more than just a student project. Although its main goal remains to provide experience and learning opportunities for students in Ohio State University's College of Engineering, it encompasses more than just education. This project and other alternative fuel motorsports projects are meant to advance the state of technology for such areas and to generate excitement about these green technologies. Motorsports inherently has a way of pushing a technology to the absolute limits of what is possible. Additionally the project is meant to portray the idea that "green" technology does not necessarily mean slow.

The a main goals of this thesis research are to improve upon the work of previous team members and address performance and reliability issues encountered by the team during the 2007 racing season. The main thrust was to perform extensive fuel cell system testing,

address shutdown conditions and improve the reliability. Also, it focused on increasing power output and the accuracy of the fuel cell models. The work done in this thesis will push the project closer to its goal of breaking 300 [mph] and advancing fuel cell technology while bringing attention to fuel cells as a viable option for transportation.

Chapter 2 :

Vehicle Information and Testing Approach

This chapter gives a brief overview of the major vehicle systems. The focus will be on the fuel cell and related systems. A brief background on fuel cell basics will be discussed. The chassis, suspension, braking, body, and parachute systems will not be discussed in depth in this paper. For further information on these aspects of the BB2 please see that following references: [5][6][7][8]. Additionally, this chapter explains the testing setup used for fuel cell system testing for the Buckeye Bullet 2.

2.1 Vehicle Systems Overview

The Buckeye Bullet 2 is far more complex in design and execution when compared to the original Buckeye Bullet. Unlike the batteries used in the BB1, the fuel cell system in the BB2 requires the use of a cooling system, gas delivery system, humidification system, and a more sophisticated control system. This means that very little has been carried over from the original car. The inverter and motor are the only two main components from the BB1 still used in the BB2.

2.1.1 Vehicle Layout

In order for the Buckeye Bullet 2 to race, it requires the coordination of multiple systems to facilitate power generation and direct that power to the wheels. Figure 2.1 shows the major component layout for the vehicle.

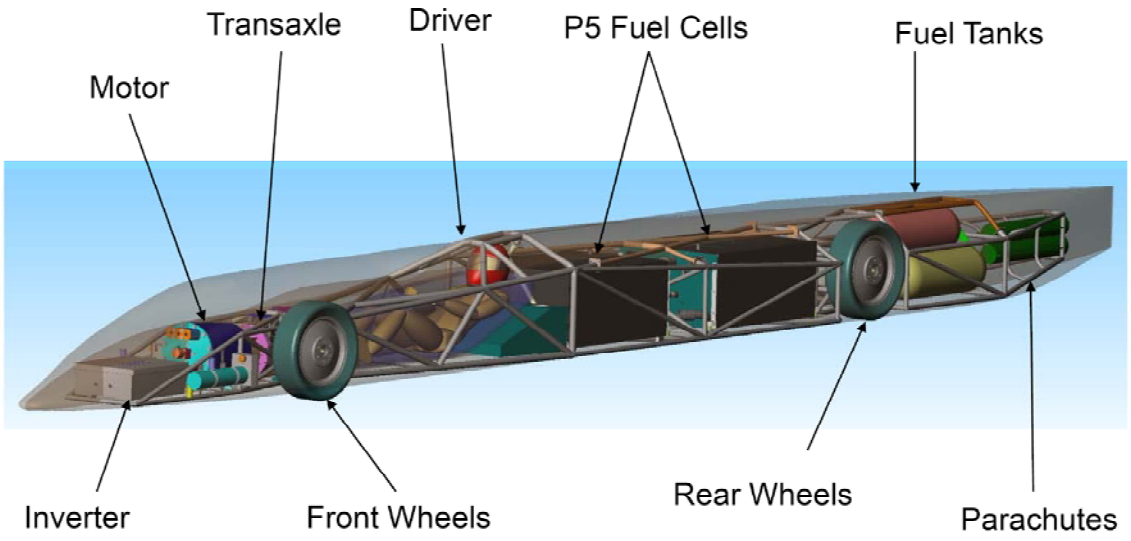

Figure 2.1: Buckeye Bullet 2 Vehicle Layout

The BB2 is a front wheel drive vehicle, with the motor and inverter situated at the front of the car. The motor was packaged in the front for several reasons. Firstly, it was placed in front of the driver for safety. Placing the motor in front places more mass in front of the driver and increased the crumple area of the car should it be involved in a front end collision. Colliding with an object head-on at the salt flats is not very likely because the flats are devoid of almost any natural object to collide with and race cars and pit areas are placed far away from the racing surface. However, the vehicle is tested at the Transportation Research Center on a test track, where there is a possibility to strike a guard rail if there is a steering or suspension failure.

Additionally, unlike most motorsports where rear wheel drive gives a handling advantage, the physics of land speed racing are slightly different. In land speed racing it is desirable to have as much weight toward the front of the car as possible. This ensures that the center of gravity is forward of the center of pressure. With this condition satisfied, if the vehicle begins to yaw, the aerodynamic forces will create a moment on the body that tends to

straighten the car. This adds aerodynamic stability to the car at high speeds. Also, since the racing occurs on salt which can have a coefficient of friction anywhere from .4 to .6 depending on the salt conditions, the rate of acceleration is much less than that of a high performance car on asphalt. This combined with a wheel base of more than 19 ft means that there is very little weight transfer under acceleration. The combination of low weight transfer under acceleration and the fact that the car is designed to have more mass in the front of the car means that the front wheels will have more traction than the rear wheels. Thus, having a properly design front wheel car is more advantageous in land speed racing.

The driver is positioned behind the front wheels, this gives him the best visibility and safety. Additionally, it gives the driver a better sense of how the car is behaving, allowing him better car control. The driver is protected by a 4130 chromoly steel cage and roll structure with head restraints. As a redundant safety system the driver is also surrounded by a carbon fiber honeycomb survival cell. On either side of the driver are the ice tanks which hold up to 180 [kg] of ice used for cooling the fuel cells. All 180 [kg] of ice will be melting in a single 90 second run.

The driver section of the car is separated from the rear portion of the vehicle by a firewall. Directly behind the driver are the two Ballard P5 PEM fuel cell modules. These modules were originally intended for use in transit city buses; producing up to 125 [kW] apiece under normal operating conditions. The two modules in use by the BB2 team have been specially modified for the specific application of land speed racing. These modifications will be discussed in detail in later chapters.

The fuel cell modules are fueled by the compressed hydrogen and heliox tanks at the rear of the car behind the rear axle. At the back of the car is the parachute system. The parachutes are the primary means of deceleration from speeds above 320 [km/h] (~200 [mph]). The vehicle also has a redundant braking system. The vehicle's mechanical brakes

are adapted from Goodrich Aerospace aircraft brakes used on a Lear Jet. These brakes function similar to a clutch with 2 carbon rotors and 3 carbon stators. Many conventional high performance automotive brake packages were considered for the vehicle, however, none of them were capable of stopping the vehicle from top speed. The Goodrich brakes have the capacity to stop the car from 500+ [km/h]. These brakes can be used for low speeds like regular automotive brakes. Although they can stop the car from 500 [km/h], performing this action will destroy the brakes. So they can only perform a high speed stop once. This is perfectly acceptable because the brakes are only a backup system in case the parachute system fails.

2.1.2 Fuel Cell System Introduction

A fuel cell is an electrochemical device that combines a fuel and an oxidant without combustion and creates electricity directly. The Ballard P5 fuel cells used for the BB2, as with many fuel cell systems, use hydrogen as the fuel and oxygen as the oxidant. The most typical kind of fuel cell used in automotive applications is the permeable electron membrane (PEM) fuel cells. PEM fuel cells work at low temperatures compared to other types of fuel cells which means that they can be started quickly. This is a strong advantage for the vehicle applications as customers are accustomed to internal combustion engines which require very short startup time. Also PEM membranes can be made very thin which allows the total stack to be more compact. Another advantage PEM fuel cells have for vehicle applications is that they do not contain any corrosive fluid that other types of fuel cells contain. [9]

The PEM fuel cell consists of membrane electrode assemblies (MEAs) sandwiched between bipolar plates. Multiple bipolar plates and MEAs are connected together to form the fuel cell stack. Each cell produces between 1.2 and .5 volts depending on its loading condition. The cells in the stack are connected in series which allows the overall stack in the

case of the BB2 to operate between 960 to 550 [V]. Figure 2.2 shows a generic exploded diagram of a fuel cell stack with multiple MEAs and bipolar plates.

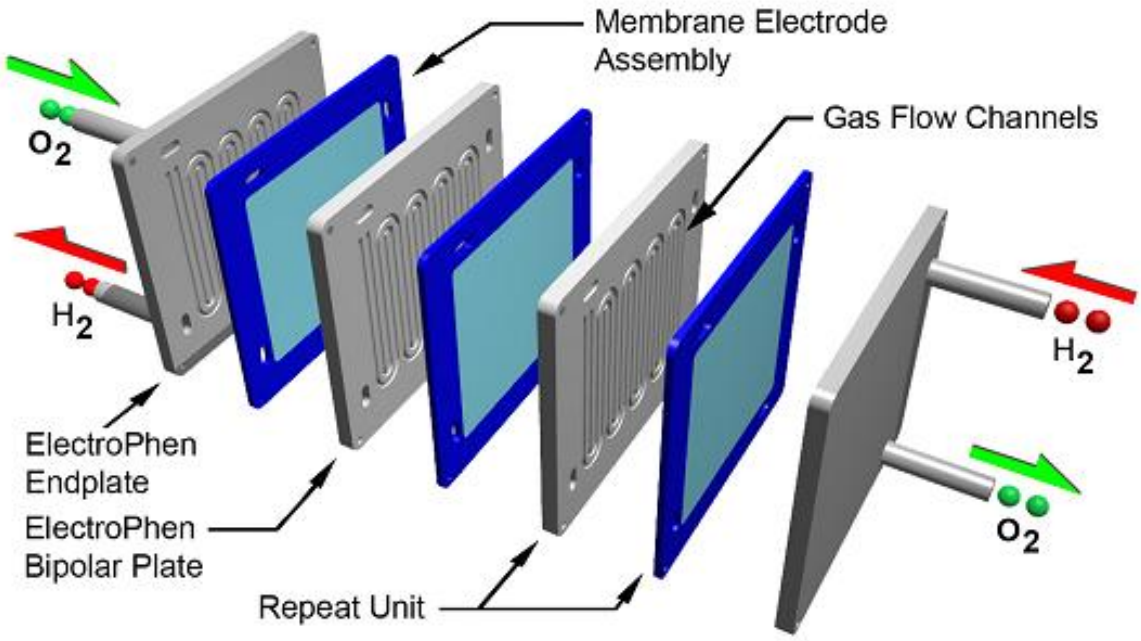

Figure 2.2: Fuel Cell Stack [10]

The MEA consists of an electrolytic polymer with catalyzed electrodes bonded to either side. The electrolyte polymer allows the transfer of H+ ions across the membrane. During operation, hydrogen is supplied on the anode side of the membrane and oxygen is supplied on the cathode. The hydrogen atom ionizes to form H+ ions on the catalyzed anode side of the membrane. The H+ ion then passes through the polymer membrane while the electron travels through the bipolar plates and recombines with hydrogen and oxygen on cathode to produce water. It is this flow of electrons that create the electric power that the fuel cell outputs. The only products from the reaction are water, electricity and heat. Figure 2.3 shows a diagram of a typical PEM fuel cell reaction.

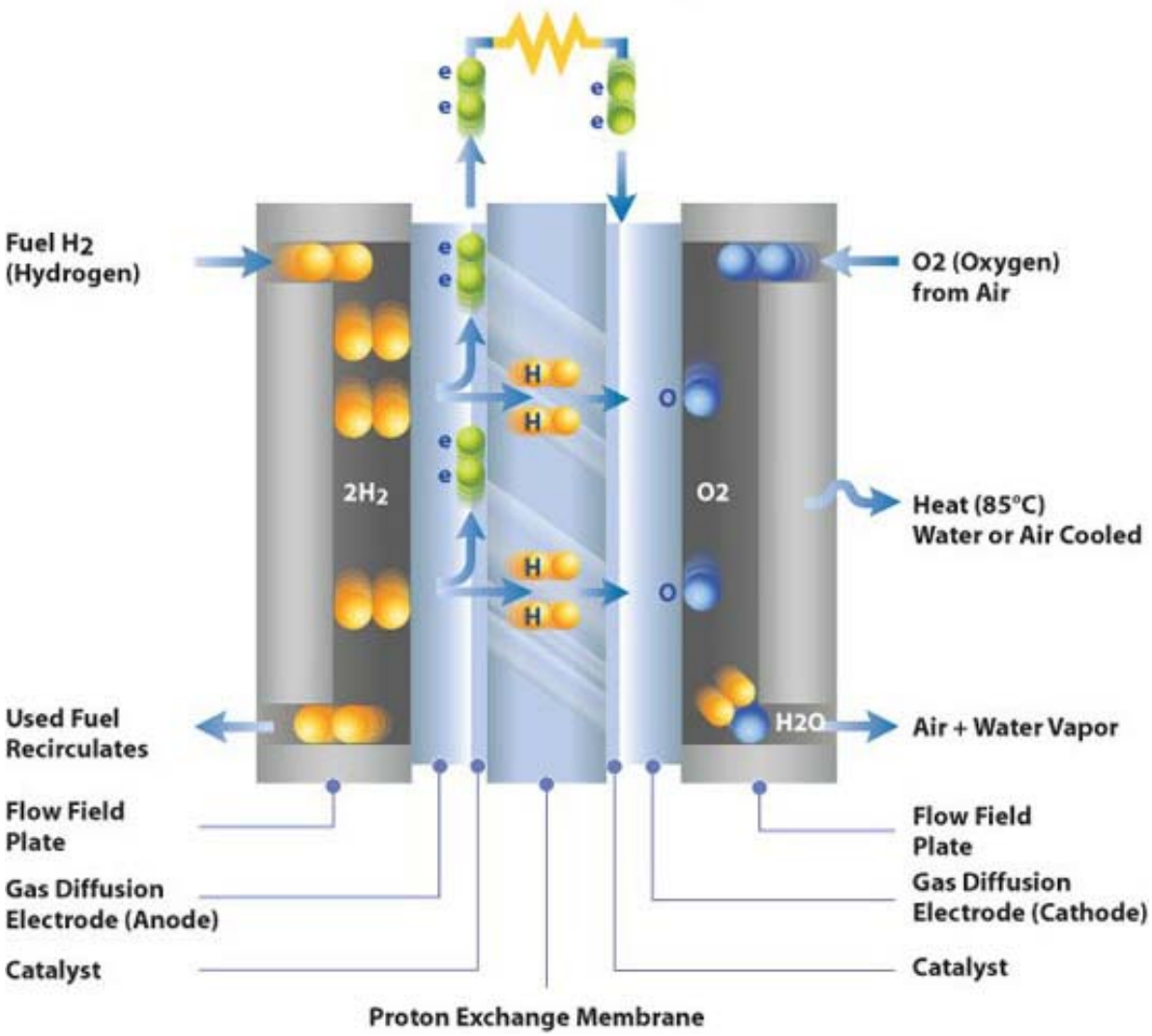

Figure 2.3: PEM Fuel Cell Membrane Reaction [11]

2.1.3 Gas Delivery System

The gaseous hydrogen that powers the fuel cells is stored at 350 [bar] in a DOT approved carbon fiber and aluminum tank. A schematic of the hydrogen delivery system is displayed in Figure 2.4. The hydrogen is stepped down from 350 [bar] to 17 [bar] by two first stage regulators plumbed in parallel. The hydrogen is further reduced in pressure inside each FCM by the hydrogen low pressure regulator. This regulator determines the pressure that is delivered to the hydrogen injectors. During idle and low current draw the pressure upstream of the injectors is approximately the same as the hydrogen loop stack pressure. Under full current draw however this pressure can increase up to the hydrogen supply pressure. Two injector nozzles are used in each stack. One nozzle is sized to supply hydrogen at idle and low current draw. The larger nozzle is used to supply hydrogen during high current draw. The original P5 module switched between the high and low flow injectors depending on the current draw. This function has been disabled on the BB2 modules for reasons discussed in chapter 3.

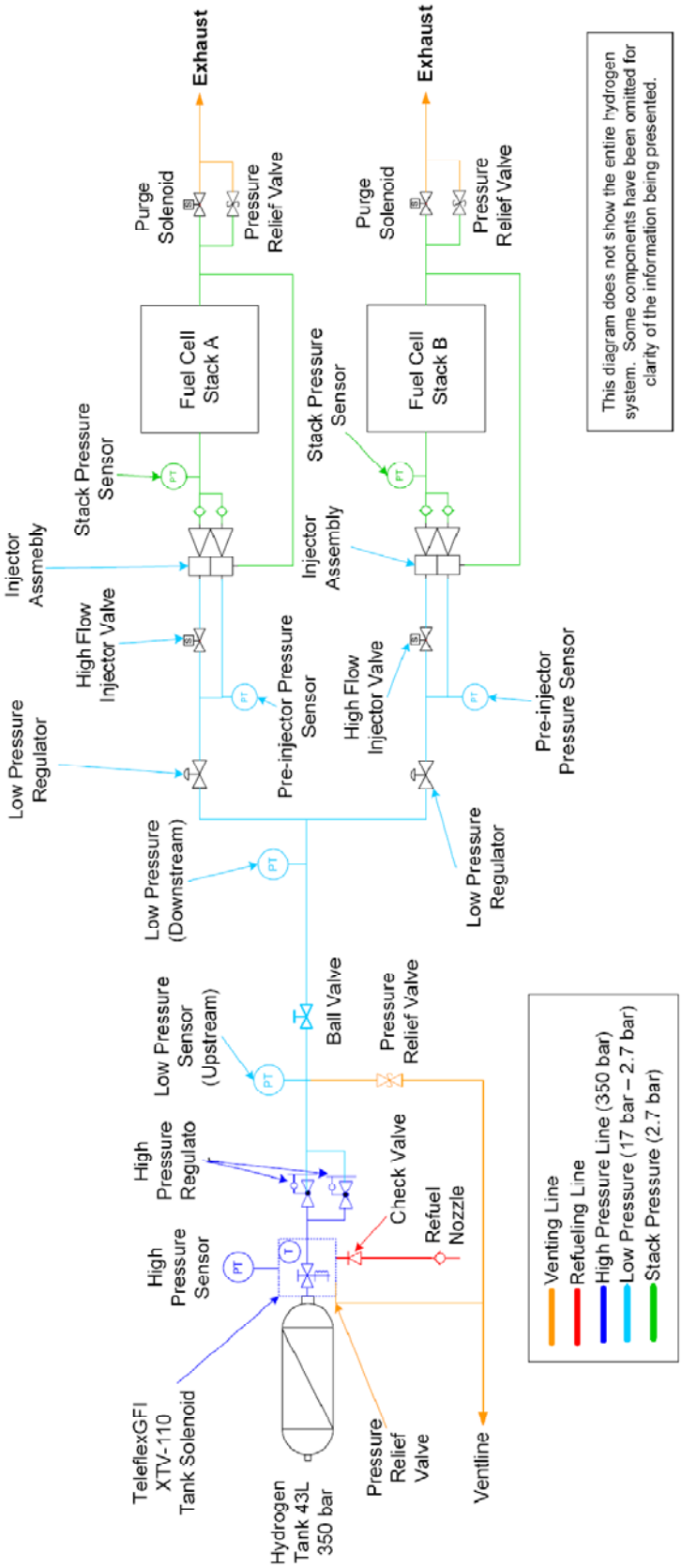

Figure 2.4: Buckeye Bullet 2 Hydrogen Supply System

Most vehicle fuel cell systems use ambient air for the oxidant in the cathode loop of the fuel cell. Like most pressurized fuel cell systems, the standard P5 module was designed to use a motor driven compressor to compress ambient air to stack pressure. The BB2 uses compressed heliox stored onboard in tanks rather than using a compressor. Using compressed heliox rather than air has several advantages. First, the vehicle does not need to carry on onboard compressor, which uses a significant portion of the energy generated by the fuel cell. A compressor can use as much as 20% of the power produced by the fuel cell stack. For the BB2 this would mean that 120 [kW] would be used to drive a compressor rather than driving the vehicle forward. Additionally, the vehicle is raced on the Bonneville Salt Flats. Any air drawn into the vehicle would contain salt particles as well as other contaminants and would thus need to be filtered. Inevitably some contaminants would enter the gas system and the stack and could reduce performance over time. Also, arguably the most important reason the BB2 runs on compressed oxidant is because it allows the use of higher concentrations of oxygen than ambient air. The vehicle currently uses a mixture of 60% helium and 40% oxygen. The higher oxygen concentration increases the power output of the modules. This is discussed in more detail in the following chapters. Helium was used rather than nitrogen as a mixing gas because it allowed for a lower mass flow rate of gas for the same molar flow rate of oxygen. A lower mass flow rate results in lower pressure drops across gas system restrictions and allows for the use of smaller pressure regulators. Performance could be increased by using even higher oxygen concentration, how 100% oxygen is very dangerous under high pressure. 40% oxygen was determined to be a good compromise between increased performance and safety. Figure 2.5 shows a schematic of the the BB2's heliox delivery system.

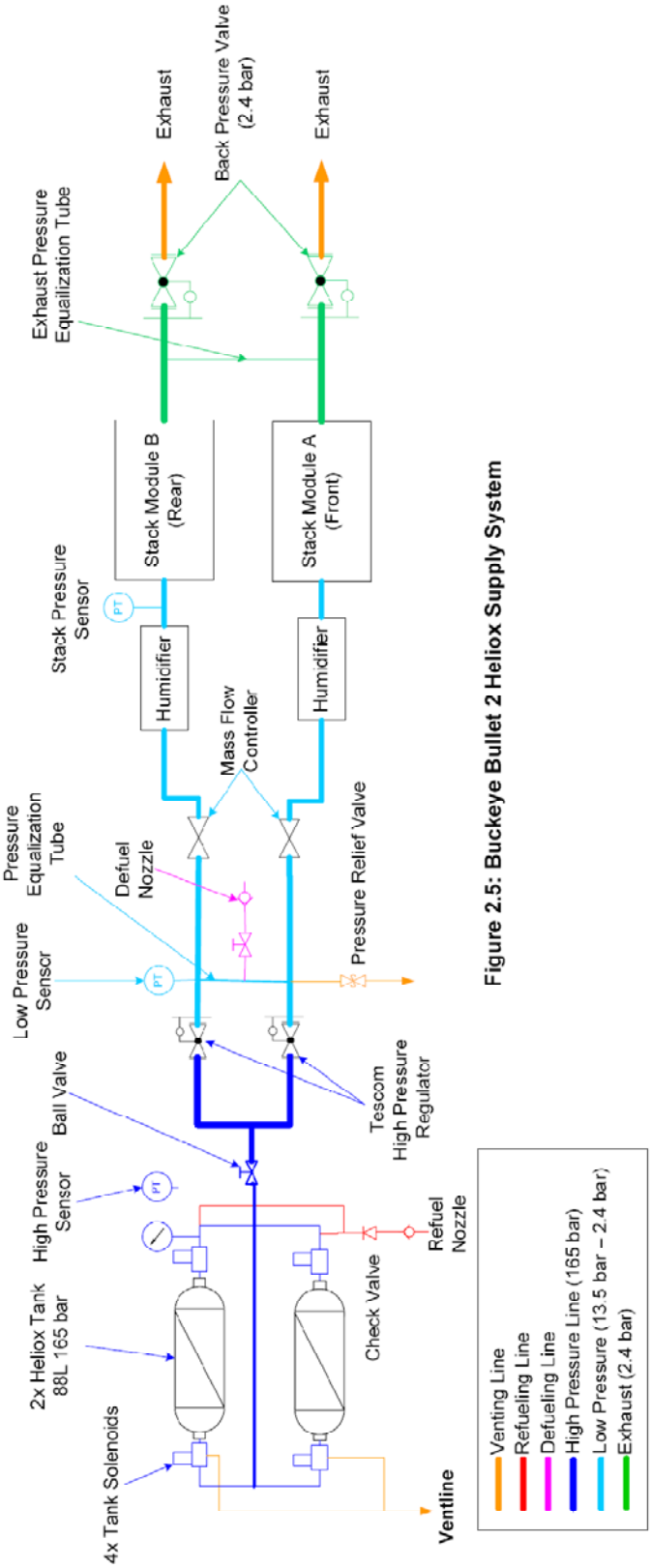

Figure 2.5: Buckeye Bullet 2 Heliox Supply System

2.1.4 Cooling System

Fuel cell systems are generally more efficient than internal combustion engines [9], however, they are still not perfect. The BB2 fuel cell system is approximately 50% efficient. This means that if it is producing 500 [kW] of electricity it is also creating about 500 [kW] of heat energy that needs to be removed from the system to ensure that it does not overheat. The fuel cell system on the BB2 is design to operate at 80^{o} C ideally. If the fuel cells reach much higher than that temperature this could damage the MEAs and reduce the power output of the stacks. The vehicle uses an ice bath to cool the modules. Ice was used as a heat sink because it has the ability to absorb large amounts of energy by utilizing the phase change from solid to liquid water. The vehicle uses 180 [kg] of ice each run. Therefore, it is important that ice is cheap and easy to obtain. The cooling system uses two isolated loops for cooling. The water flowing through the stack is isolated from the water flowing through the ice tanks. This is because the water flowing through the stack is in contact with the bipolar plates and thus must be deionized to avoid conducting electricity. Heat from the fuel cell water loop is transferred to the ice tank loop through two heat exchangers mounted on either side of the forward fuel cell module. Using two isolated loops allows the water in the ice side to be relatively "dirty", meaning that any source of ice can be used in the ice tanks.

2.1.5 Electric Motor

The BB2 uses the same motor and inverter as the original Buckeye Bullet. The motor is a three phase AC induction motor and was custom made for the Buckeye Bullet program. It is specially designed for land speed racing. It is able to deliver a large amount of power over a short duration. The motor is capable of running at 520 [kW] for approximately 2 minutes. It can perform two runs like this within an hour of each other.

2.1.6 Control System

The BB2 uses sophisticated multilevel control system. Figure 2.6 shows an overview of the BB2 control system. The Motohawk controller is the top level controller that controls and coordinates between the other control devices. The Motohawk receives input from the driver and the sends the appropriate commands to the inverter and Ballard controller. It also monitors select data channels and relays information to the driver via the Bosch display. The driver is able to see information such as speed, motor rpm, gear selection, as well as vehicle warnings such as low hydrogen or heliox pressure. The same controller and software used in the Ballard Bus Program has been retained for use in the BB2. This controller controls all fuel cell functions and control. The original software from the Ballard Buses has been specially modified for the use of the BB2.

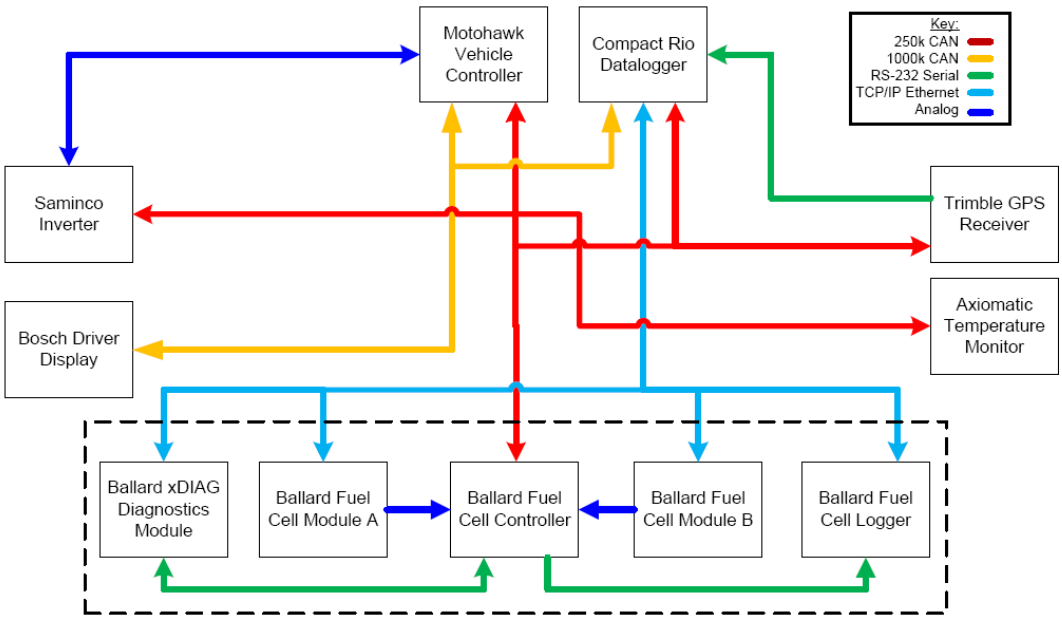

Figure 2.6: Buckeye Bullet 2 Control System Overview

2.1.7 Data Acquisition System

Data collection is very important for prototype vehicles like the BB2. Without the proper data available it is impossible to properly assess vehicle issues and failures. Data is collected for each test and run of the vehicle. The vehicle has two data collection systems. The Ballard data logger from the Ballard Buses is used to monitor data channels from inside the fuel cell module such as stack pressure, temperature, control valve positions, heliox mass flow rates, voltage, current, hydrogen leak detectors, smoke detectors etc. The voltage of each cell row is also measure using the cell voltage monitors (CVMs). The individual cell voltages are recorded using the Ballard data logger. The CVM measurements are very important in diagnosing system issues. Low cells and reversed cell are symptoms of oxidant or fuel starvation at the stack or flooding inside the module. Low cells are discussed further in chapter 3. The National Instrument Compact Rio also functions as a data logger for the other vehicle systems. This device records motor rpm, speed, cooling system temperatures, gas supply pressures, etc. A more in depth list of Compact Rio data channels is shown in Table 2.1. This list is not comprehensive.

Catergory	Sensor
Cockpit	Throttle Pedal Input
Cockpit	24V Battery Voltage
Cockpit	12V Battery Voltage
Cockpit	Clutch Limit Switch
Cockpit	Clutch Pressure
Cockpit	Front Break Pressure
Cockpit	Rear Break Pressure
Cockpit	Brake Power Assist Accumulator Pressure
Cockpit	Control System Active LED
Cockpit	Up Shift Signal
Cockpit	Down Shift Signal
Driveline	Motor Speed
Driveline	Motor Temperature
Driveline	Transmission Temperature
Driveline	Transmission Gear
Driveline	Torque Reference to Inverter
Driveline	Inverter High Voltage
Cooling	48V Battery Voltage
Cooling	Fuel Cell Cooling Loop Pump Command
Cooling	Ice Bath Cooling Loop Pump Command
Cooling	Coolant Pressure Module A
Cooling	Coolant Pressure Module B
Heliox System	Heliox Tank Pressure
Heliox System	Heliox Low Pressure
Heliox System	Heliox Pressure Before MFC
Heliox System	Heliox Pressure at Stack Inlet FCM A
Heliox System	Heliox Pressure at Stack Inlet FCM B
Hydrogen System	Hydrogen Tank Temperature
Hydrogen System	Hydrogen Tank Pressure
Hydrogen System	Hydrogen Low Pressure upstream
Hydrogen System	Hydrogen Low Pressure downstream
Hydrogen System	Hydrogen Pressure Before Injector FCM A
Hydrogen System	Hydrogen Pressure Before Injector FCM B
Hydrogen System	Hydrogen Pressure at Stack Inlet FCM A
Hydrogen System	Hydrogen Pressure at Stack Inlet FCM A
Hydrogen System	Hydrogen Pressure at Stack Outlet FCM A
Hydrogen System	Hydrogen Pressure at Stack Outlet FCM B
Fuel Cell	FCM B Voltage
Fuel Cell	FCM A Voltage
GPS System	GPS Speed
GPS System	GPS Heading

Table 2.1: BB2 Data Acquisition Channels

2.2 Fuel Cell System Test Setup

It was clear after the 2007 racing season that one of the largest issues facing the BB2 team was the need for better and easier procedures for testing the fuel cell systems. Prior to the 2007 racing season there were only two main methods generally available to the Buckeye Bullet team members for load testing the fuel cell systems. These methods were dynamometer testing and track testing. Both of these test methods have advantages and disadvantages for testing the fuel cell systems. However, both of them require extensive setup time and effort.

2.2.1 Dynamometer Testing

A dynamometer is a machine that measures torque and speed of a motor and absorbs the power output of the motor. The Center for Automotive Research at the Ohio State University has two 745 [kW] (1000 [hp]) dynamometers that are available for BB2 team use. During dynamometer testing it is required to remove the motor from the vehicle to connect it to the dynamometer. During dynamometer testing, electric power it generated by the fuel cells and sent through the inverter and into the motor. The motor transfers the electric power into mechanical energy which is absorbed by the dynamometer.

This method of testing is useful for testing the overall driveline system and testing how the motor, inverter and fuel cell systems work together. However, it takes two team members working for an entire day to remove the motor from the car and setup the vehicle for dynamometer testing as well as another day to do the reverse operation. For most of the testing performed in 2008 the team was only interested in testing the fuel cell system. The inverter and motor add additional variables to the test setup. Additionally, dynamometer testing results in additional wear to the motor. Again, the motor is custom built and not easily replaceable.

2.2.2 TRC Testing

The vehicle is track tested at the Transportation Research Center (TRC) in East Liberty, Ohio. This is the only place other than the salt flats where the BB2 can run under its own power. TRC has many testing areas including a dynamic handing course, gravel road, durability testing areas and a 7 mile outer oval course. The BB2 tests on the Vechile Dynamics Area (VDA) which consists of a large ~2 mile figure-8 circuit. An aerial view of the VDA is shown in Figure 2.7.

Figure 2.7: TRC - Vehicle Dynamics Area

TRC testing is excellent for testing the entire vehicle. It not only tests the fuel cell systems but also the transmission, suspension, brakes and parachute system. However, track testing is less desirable if one only wants to test the fuel cell system. During TRC testing the vehicle is able to test up to 160 [km/h]. Although this sounds fast for any vehicle, the BB2 does not even leave first gear at this speed. In fact, most of the testing performed at TRC is not at full power because the vehicle spends most of the time at lower speeds where the motor is not yet into its peak power region. Therefore, the fuel cell system cannot be adequately tested at full power at TRC. Also, getting the car to the track and preparing it for testing requires the effort of many team members and requires packing the car and support

equipment and transporting it to TRC. A picture of the BB2 testing at TRC is shown in Figure 2.8.

Figure 2.8: The Buckeye Bullet 2 testing at TRC

2.2.3 Load Bank Testing

In response to the issues with the current testing methods a new fuel cell testing method was necessary. A load bank was constructed to convert the electrical energy produced by the fuel cells into heat energy that is then dissipated into the atmosphere. The load bank consists of nine Avtron resistors ranging from 7.80 Ω to 5.10 Ω. The resistors can be switched on individually, allowing the fuel cells to be run at nine discrete power levels from low power up to full power. A picture of the load bank is displayed in Figure 2.9.

The resistors are cooled by a 11 [kW] three phase electric fan. When used with the fan, the load bank is able to dissipate the 600+ [kW] that the two fuel cells combined can generate for the 90 second duty cycle over which the car will typically run. Additional the load bank can be used for short duration testing (<10 seconds) without cooling. This is useful because it makes it possible to test the fuel cell on the salt flats without running the

car. Therefore, short tests can be performed in the pits without wasting valuable time on the salt flats. One of the greatest advantages of the load bank is that it allows the fuel cell system to be tested regardless of the condition of the rest of the vehicle. This means that the fuel cells can be tested if the rest of the vehicle is disassembled or if the vehicle has just been run on the salt. It takes less than 5 minutes to transition from a track ready car to the load bank configuration. To transition to fuel cell testing the high voltage cables only need to be removed from the inverter and plugged into the load bank. This saves valuable time during testing and allows fuel cell system issues to be addressed quickly and separately from other vehicle systems.

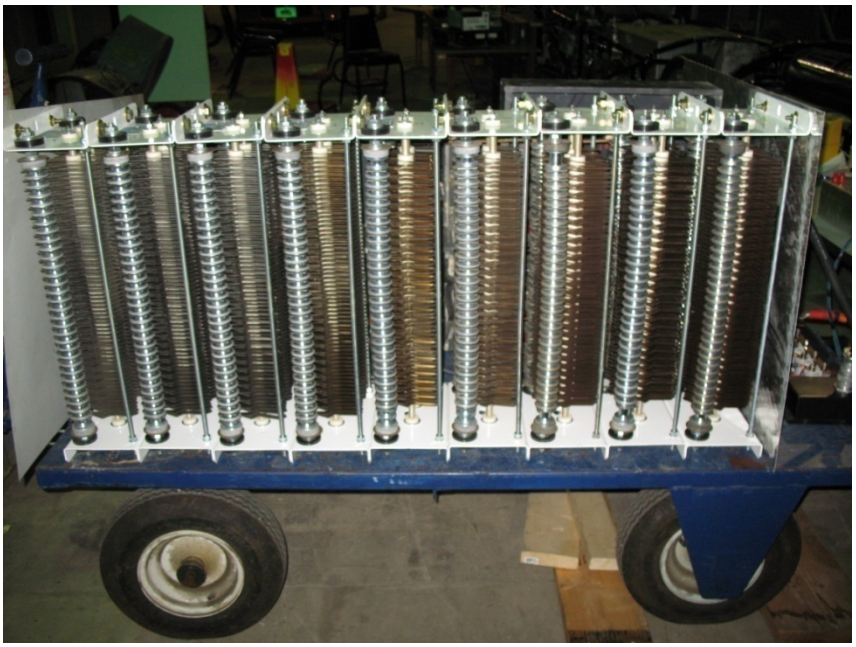

Figure 2.9: BB2 Fuel Cell Testing Load Bank

Chapter 3 :

Vehicle Design Improvements and Modifications

Land speed racing requires very unique design considerations for vehicles compared to road cars and even other types of motorsports. This means that the requirements for the fuel cells used for the Buckeye Bullet 2 are very different from those for which they were originally designed. The Ballard P5 fuel cell modules were originally designed for city transit buses that run at moderate power levels for an extended period of type with varying power output. The BB2 runs for very short durations, usually under 90 seconds, and at full power output for close to 85% of its run time. Therefore, the P5 fuel cell modules underwent several modifications to optimize their design for land speed racing. This chapter will give a brief review of the BB2's first racing season in 2007 and highlight the changes that were made to the fuel cell systems before the 2008 season. This chapter also contains analysis of the over pressure events that occurred during the 2008 season.

3.1 Review of 2007 Racing Season

The BB2 was first raced on the Bonneville Salt Flats during Speed Week 2007. The BB2's highest recorded speed during that week was 324.502 [km/h] (201.636 [mph]). The car reached a speed of 360.977 [km/h] (224.301 [mph]) during World Finals in October 2007. This became the fastest ever recorded speed for a hydrogen vehicle beating the Ford 999's top recorded speed of 333.612 [km/h]. It should be noted that these are not

considered records under the SCTA because both the BB2 and the Fusion 999 are categorized at straight electric vehicles in the E3 class. Therefore, the speed they would need to break to be considered for a recorded is the all out electric land speed record set by the original Buckeye Bullet at 508.485 [km/h]. The BB2 went on to set a FIA sanctioned world record for the world's fastest fuel cell vehicle at 212.641 [km/h] (132.129 [mph]) during a private FIA meet following World Finals in 2007. All of the speeds attained during the 2007 racing were fantastic results that pushed the envelope of fuel cell technology. However, all the attempts fell short of the vehicle's original design goals to break 300 [mph] and contend with the BB1's record for the world's fastest electric car.

There were many issues that plagued the 2007 racing season for the BB2. Keep in mind that this was the first year the vehicle had ever been track tested or raced. It took the original Buckeye Bullet three years of racing before it set the mark at the current record. The BB1 also set its record using batteries rather than fuel cells. Although batteries contain their own issues and pitfalls, the fuel cell system is massively more complex than the battery packs. This can be easily illustrated by looking at the amount of data being record by the two vehicles. The BB1 originally only recorded 4 data channels: vehicle speed, motor rpm, voltage and current. The BB2 monitors hundreds of data channels from voltage and current to gas system pressures, cooling temperatures, solenoid positions, hydrogen sensors, etc.

Given the enormous amount of complexity, the team was still able to set a world record during that first racing season. However, several issues still needed to be

addressed before the following racing season in order to achieve the program goals. A new primary goal was set for the 2008 season: develop a reliable fuel cell system.

Most aborted runs during the 2007 season were a result of an automatic vehicle shutdown. The Ballard controller monitors a variety of data channels and will shutdown the fuel cell system when a number of conditions are met. These shutdowns are triggered to prevent damage to fuel cell components and to ensure safety. The shutdowns during the 2007 season were most commonly caused by detection of hydrogen leaks and low cell voltages.

As part of the safety strategy, the Ballard controller monitors the hydrogen concentration inside each module. A hydrogen sensor is placed in front of an exhaust fan on the outer casing of each module. A vent on the front of each module allows ambient air to be drawn into the module. This reduces the chances that a small hydrogen leak can lead to a buildup of hydrogen in the module and result in a hydrogen concentration above the flammable limit. All the air in the module that is drawn out by the exhaust fan passes over the hydrogen detector. Hydrogen is flammable at 4% in air. The Ballard controller will shut down both modules and close the hydrogen tank solenoid if the hydrogen sensor registers a reading of 50% of the lower flammability limit for hydrogen (2% hydrogen concentration) for longer than ~2-3 seconds. Several run attempts during the 2007 racing season were aborted due to hydrogen leaks. The reaction to these hydrogen leaks is discussed later in this chapter.

Another common shutdown condition for the vehicle in 2007 was low or reversed cell voltages. Each voltage of the total 1920 individual cells in the BB2 is monitored and recorded during the run. If any cell reads below .2 [V] for a short period (~5 seconds) the

modules will shutdown. These low cells are caused by a number of problems. Low cells can be caused by low oxygen or hydrogen concentration on the cathode and anode, respectively. The low reactant concentration can be attributed to restrictions in the supply system, improper regulator settings resulting in low reactant pressure and reactant leaks. Also, a low cell can be caused by water flooding. If the pores on an electrode or the gas diffusion layer flood this will block the reactants from reaching the catalyst sites. Product water is removed from the stack by the flow of reactant through the stack. If the reactant velocity is not high to remove the product water adequately, reactant starvation will occur. The rate at which water produced in the fuel cell is directly proportional to current. Although water is not produced on the anode, water removal from the anode is still a concern. Product water will travel through the membrane and collect on the anode; therefore, flooding can occur there. A reversed cell is one that actually measures a negative voltage. A reversed cell is caused by a low concentration of hydrogen.

These low and reversed cell essentially become resistors in the stack. They reduce the overall stack power output. They also generate heat and if not addressed can cause serious damage. The heat generated in combination with a catalyst can cause hydrogen ignition if there is an internal stack leak that allows the correct concentration of oxygen and hydrogen to occur. Also, the low and reversed cell can cause permanent damage to the membranes which can affect their power output even after the cell returns to normal operating voltage.

The largest issue facing the team at the end of the 2007 season was low and reversed cells. The most significant reason for these low cells was hydrogen starvation in

the anode loop. The diagnosis and reaction to these failures is discussed in detail in the following sections.

3.2 Hydrogen Leaks and Detection

Hydrogen has the lowest molecular weight and viscosity of any gas, therefore, it has the highest leak rate compared to other gases and is more difficult to contain [12]. It is very expensive and difficult to make a hydrogen system that is completely sealed. The greatest leak potential is not within the stainless steel fittings that supply the fuel cells but rather in the stacks themselves. There is always an accepted leak rate when dealing with hydrogen systems. The BB2's specification for acceptable leak rate at operating pressure for one module is 2.5 [slpm] of hydrogen.

The air within each module is evacuated continuously with an exhaust fan on each module. This reduces that chances that hydrogen will build up within the module and reach a potentially flammable limit.

There are several methods that the BB2 uses to check for leaks in the hydrogen system. The most extensive method is to connect the module to a leak checking device. The leak check device allows the system to be pressurized and then measures the flow rate of gases flowing through the device. This effectively quantifies the leak rate. The coolant, heliox and hydrogen leak rates can be measured individually. Additionally the cross leak rates between anode and cathode and coolant can be measured. This tool not only measures the line leaks within the module but also the leak rates within the stack.

Another form of leak check that is less extensive and easily performed involves pressurizing the system by opening the fuel tank and closing the purge valve. Then each

fitting needs to be either sprayed with soapy solution that indicates leaks by bubbling or a hydrogen detector can be used to check each fitting for leaks.

In order to reduce the vehicle shutdowns due to hydrogen leak detections, the Buckeye Bullet team adopted a more rigorous leak checking schedule. Under normal operation the fuel cell modules would be leak checked after several hundred hours of operation. During the 2008 racing season, each BB2 module was subjected to a full metered leak check using a leak check device before each trip and then leak checked on the salt using a hydrogen detector. This significantly reduced the hydrogen leaks detected during operation.

3.3 Module Hardware Changes

The two fuel cell modules used for the BB2 are specially modified for the unique characteristics of land speed racing. The BB2 modules run at a much higher power level than the original P5 specification and thus the hydrogen system needed to be changed to account for the increased hydrogen flow. Also, some systems were able to be removed to reduce overall vehicle weight.

3.3.1 Hydrogen Injector Assembly

The amount of hydrogen consumed on the anode is directly proportional to the current draw. If the hydrogen supply system to the stack is not able to flow enough hydrogen, the concentration of hydrogen in the stack will decrease leading to hydrogen starvation on the stack. Hydrogen starvation results in low cell voltages as previously discussed. Additionally, even if the proper concentration of hydrogen is maintained on the stack, if the hydrogen flow rate is not high enough flooding in the anode can occur.

For these reasons the hydrogen is circulated through the stack to ensure that there is adequate flow velocity to remove product water. To facilitate this action some fuel cell

systems use an electric pump to recirculate the hydrogen. The P5 module uses a jet pump to recirculate hydrogen. The flow of the hydrogen through the stack is driven by a combination of hydrogen being consumed in the reaction and the momentum of the pressurized hydrogen entering the anode loop through an orifice. A diagram of this system is shown in Figure 3.1.

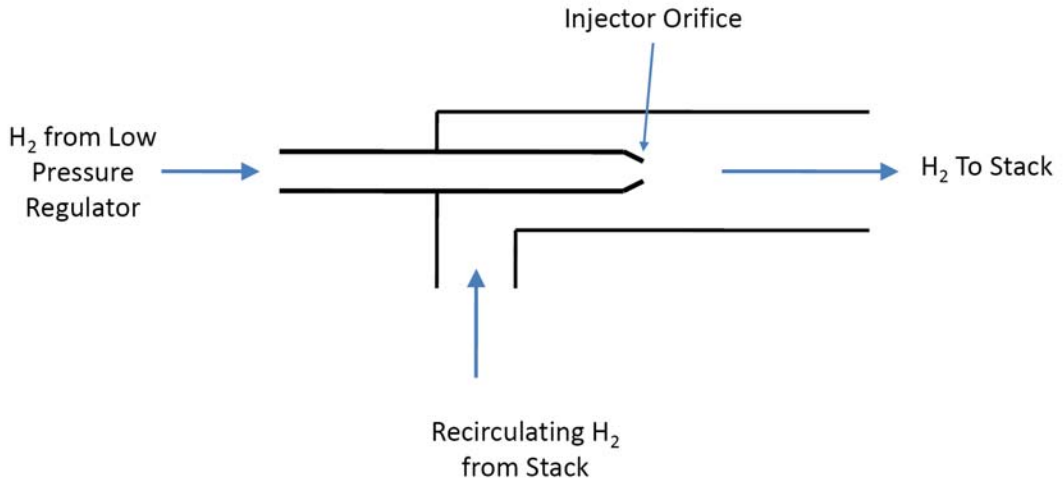

Figure 3.1: Hydrogen Recirculation System

The hydrogen flow rate through the injector orifice is dependent on the orifice sizing and the hydrogen inlet pressure. Each module contains one low flow and one high flow injector for low current and high current, respectively. The normal P5 module will switch on the high flow injector for high current draw. The low flow injector is always open.

The main issue during early testing in Spring 2008 was global hydrogen starvation in both fuel cell modules. From Figure 3.1 it can be seen that hydrogen pressure in both stacks drops off quickly at current draws greater than 600 combined amps. The supply pressure to the injector assembly droops to ~ 9 [bar] during this high current area.

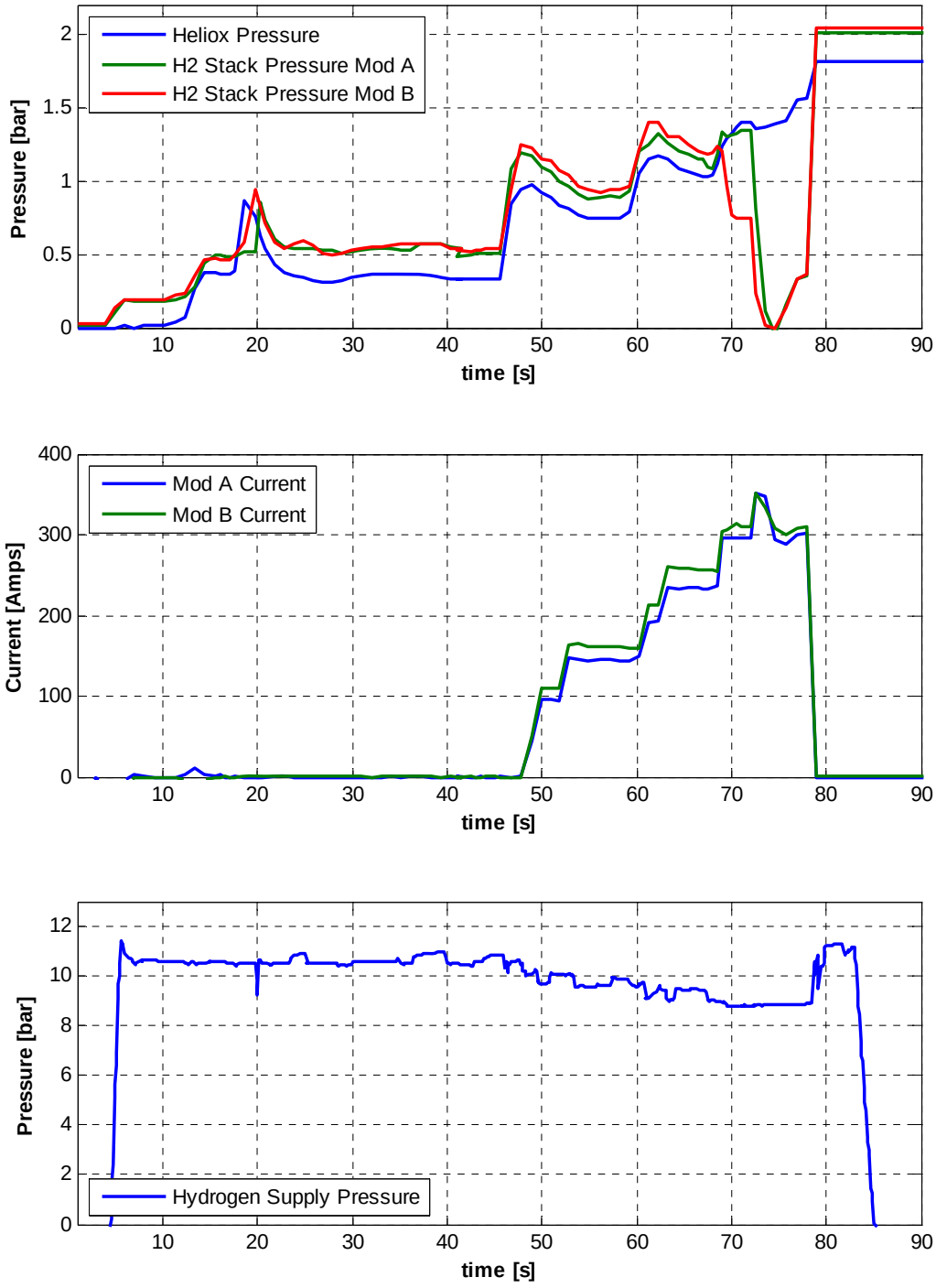

Figure 3.2: April 5 Load Cell Test Data

Over several tests the supply pressure was increased to ~14.1 [bar] at fuel cell module inlet. This increased the maximum possible current draw with some success, however, hydrogen starvation continued to be a problem. Further increase of the hydrogen pressure was not possible due to the rated pressure of certain hydrogen system components.

The mass flow rate needed is directly proportional to the current draw. The desired mass flow rate of hydrogen can be determined by calculating the hydrogen consumed in the fuel cell reaction:

$$\dot{m} = \frac{I}{2F}\left(M_{H_2}\right)\left(N_{cells}\right)$$

where

$\dot{m}$=desired mass flow rate of hydrogen ([g/s])
I = Current draw [A]
F=Faraday's Constant (96485 [C/mol])
M_{H2}= Molecular mass of hydrogen (2.016 [g/mol])
N_{cells}= 960

$$\dot{m} = \frac{500[A]}{2\left(96485\left[\frac{C}{mol}\right]\right)}\left(2.016\left[\frac{g}{mol}\right]\right)(960[cells])$$

$$\dot{m} = 5.015[g/s]$$

The idle jet is able to deliver approximately 0.4 [g/s] of hydrogen under the described loading condition. Therefore, the high flow injector needs to deliver 4.615 [g/s]. It should be noted that normally more hydrogen is injected into that stack than is consumed for the reaction. The excess hydrogen is purged during the normal purge cycling and also leaks through the stack into the cathode loop. The hydrogen that leaks into the cathode loop is carried out with the exhaust. The hydrogen that is purged exits the vehicle through the exhaust. The purge valve periodically opens to remove helium and oxygen contaminants that leak over from the cathode and lower hydrogen concentration on the anode. The contaminant buildup in the anode is very minimal in 90 seconds. Therefore, the purge valve is always

closed above 300 [A] per module. Eliminating the purge cycle at high current draw helps to maintain hydrogen pressure. Because no hydrogen is purged during high current draw and very little leaks across the stack, the excess hydrogen entering the stack will be ignored for the following calculations.

The actual mass flow rate of the hydrogen entering the stack through the high flow injector is determined by the isentropic choked flow through a nozzle equation [13]:

$$\dot{m} = p_o A^* \sqrt{\frac{\gamma}{RT_o}\left(\frac{2}{\gamma+1}\right)^{\frac{\gamma+1}{\gamma-1}}}$$

where

p_o = absolute pressure before the injector [Pa]
A^* = area of the orifice [m^2]
R = Ideal Gas Constant for Hydrogen (4124 [J/(kg*K)])
T_o = temperature before the injector [K]
γ = specific heat ratio for hydrogen (1.41)

During the 2007 racing season the high flow injector orifice was 2.74 [mm] in diameter. For the high flow injector with an orifice size of 2.74 [mm] at 10 [barg] before the injector (note that 10 [barg] would correspond with 14.1 [barg] at the module inlet), the mass flow rate is calculated as follows:

$$\dot{m} = (9.976 * 10^5[Pa])(5.896 * 10^{-6}[m^2]) \sqrt{\frac{1.41}{\left(4124\left[\frac{J}{kg*K}\right]\right)(273[K])}^{\frac{1.41+1}{1.41-1}}}$$

$$\dot{m} = 3.804 \text{ [g/s]}$$

This value shows that the mass flow rate through the choked flow injector is not sufficient to supply the reaction at high current. Therefore, fuel starvation in the stack was caused by the orifice of the injector being sized to small.

The high flow injector on the jet pump was drilled out to 3.048 [mm] in 2008. The maximum mass flow rate through the new orifice size is determined to be:

$$\dot{m} = (9.976e5[Pa])(7.297e-6[m^2])\sqrt{\frac{1.41}{\left(4124\left[\frac{J}{kg*K}\right]\right)(273[K])}}^{\frac{1.41+1}{1.41-1}}$$

$$\dot{m} = 4.708\,[g/s]$$

This hydrogen flow rate is sufficient to power one module up to 500 [A]. The BB2 usually only operates closer to 450 [A] which gives the system a margin to account hydrogen cross leaks and supply temperature and pressure deviations.

The actual flow rate entering the stack for a given current draw is determined by the pressure upstream of the injector. This pressure is varied based on the difference in pressure between the anode and cathode. Therefore, only the hydrogen that is needed to carry out the reaction is injected. The ratio of the fuel consumed and the fuel circulated through the stack is known as the stoichiometric ratio. It should also be noted that even though only the amount of fuel necessary for the reaction is injected that does not mean that the fuel stoichiometric ratio is 1.0. The excess fuel recirculates through the stack and thus increases the ratio of fuel flow and fuel consumed.

Further testing revealed intermittent hydrogen starvations at medium to high current draws. It was determined during testing that it is possible for the high flow injector valve to fail in the closed position. This valve is a normally open valve and because of its design is it possible to fail closed. Due to the frequency of this failure the high flow injector valve was removed. This valve allows the vehicle to run on the idle jet at low current. This is advantageous because the velocity of the incoming hydrogen is greater under low current when only the idle jet is open. This allows for greater hydrogen circulation and a higher stoichiometric ratio at low current. Again, the high stoichiometric ratio is desirable because

it helps remove water from the anode and ensures high hydrogen pressure and concentration downstream in the stack. However, because the BB2 only operates at low power for a very short amount of time, the valve was removed so that the BB2 always runs with both injectors open.

3.3.2 Weight Reduction

Weight is the enemy of any high performance vehicle. Weight is not directly related to the top speed of a vehicle. The absolute top speed occurs when the force pushing the car forward by the drivetrain and the wheels equals the aerodynamic and rolling resistance forces pushing the vehicle backwards. Therefore, top speed is directly a function of engine power, traction, rolling resistance and aerodynamic resistance. However, the BB2 is accelerating even through the last timed mile. Therefore, any weight reduction and subsequent increase in acceleration results in a higher exit speed in the final timed mile. So reducing weight results in a higher recorded speed. In the 2007 racing season the BB2 weighed approximately 2700 [kg] with a driver and loaded with cooling ice. Throughout 2008 many improvement were made to the BB2 to reduce weight where possible. The cooling system and gas delivery systems were revised to utilize light weight materials and reduce complexity.

Additionally, unnecessary systems were removed from the fuel cell modules in order to reduce weight. The aluminum covers for the fuel cell panel were replaced with carbon fiber panels or thinner walled aluminum panels. Also, the exhaust water recapture system was removed. Normally the product water from the fuel cell stack is removed from the exhaust and used in the humidification system. This eliminates the need to refill the humidification system with water during the bus operation. However, for the BB2 application it is lighter to actually store more water on board and remove the water recapture system.

All the weight reduction projects resulted in approximately 220 [kg] of weight being removed from the vehicle.

3.4 Overpressure Event Analysis

During Speedweek 2008 the fuel cell system showed remarkable improvement in reliability compared to the previous season. Throughout the first four days of racing there were no aborted runs due to fuel cell issues. On August 23, 2008 after two aborted runs due to a failure of the humidification pump on module B, the third run of the day resulted in shutdown due to a hydrogen leak detection. After pulling the vehicle back into the pit area and investigating further, it was discovered that a stack seal had be damaged by a pressure spike in both the anode and cathode loop in module B. The pressure spike was attributed to a malfunction of the mass flow controller (MFC) for module B. After bench testing MFC B after the event, it was concluded that the MFC had failed due to an electrical failure caused by corrosion and water intrusion on the MFC's circuitry. At the time, the MFC for module A did not exhibit this problem behavior. MFC B was subsequently replaced with a new MFC of the same model.

During the FIA meet on September 26, 2008, the vehicle experienced a similar over pressure event resulting in a blown seal in the fuel cell stack. The escaping hydrogen and heliox ignited due to an unknown source and caused minor damage to the vehicle. The majority of the damage occurred to the vehicle's body panels and the fuel cell module panels. All the major vehicle systems and more importantly the driver survived the event without any harm.

3.4.1 Overpressure Event Data

Data from both over pressure events are very similar, thus we will focus on the more severe over pressure event during the FIA meet. Figure 3.3 shows the stack pressures during

the overpressure event during the FIA meet in September 2008. From the data it can be seen that the anode and cathode pressure spike in both modules just prior to hydrogen leak detection. It should be noted that the pressure sensors used at the stack level saturate at 3.2 [bar]. Therefore, during the pressure spike, it is unclear of the actual pressure on the stack. It is only known that the pressure is equal to or greater than 3.2 [bar]

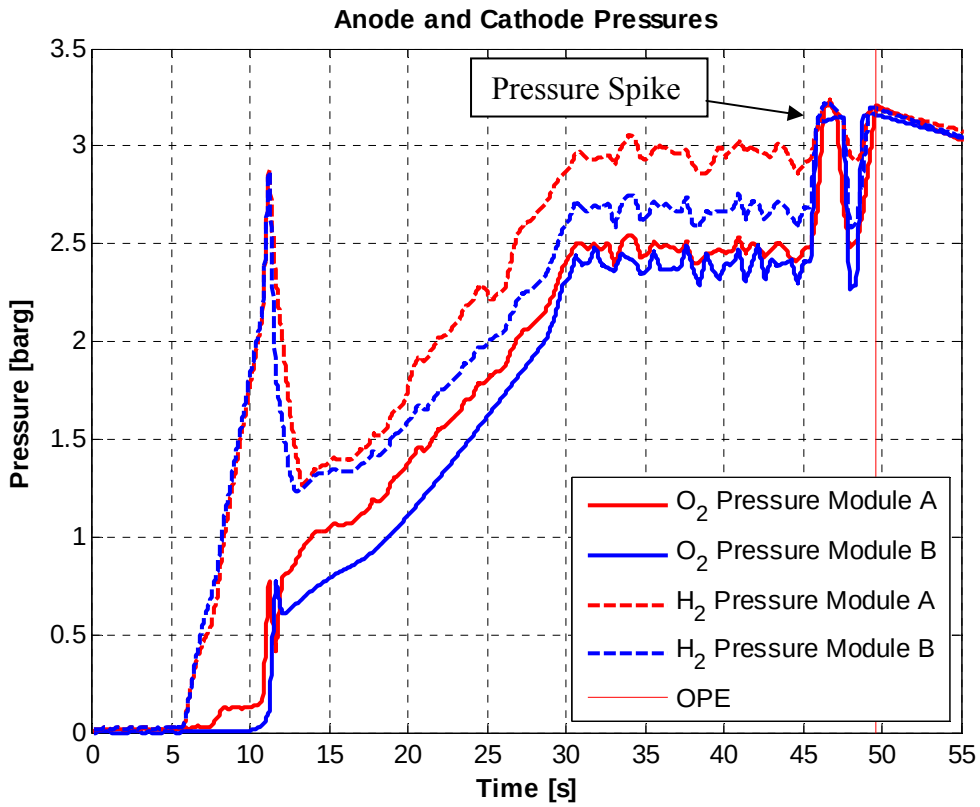

Figure 3.3: Stack Pressure Data for for September 26, 2008

Figures 3.4 and 3.5 show the pressure data taken from the September 26 run for the hydrogen and oxygen systems respectively. Figure 3.4 also shows the hydrogen detection sensor reading. Figure 3.5 also shows the mass flow rate through the mass flow controllers.

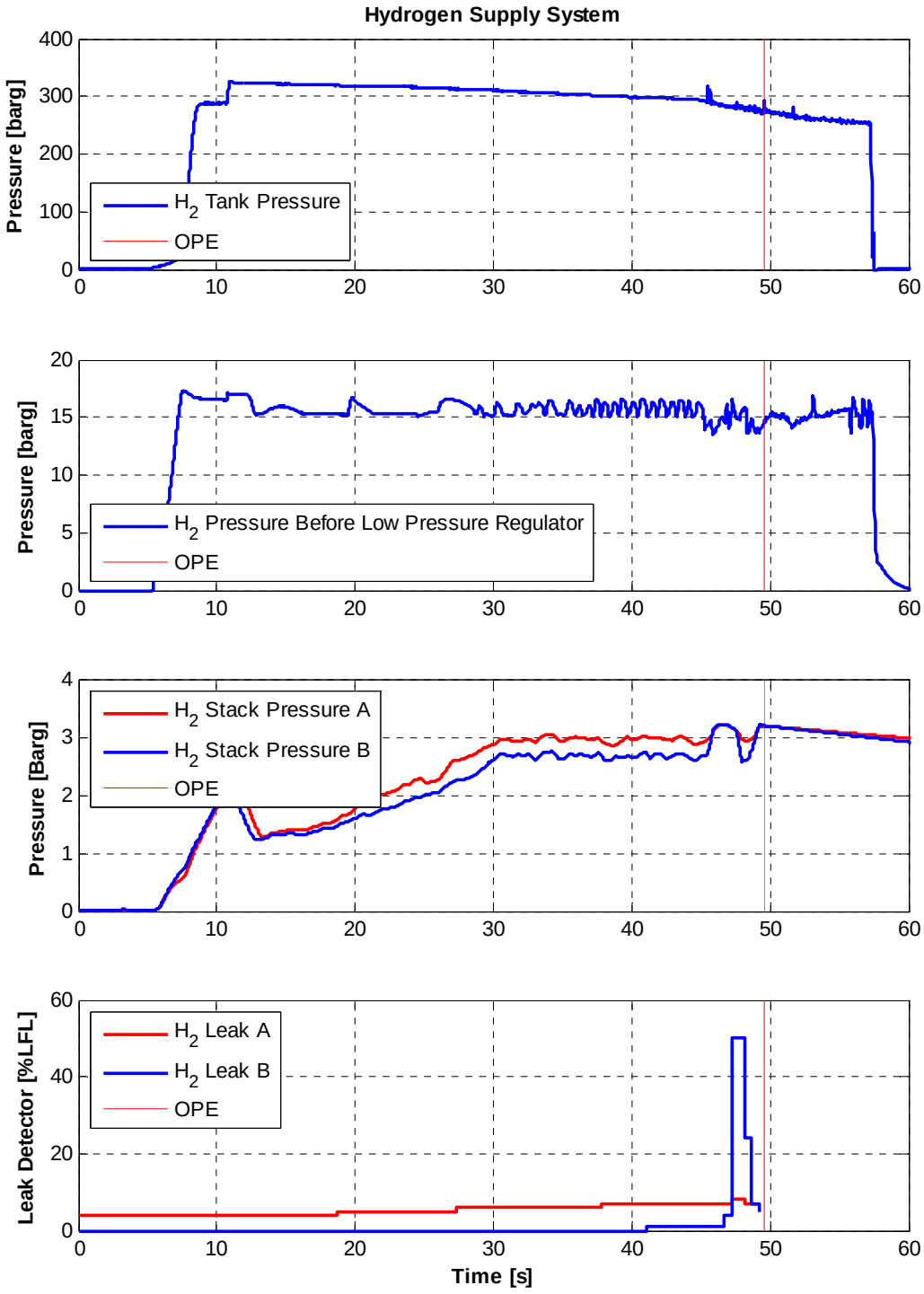

Figure 3.4: Hydrogen Supply System Data for September 26, 2008

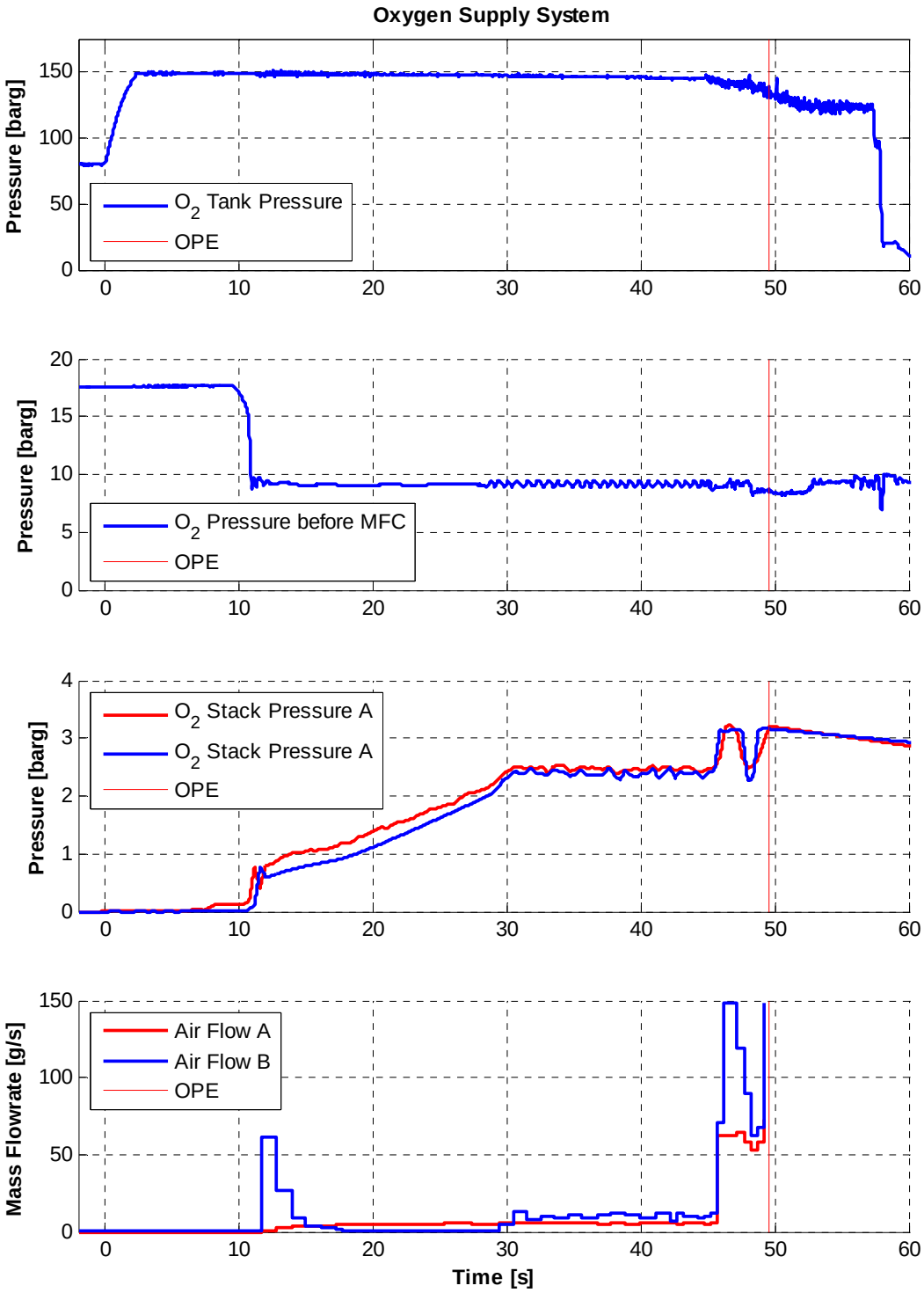

Figure 3.5: Oxygen Supply System Data for September 26, 2008

Analysis of the data in Figures 3.4 and 3.5 indicate that the pressure spike is likely caused by a sudden uncontrolled increase in mass flow rate through MFC B. Because the backpressure valve and fuel cell stack represent resistances to flow, an increase in mass flow rate above the designed flow rate would result in an increase in cathode pressure. The mass flow controllers have already proved to be unreliable in previous tests. The MFCs often overshoot when reacting to step inputs resulting in mass flow rates above the command value.

It should be noted that the hydrogen pressure on the stack is controlled by the low pressure hydrogen regulator. This regulator references the stack air pressure and will adjust the hydrogen pressure to be greater than the heliox pressure by a predetermined amount. Therefore, a pressure spike on the cathode would result in an even higher pressure spike on the anode. Figure 3.6 shows the pressure just downstream of the hydrogen low pressure regulator and upstream of the hydrogen injector.

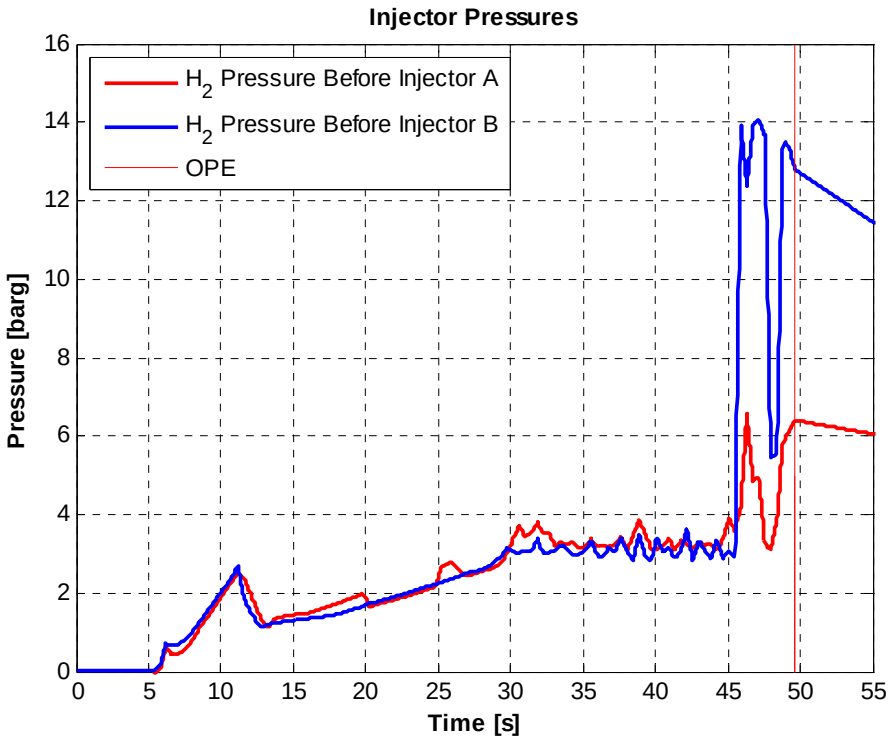

Figure 3.6: Hydrogen Injector Pressures

3.4.2 Theoretical Mass Flow Rate through MFC

During the overpressure event the MFC feedback signal was saturated at 150 [g/s] of heliox, therefore, it is not possible to know how much heliox was actually flowing into the system. In order to account for the worst case scenario, it can be assumed that the mass flow through the MFC was governed by the choked flow condition through the MFC orifice. The equation below describes the gas flow through the mass flow controller for its given flow coefficient [14]. This equation is used because the large pressure drop across the valve resulting in sonic choked flow.

$$Q = 1.471 N_2 C_v P_1 \sqrt{\frac{1}{SG * T_1}}$$

$$= (1.471)(6950)(6.0)(13.5)\sqrt{\frac{1}{(.5247)(293.15)}}$$

$$= 2.480e4\ [slpm] = 261.2\ [g/s]$$

Where

Q = Volumetric Flow Rate [slpm]
N_2 = Constant based on units [6950]
SG = Specific Gravity
C_v = Flow Coefficient [6.96]
P_1 = Upstream Pressure [bar]
T1= Upstream Pressure [K]

This suggests that if the mass flow controllers failed in the open position that the resulting gas flow rate would be 261 [g/s]. This is assuming an upstream pressure of 13.5 [bar]. It should be noted that the upstream pressure was 13.5 [bar] during the overpressure event in August. However, the upstream pressure was lowered to 9.5 [bar] before the overpressure event in September. An upstream pressure of 9.5 [bar] would correspond to a max flow rate of 184 [g/s] of heliox. For the system model developed in the following section the worst case flow rate of 261 [g/s] from the August overpressure event will be used

for the model input. Figure 3.7 shows the recorded data sample and the theoretical maximum flow values. The input to the heliox system model is a combination of recorded data values with the theoretical maximum flow values.

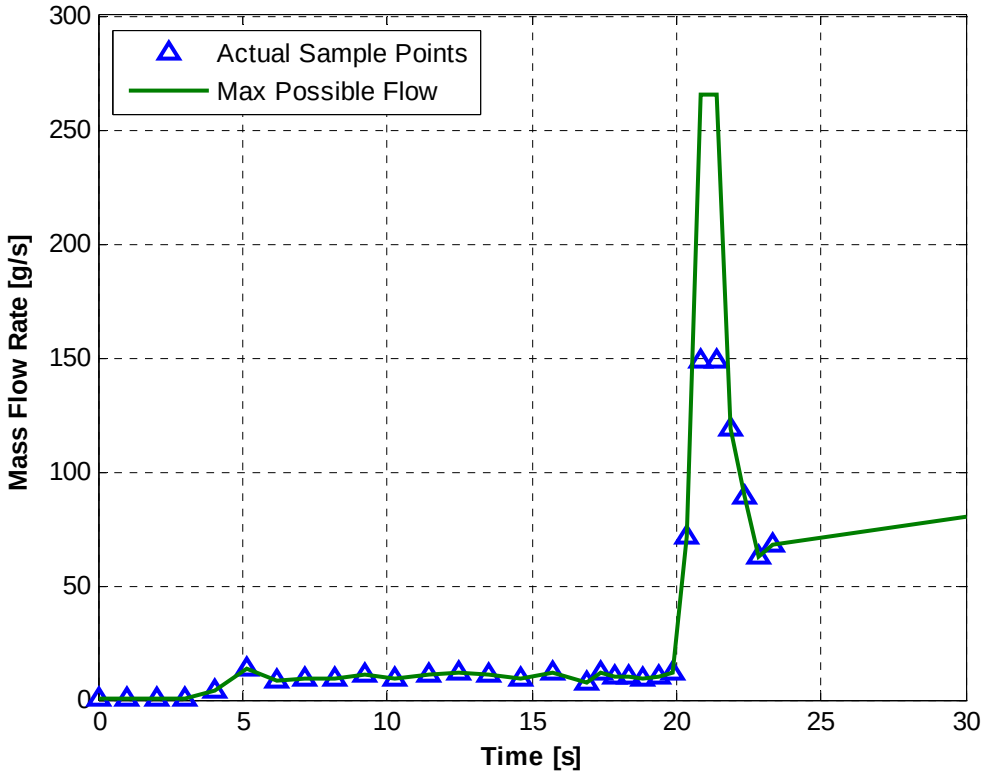

Figure 3.7: Heliox System Model Inputs

3.4.3 Overpressure Event Model Development

In order to validate that a sudden increase in mass flow rate is capable of causing the observed pressure spikes, a model was developed of both the 2007 and 2008 heliox systems. Several assumptions were made in the model for the heliox system. The gas is assumed to follow the ideal gas law. The effect of humidification is not considered in the model at this stage. All of the gases are assumed to be dry. The temperature from the inlet and exit is assumed to be constant at 80° C, which is the normal operating temperature of the fuel cell stacks. The exhaust and inlet gases are considered to be the same composition. In other

words, the oxygen is not consumed through the stack. These assumptions are made because both overpressure events occurred during low current draw which means that very little oxygen was consumed and very little produce water was being produced. These assumptions do reduce the accuracy of the model, however, this model is intended to determine within relative accuracy whether the system will produce a pressure spike with a given input.

The inlet and exit manifold were modeled using a lumped volume approach. Here the conservation of mass resulting in:

$$\frac{dm}{dt} = \dot{m}_{in} - \dot{m}_{out}$$

Adapting this equation into the ideal gas law produces:

$$\frac{dP}{dt} = \frac{RT}{V}(\dot{m}_{in} - \dot{m}_{out})$$

Where

m = mass of the gas in the control volume [kg]
$\dot{m}$ = mass flow rate in or out of the control volume [kg/s]
t = time
P = pressure [N/m^2]
V = volume of the manifold [m^3]
R = Gas Constant for Heliox [546.9 J/(kg*K)]
T = Temperature [K]

The back pressure on the stack is regulated by the back pressure valve (BPV). The mass flow rate through the back pressure valve is dependent on the back pressure and the original pressure setting. The mass flow rates through the BPV for a given pressure are given by the manufacturer. After correcting the manufacturer's data for use with heliox the curve shown in Figure 3.8 was developed for the model. The manufactures data gave a curve of back pressure dependent upon the flow rate. Because the model requires a discrete flow rate dependent on the back pressure, a curve fit of the manufactures data was used.

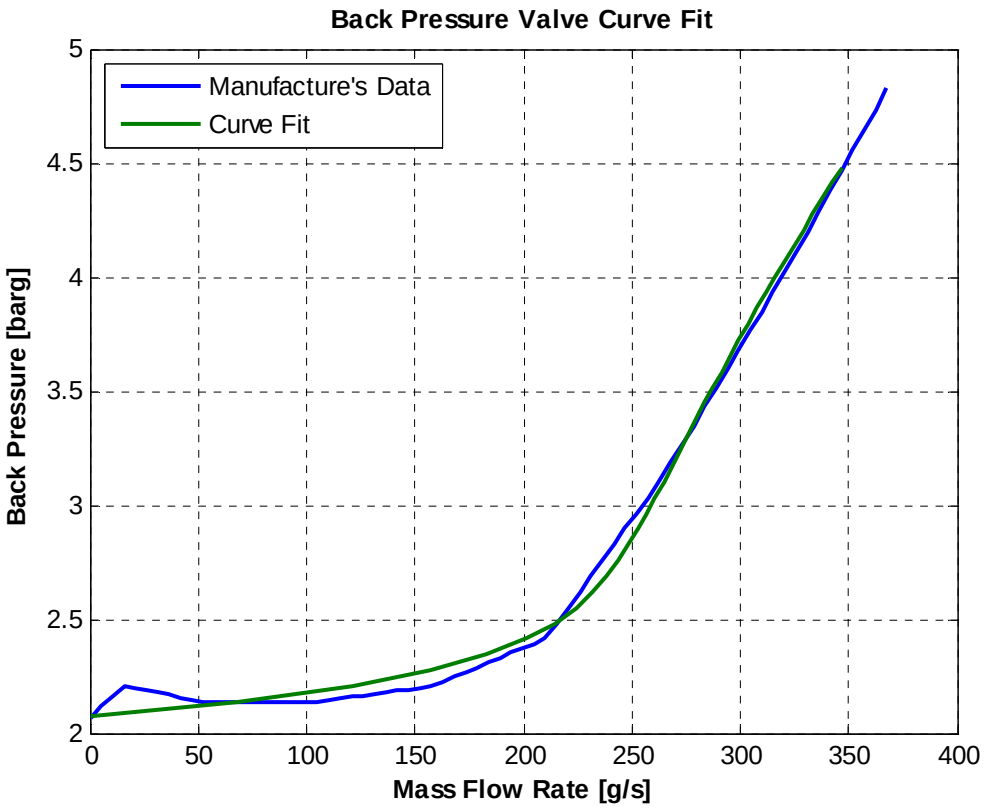

Figure 3.8: Back Pressure Valve Mass Flow Rate

Through the normal operating area of the BB2, the pressure drop across the stack behaviors almost linearly. Figure 3.9 shows a linear curve fit with the experimental pressure drop across that stack.

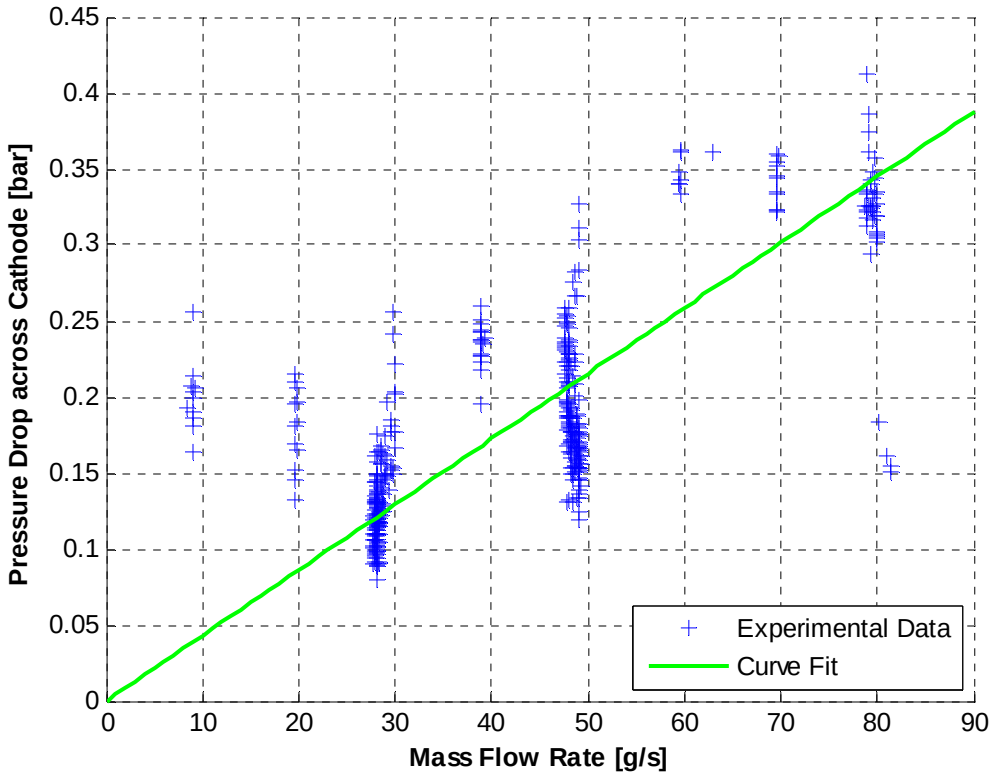

Figure 3.9: Pressure Drop across Cathode

The pressure drop across the stack may not perform linearly during the overpressure events where the mass flow rate is much higher than the normal operating conditions. However, the geometry of flow channels inside the stack and other necessary information to create a more accurate model of the stack is not available to the BB2 team at this time. Therefore, a linear stack flow resistance will be used for the heliox system model.

The main question to answer in performing this analysis is why there were two over pressure events in 2008 and no over pressure events in 2007. The overall stack pressure in 2008 was higher than in 2007, however, during normal operation the anode and cathode pressures remained below the 3.1 [bar] burst pressure of the stack. The only physical changes to the heliox system between 2007 and 2008 was in the exhaust. In the 2007 the exhaust from each module entered a single large exhaust tube that ran the length of the car and exited the rear. In the 2008 exhaust system the overall length and subsequently the

volume of the exhaust was reduced to remove weight. Each module exhausted through a separate backpressure value. The back pressure was equalized between the modules by a 12.7 [mm] (0.5 [inch]) cross-over tube. The 2007 and 2008 exhaust systems are compared in Figure 3.10.

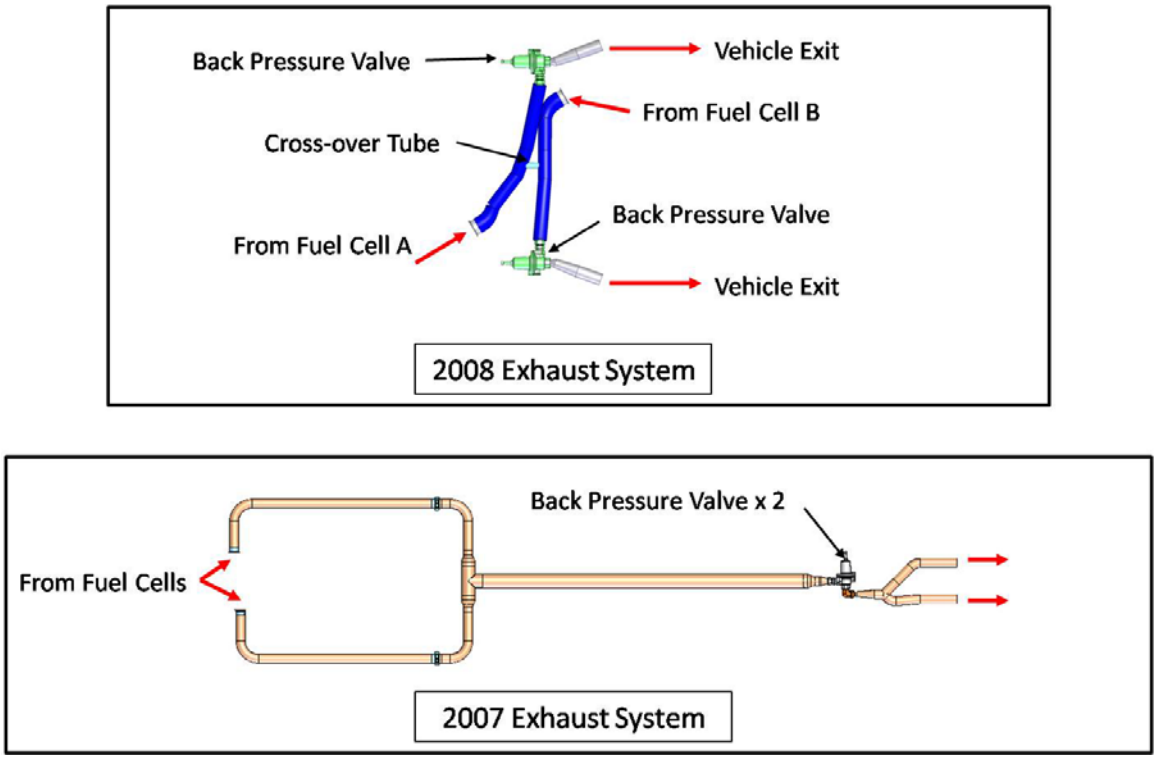

Figure 3.10: 2008 and 2007 Exhaust Comparison

For the heliox system model the cross over tube was modeled using compressible flow with friction through a tube [13]. The flow rate through the tube is dependent on the ratio between module A and module B back pressure. The resulting curve is shown in figure 3.11. The mass flow rate through the cross over tube increases with increasing pressure ratio.

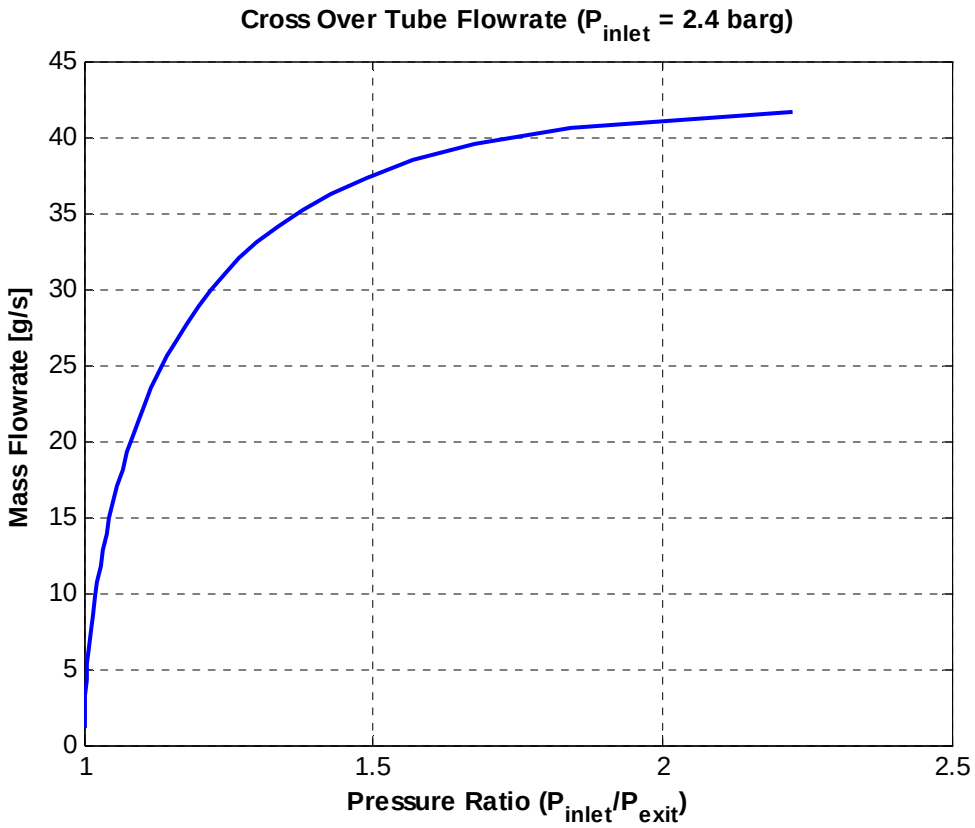

Figure 3.11: Mass Flow Through 12.7 mm Cross Over Tube

For the full Simulink model of the heliox system refer to the Appendix.

3.4.4 Overpressure Event Model Results

Both the 2007 and 2008 system parameters and volumes were integrated into the heliox system model. The mass flow rate exiting MFC B in the system model is described by the measured data with the addition of theoretical data where the sensor has been saturated. The mass flow rate exiting MFC A is the actual mass flow rate measured from the test data for the September 26 run. Figure 3.12 shows the system inputs used for the comparison between the 2007 and 2008 systems.

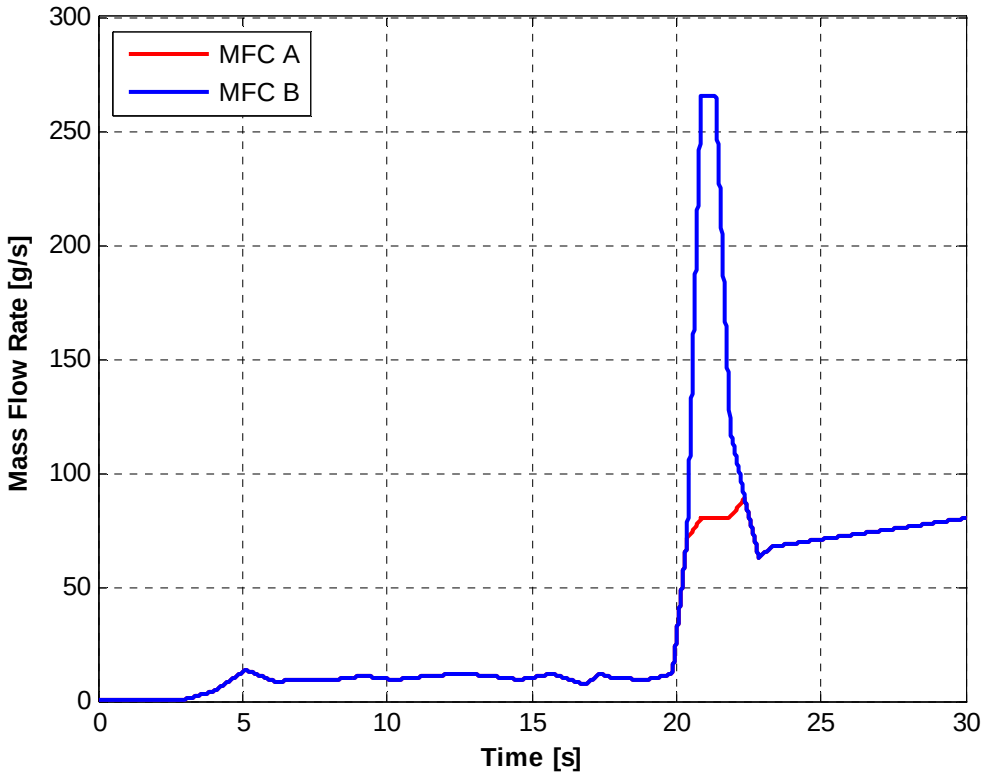

Figure 3.12: Heliox System Model Inputs

The results of the system model are shown in Figure 3.13.

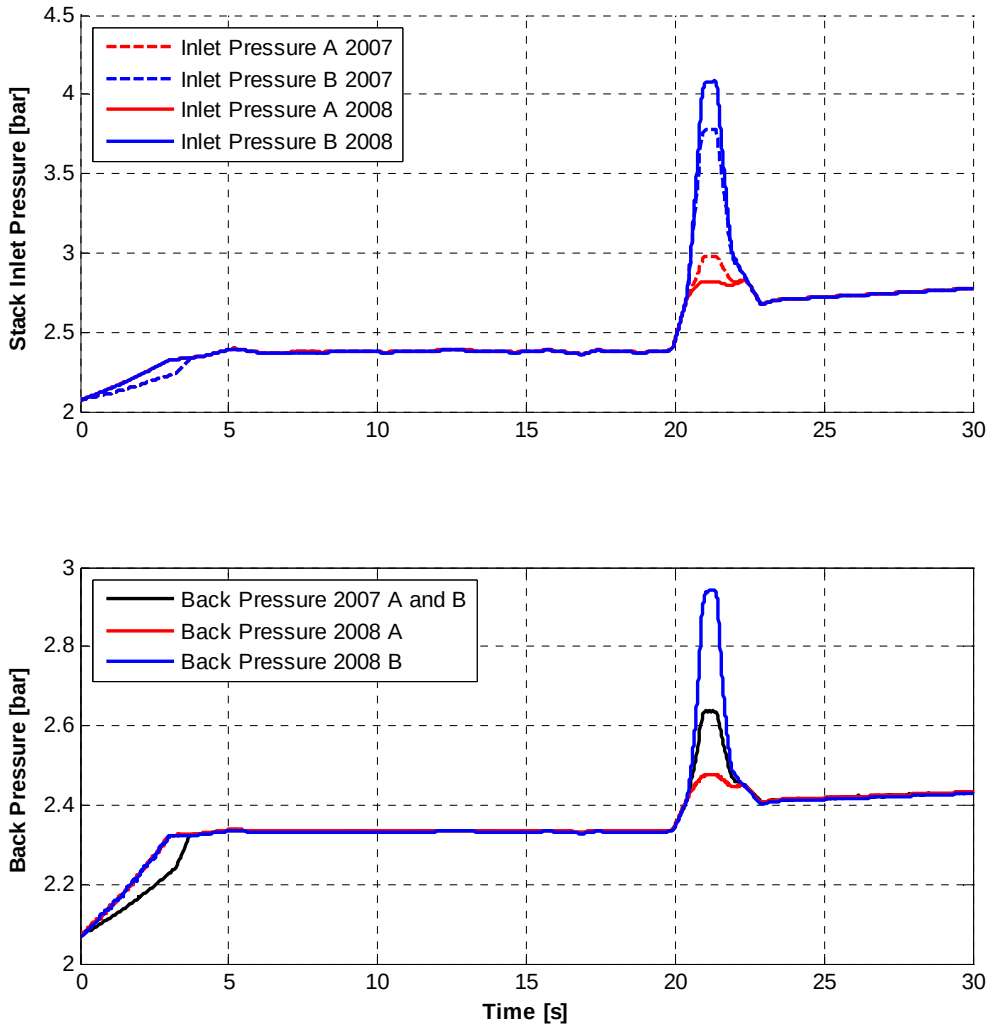

Figure 3.13: Heliox System Model Results (2007 and 2008 Comparison)

The model accurately predicts that a pressure spike in the cathode does occur in module B if the mass flow rate through MFC B does increase to 261 [g/s]. From Figure 3.13 it is obvious that the 2007 system would result in a lower pressure spike with the same mass flow input and the same stack pressure settings.

Initially it was theorized that the decrease in exhaust volume between 2007 and 2008 was the main contributing factor that lead to the overpressure events. The idea being that a larger exhaust size gave the system a larger capacitance and the short duration increase in the

mass flow rate would not significantly increase the back pressure. However, increasing the volume in the 2008 model showed very little difference in output pressure.

It is more likely that the effect of having the excess flow regulated by two back pressure valves in the 2007 system as opposed to the individual valves in the 2008 system was the cause of pressure spike. Again, in the 2007 system the exhaust exited both fuel cell modules and entered a common exhaust tube. Two back pressure valves were placed downstream of this common exhaust. In the 2008 system the module exhausted through individual back pressure valves. The back pressure was intended to be equalized using a 12.7 [mm] (0.5 [in]) cross over tube between the two exhaust tubes. The Simulink model shows that the 12.7 [mm] cross over tube does not adequately equalize pressure between the two modules. Therefore, the increased mass flow through FCM B is not completely shared with the BPV for FCM A. The mass flow rates through each BPV and the cross over tube are shown in Figure 3.14.

Increasing the size of the cross over tube aids in increasing the cross over flow rate and subsequently equalizing the pressure between module A and B. Figure 3.15 shows resistance values for various sized cross over tubes. Increasing the cross over tube diameter to 50.8 [mm] (2.0 [in]) effectively equalizes pressure between module A and B. The pressure varies by less than 1% between the two exhaust pressures with a 50.8 [mm] cross over tube. This means that the model solution for the 2008 system with a 50.8 [mm] cross over tube approaches 2007 model results. Figure 3.16 shows a comparison between the 2007 system and the 2008 system with a 50.8 [mm] cross over tube.

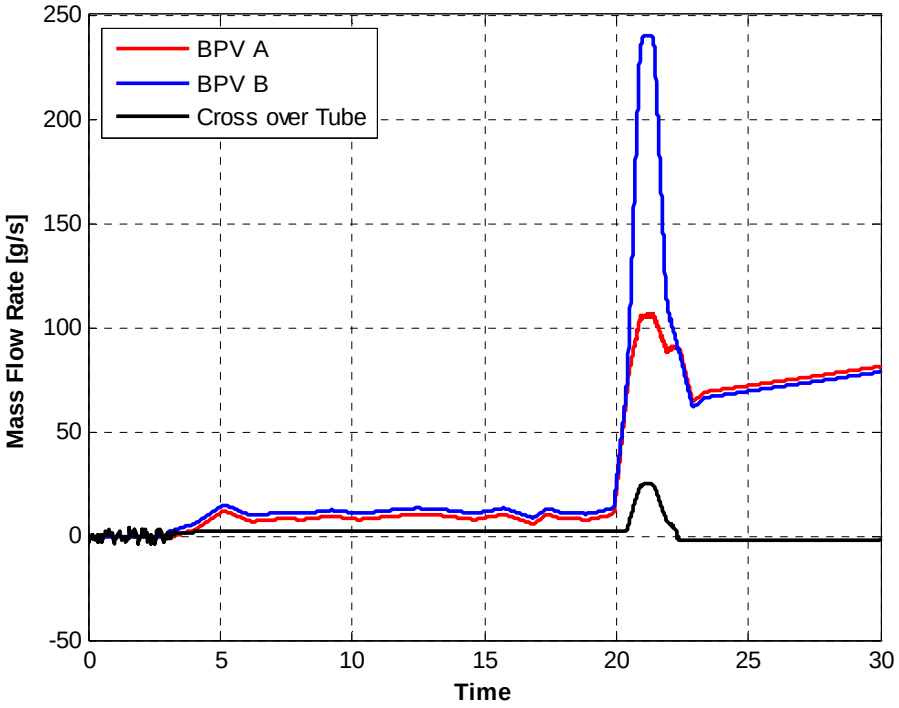

Figure 3.14: Heliox Mass Flow Rates Through BPVs and Cross over Tube

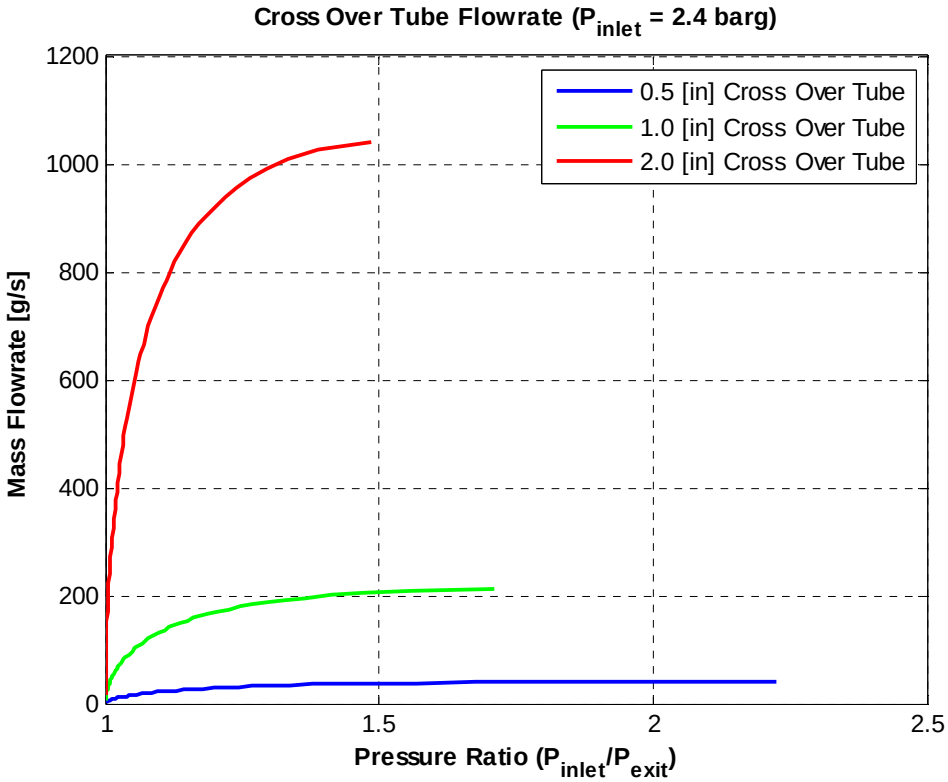

Figure 3.15: Cross Over Tube Flow Rate with Varying Diameter

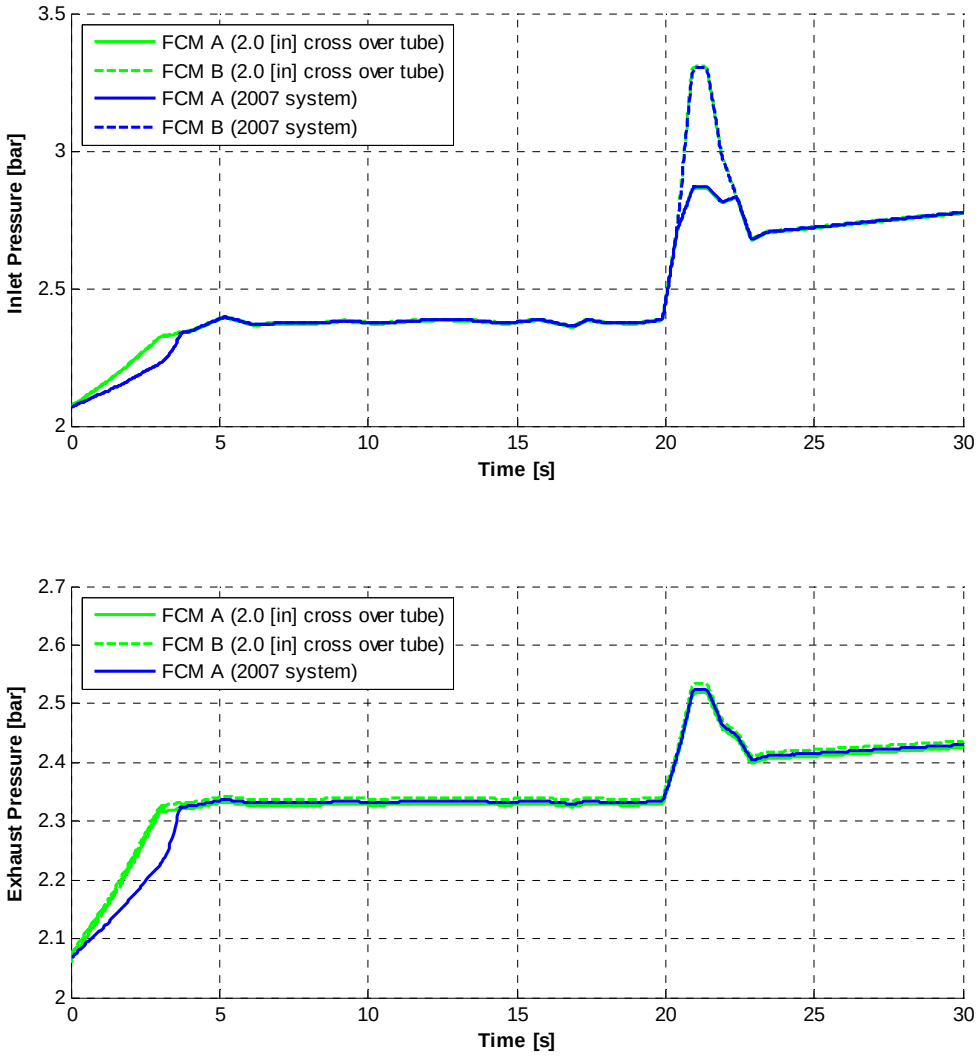

Figure 3.16: 2007 Heliox System and 2008 Heliox System with 50.8 [mm] Cross Over Tube Simulation Results Comparison

These results indicate that the 2008 exhaust setup with a 50.8 [mm] cross over tube does have comparable performance to the 2007 system. However, the model still indicates a pressure spike above 3.1 [bar] which is the rated burst pressure of the stacks. These results are obtained considering an operating inlet cathode pressure of 2.4 [bar] which reflects the 2008 pressure settings. The overall stack pressure could be reduced to account for this potential overshoots in the mass flow rate. However, this would decrease the fuel cell's

potential power output. Therefore, it is desirable to keep the stack pressures at the current level and formulate a system to either eliminate the mass flow rate overshoots or to mitigate pressure spikes associated with such mass flow rate increases. This topic will be discussed further in Chapter 5.

Chapter Summary

The BB2 team was able to accomplish great result during the 2007 racing season. However, vehicle shutdowns due to low cell voltages and hydrogen leaks prevented the vehicle from performing at its best. To combat the low cell voltages, the hydrogen injector assembly was modified to accommodate the increase hydrogen flow rate needed for the higher power levels that the BB2 operates at. The hydrogen leaks were addressed by simplifying the hydrogen delivery system and improving the leak checking procedure.

During the 2008 season two overpressure events damaged the fuel cell stack used for the BB2. System modeling and analysis reveal that the cause of the pressure event was a malfunction in one of the heliox mass flow controllers. Although the same MFCs were used during the 2007 no overpressure events were observed during the 2007 season. Changes in the exhaust system and overall higher operating pressures were determined to be the reason for these events during the 2008 season. Further system modifications will need to be done to ensure these failure do not happen again.

Chapter 4 :

Performance Results

The main focus of this research is to improve the reliability and performance of the Ballard power plant used in the BB2. Large amounts of data are recorded during each run and test session. Being able to identify factors that characterize a good run and a bad run are essential. From a passenger car perspective, there are many considerations when judging the performance of a fuel cell system. Such systems are designed to balance power output, efficiency, cost, durability, longevity, safety and reliability. For the BB2 fuel cell system, safety, of course, remains the principle criteria when analyzing post run results. The second important criteria would be the power output. Modeling of the stack is important for gauging the effect of changes on overall stack performance.

The stack model developed in this thesis is used in the overall vehicle simulator as well as in the vehicle control code. This model helps to determine the theoretical top speed of the vehicle. It can also be used to determine the amount of ice necessary to cool the vehicle during a run. Additionally the vehicle gear ratios are determined by using the simulator.

4.1 Fuel Cell Model

There are many models that have been developed in the literature for fuel cells. These models vary greatly in their complexity and modeling approach. The type of model and complexity level needs to match the function, resources and desired data for the specific

project. For the BB2 the model and polarization curves are used for determining performance and power output. Also the polarization curves are used in overall vehicle modeling which is used to determine the top speed of the vehicle, cooling strategy and gear ratios. Also the polarization curve is used in the control for determine the current request. The model is not used for prediction of fuel cell stack performance outside of the testing conditions. This reduces the required complexity of the model. Many of the required specifications for complex mechanistic models are not know to the BB2 team. Therefore, an empirical model will be adopted for the use of the BB2 project.

4.1.1 Fuel Cell Model Definition

Hydrogen fuel cells combine hydrogen and oxygen to form water. The overall reaction that takes place in a fuel cell is described by the following equation:

$$H_2 + \frac{1}{2}O_2 \rightarrow H_2O$$

Based on this equation and thermodynamic principles, the ideal cell voltage can be characterized by the Nerst Equation which is as follows [9]:

$$E = E^o - \frac{RT}{2F}\ln\left(P^*_{H_2}\left(P^*_{O_2}\right)^{0.5}\right)$$

Where:

E = thermodynamic equilibrium potential [V]
E^o = reference potential [V]
R = gas constant (8.3143 [J/(mol*K)])
T = temperature [K]
F = Faraday's constant (96485 [C/mol])
P_{H2}* = partial pressure of hydrogen [atm]
P_{O2}* = partial pressure of oxygen [atm]

This equation reduces to [15]:

$$E = 1.229 - 8.5 * 10^{-3} * (T - 298.15) + (4.3085 * 10^{-5})(T)\left[\ln\left(P^*_{H_2}\right) + 0.5\ln\left(P^*_{O_2}\right)\right]$$

This potential represents the ideal cell voltage under no load. The actual cell voltage is the sum of the ideal voltage and the sum of the losses. The three primary losses for a fuel cell are the activation, ohmic and concentration losses.

Activation losses are a result of the voltage lost in driving the chemical reaction that transfers the electrons to or from the electrode [9]. For the BB2, there are several ways to decrease the activation losses. Raising the cell temperature increases the rate of reaction at the anode and cathode and thus decreases the activation losses. Increasing the reactant concentrations decreases the activation losses by more efficiently occupying catalyst sites. Increasing the concentration of reactants can be achieved either by increasing the mole fraction of the reactant within the mixture (not applicable for the anode because the hydrogen concentration is already 100%) or by increasing the pressure. Additionally MEA designers can decrease activation losses by using more effective catalysts and increasing the roughness of the electrodes which increases the surface area and subsequently increases catalyst reaction sites [9].

Ohmic losses are caused by the internal resistance of the stack materials to the flow of electrons. These losses are the same as any electrical resistive losses in electrical systems. These losses can be minimized by using electrodes and other conductive components with the high conductivity and making the electrolyte as thin as possible [9].

Concentration losses or sometimes referred to as mass transport losses are the result of the change in concentration of the reactants at the surface of the electrodes as the fuel is used [16]. These losses can be minimized by increasing pressure and reactant concentration.

Figure 4.1 depicts the typical polarization curve for a PEM fuel cell. From the figure, it can be seen that activation losses dominate the behavior of the polarization curve under low current draw. The ohmic losses then determine the behavior in the middle portion. Concentration losses dominate the very high current draw.

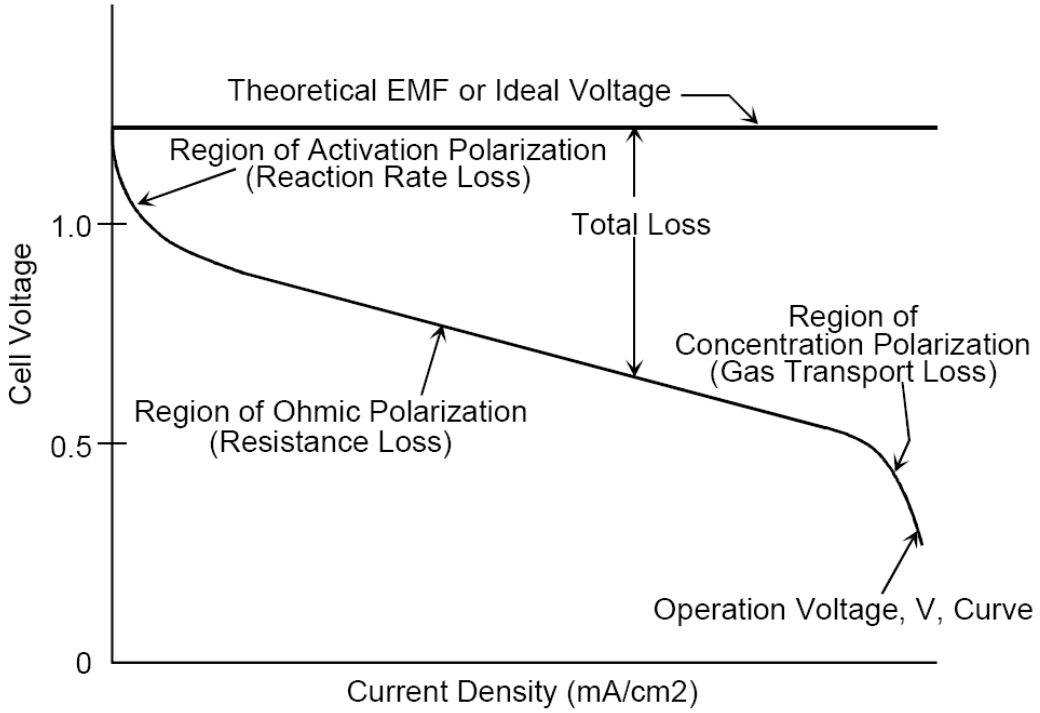

Figure 4.1: Generic Polarization Curve for a PEM Fuel Cell [17]

From experimental data the BB2 does not appear to enter this region where concentration losses dominate. Therefore the modeling of the stack will ignore these losses. In doing so the trends and power curves obtained from the experimental data will accurately capture the performance of the modeling within the experimentally tested ranges. However, the acquired data will not accurately predict fuel cell performance above these values.

The total fuel cell voltage can be characterized by the sum of the ideal open circuit voltage with the activation and ohmic losses [15]:

$$V = E + \eta_{act\ total} + \eta_{ohmic}$$

Where:

V = cell voltage [V]
E = thermodynamic potential as described by the Nerst Equation [V]
$\eta_{act\ total}$ = total activation losses [V]
$\eta_{act\ total}$ = total ohmic losses [V]

The total activation losses are a sum of the activation losses at the cathode and anode:

$$\eta_{act\ total} = \eta_{act\ anodic} + \eta_{act\ cathodic}$$

Again, the individual parameters for the stack to mechanically determine the anode and cathode activation losses independently are not know. Therefore, the anodic and cathodic activation losses will be lumped together in one expression. The value for the total activation losses can be determined empirically from the following formula [15]:

$$\eta_{act\ total} = \xi_1 + \xi_2 + \xi_3\left[\ln\left(c_{O_2}^*\right)\right] + \xi_4 T[\ln(i)]$$

Where:

ξ_1, ξ_2,ξ_3, ξ_4 = parametric coefficients
T = temperature [K]
c_{O2}*=concentration of oxygen [mol/cm^3]
i = Current [A]

The oxygen concentration on the cathode is dependent on the partial pressure of the oxygen and the temperature. It can be determined by the following equation[15]:

$$c_{O_2}^{interface} = \frac{P_{O_2}^{interface}}{5.08 * 10^6 \exp\left(-\frac{498}{T}\right)}$$

Where P_{O2} is that partial pressure of oxygen. The temperature and pressures used to develop this model will be taken at the average across the stack. This simplification is adequate for the purposes of this empirical model.

The ohmic losses are a function of the internal resistance, $R^{internal}$, of the stack and the current draw. The ohmic losses can be determined by the following equation:

$$\eta_{ohmic} = -iR^{internal}$$

Where the internal resistance, $R^{internal}$, is determined by the following parametric equation[15]:

$$R^{internal} = \xi_5 + \xi_6 T + \xi_7 i$$

4.1.2 Parameter Effect on Fuel Cell Stack Voltage

The sample data for the empirical analysis comes from both testing on the load bank and from data recorded during Bonneville runs. Figure 4.2 and 4.3 shows experimental data collected from these events. Figures 4.2 shows the effect of increasing average stack temperature on the fuel cell performance. It can be seen from Figure 4.2 that increasing the temperature increases the voltage of the stack for a given current draw. Again, this is because increasing the temperature increases the rate of reaction and decreases the activation losses [9].

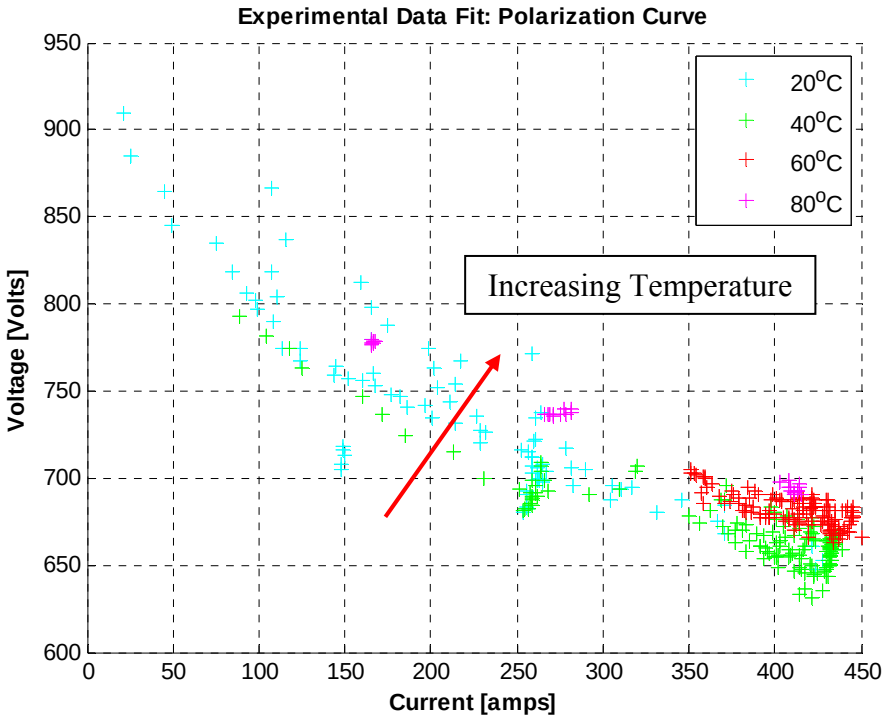

Figure 4.2: Effect of Temperature on Polarization Curve

Figure 4.3 shows that effect of increasing the overall stack pressure on fuel cell performance. The pressure here is the average cathode pressure. The anode pressure is reference from the cathode pressure and thus increasing the cathode pressure results in an increase in anode pressure. Increasing the pressure in both the anode and cathode increases

the concentration of reactants and increases the catalyst site utilization. This increases the overall stack voltage.

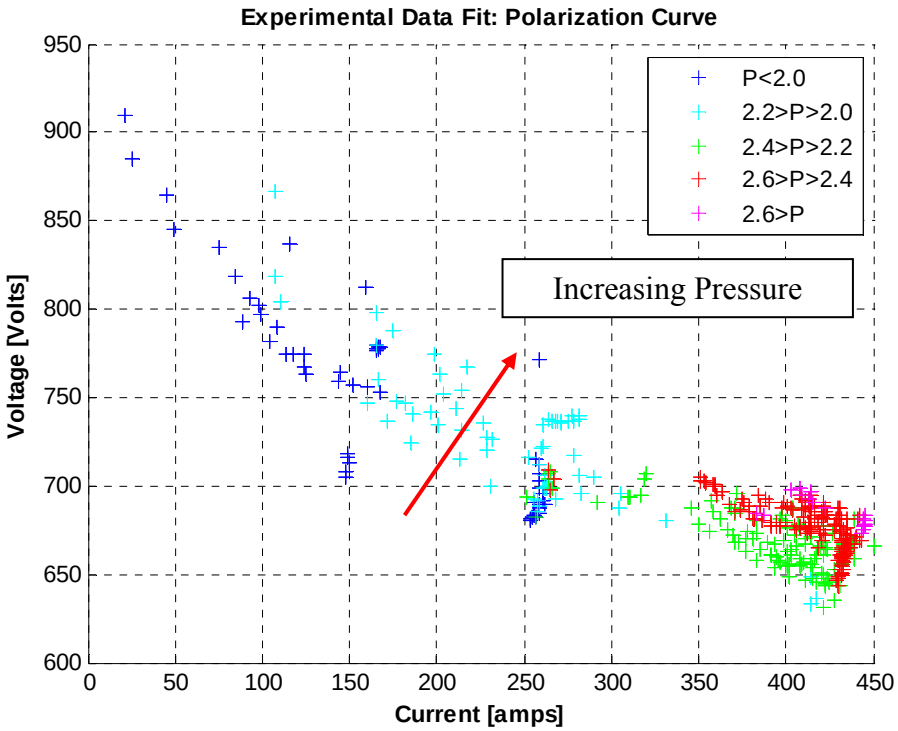

Figure 4.3: Effect of Pressure on Polarization Curve

One of the major advantages that the BB2 has over other fuel cell vehicles is that the BB2 carries its own oxidant on board. This allows that BB2 to run on higher concentrations of oxygen than the surrounding air. Figure 4.4 shows the effect of increasing the oxygen concentration. This data was obtained from short stack testing performed at Ballard. Regular air, heliox and pure oxygen were used for the test. The test clearly indicates that pure oxygen has the highest voltage for a given current draw. However, pure oxygen is very dangerous. At high pressure even stainless steel is flammable in the presence of pure oxygen. Therefore, the BB2 uses a safer concentration of 40% oxygen to 60% helium.

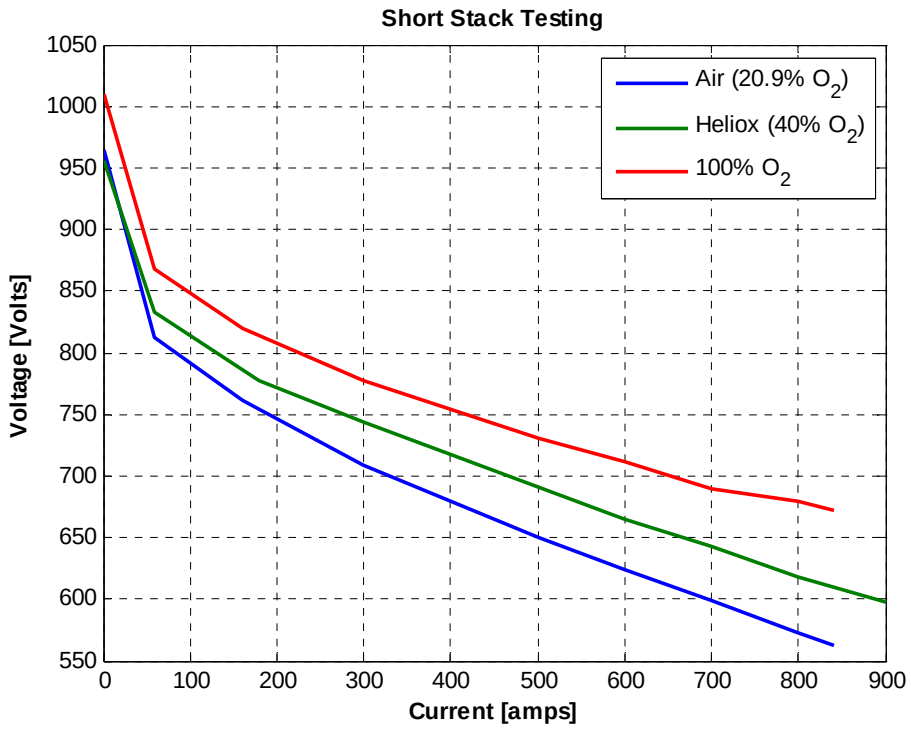

Figure 4.4: Oxygen Concentration Effect on Stack Performance

4.1.3 Model Results

The empirical equations described in section 4.1.1 were solved using the least squares linear regression method. The values obtained for $\xi_{1\text{-}7}$ are shown in Table 4.1 and 4.2.

$\xi 1$	0.8097
$\xi 2$	$-6.473*10^{-3}$
$\xi 3$	$-3.076*10^{-4}$
$\xi 4$	$1.533*10^{-4}$

Table 4.1: Activation Losses Empirical Constants

$\xi 5$	$9.190*10^{-4}$
$\xi 6$	$-1.985*10^{-6}$
$\xi 7$	$1.003*10^{-7}$

Table 4.2: Ohmic Losses Empirical Constants

The breakdown of the activation and ohmic loss components of the total voltage reduction are shown graphically in Figure 4.5. The model clearly shows that the activation

losses build quickly at low current values and then remain mostly constant at mid to high current levels. The ohmic losses build steadily throughout the current range.

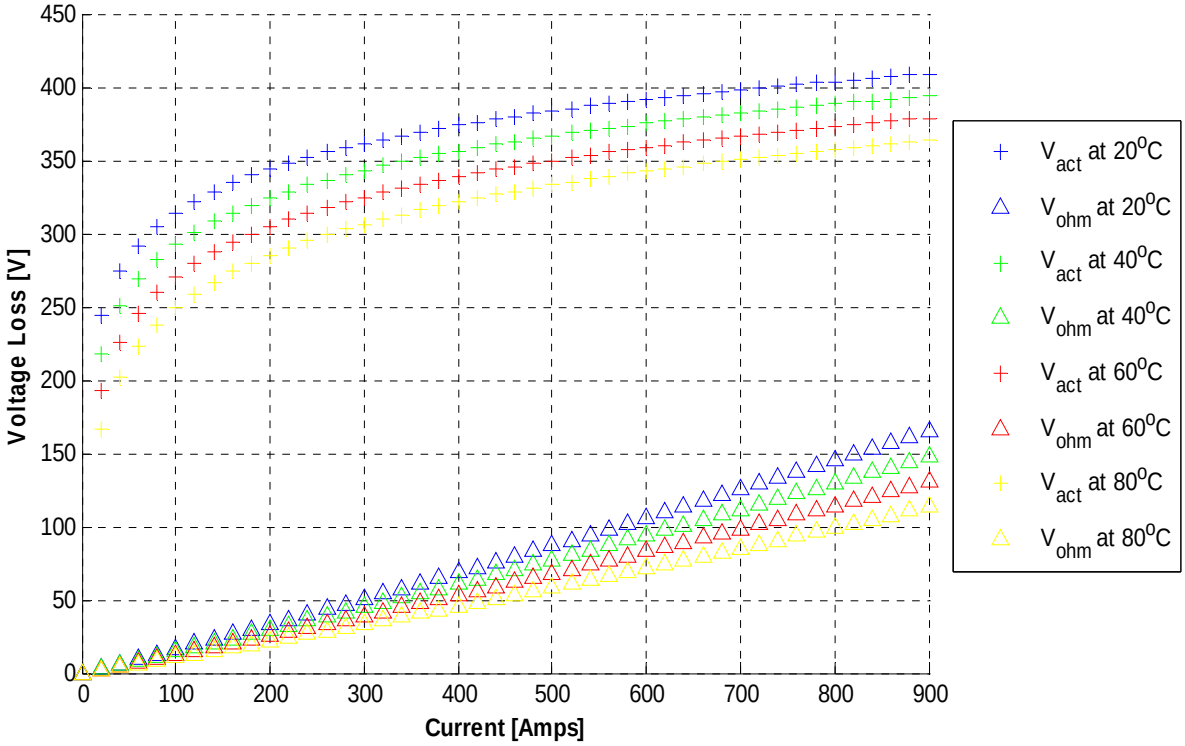

Figure 4.5: Activation and Ohmic Losses

The resulting polarization curve from the model is displayed in Figure 4.6. The power generated by the fuel cells is given in Figure 4.7. Each figure gives the model voltage for a given current as a function of temperature. The temperature of the fuel cell stack varies throughout the run. The stacks start out at 20°C at the beginning of the run. The stack then heats up as the run progresses. The stacks are actively cooled to maintain 80°C as the maximum operating temperature. From Figure 4.7, the model indicates that at 80°C the maximum power output of the stack is close to 600 [kW]. This matches the maximum power observed during load cell testing.

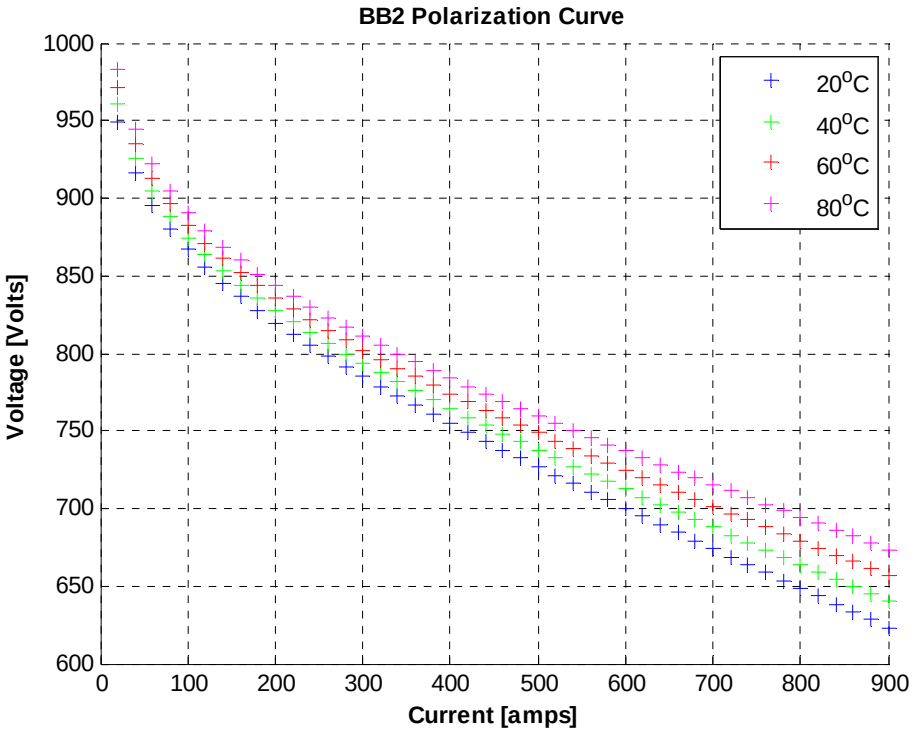

Figure 4.6: BB2 Polarization Curve at 2.5 [barg] Stack Pressure

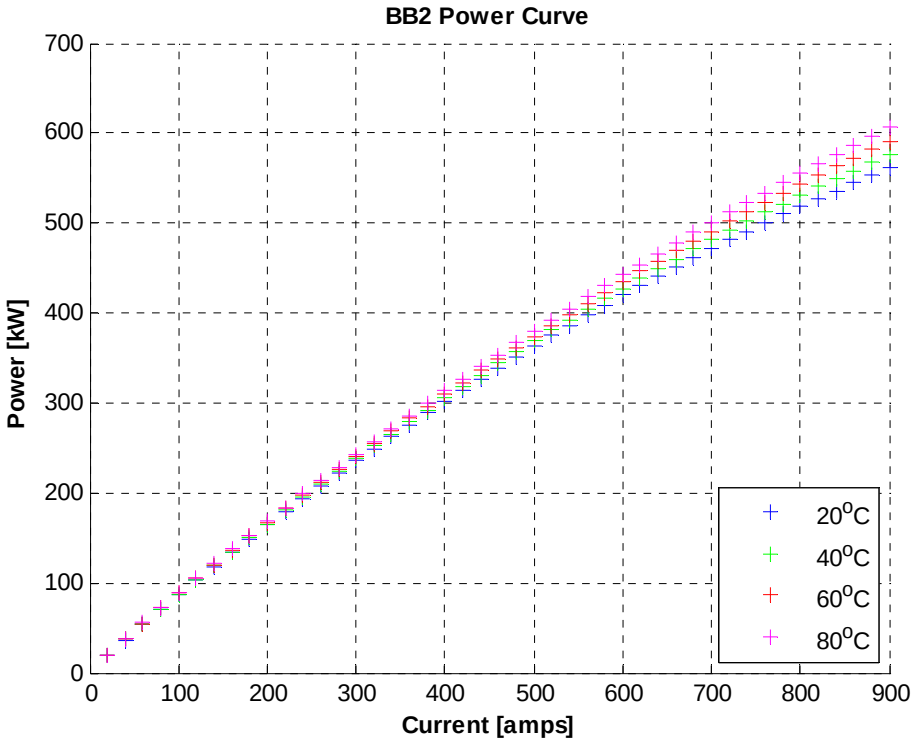

Figure 4.7: BB2 Power Curve at 2.5 [barg] Stack Pressure

The main focus of the testing during the 2008 season was to increase the fuel cell reliablility. This was certainly accomplished. During Speedweek 2008 there were no fuel cell system related vehicle shutdowns the first four days of racing. In addition to improved reliability the team was able to improve the performance and maximum power output of the Ballard P5 FCMs. Figure 4.8 shows a comparison of the theoretical polarization curve for the 2007 and 2008 racing season. Figure 4.9 shows a comparison of the corresponding power curve for the 2007 and 2008 season. For these figures the 2008 data was obtained from the model previously discussed. The 2007 curves were obtained from empirical values determined in [6]. Both were calculated using a stack pressure of 2.5 bar at 80°C. The improvement in the overall stack performance can be attributed to several changes. The most significant change would be in the increased hydrogen flow rate at high current.

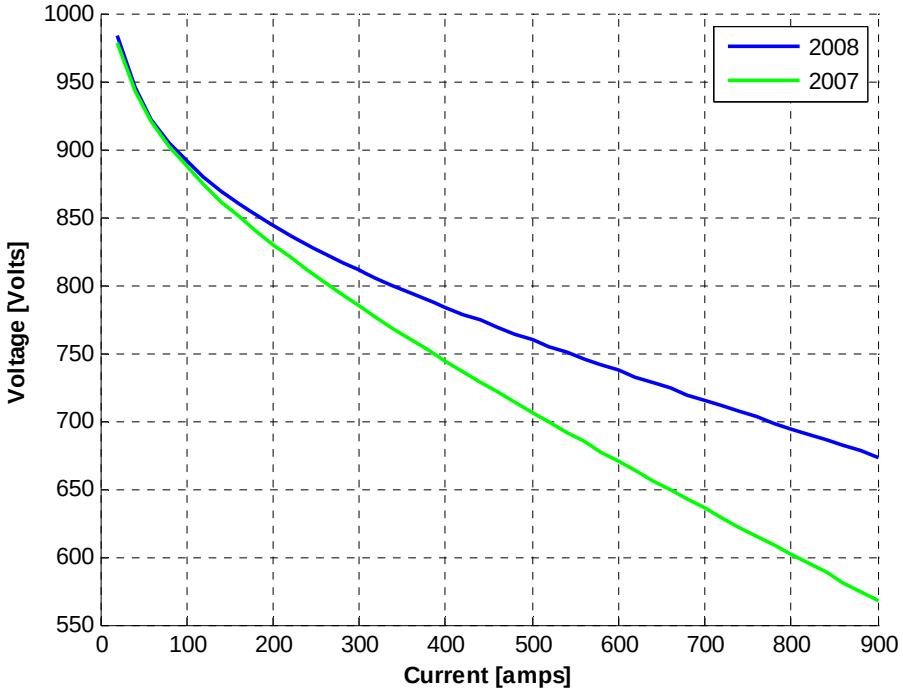

Figure 4.8: BB2 2007 vs. 2008 Polarization Curve Comparison

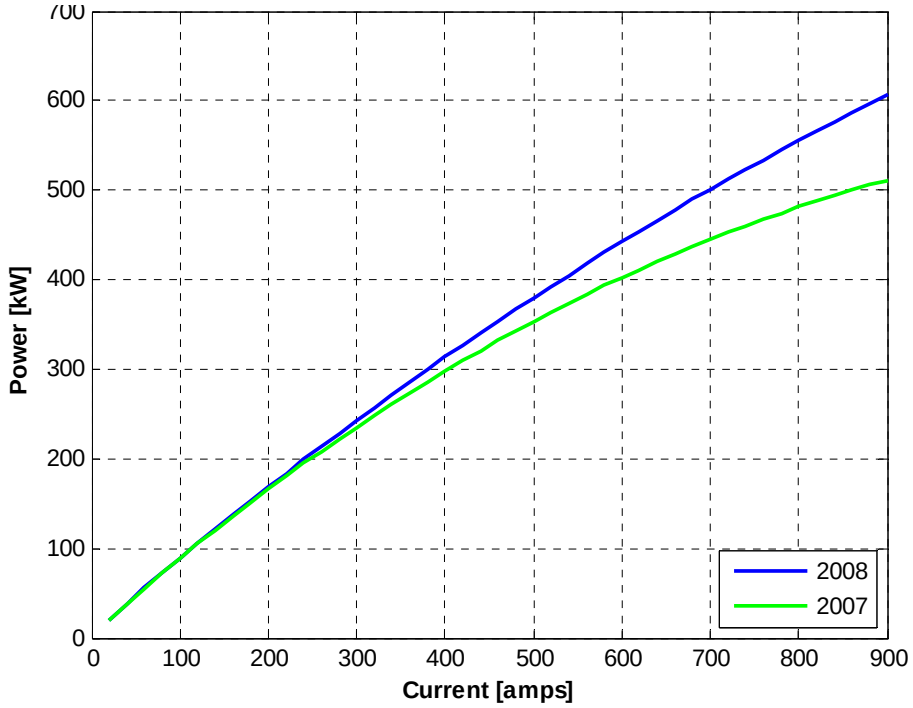

Figure 4.9: BB2 2007 vs. 2008 Power Curve Comparison

4.2 Fuel Cell Model Application

The fuel cell model developed in this thesis is used for several reasons. The empirical constants that are determined for the fuel cell performance can be input into the total vehicle model for use to determine the vehicle's theoretical top speed. For more information able the BB2's total vehicle model and its development refer to [6].

The theoretical polarization curve is also utilized by the vehicle's control code. The Motohawk controller receives input from the driver and requests a certain current level from the Ballard controller. The Ballard controller uses the current request to determine the mass flow rate of the heliox and other system parameters. The throttle input of the driver corresponds to the percent of maximum power based on the motor's power/speed curve. This desired power is then converter to a current request using the theoretical polarization curve. Figure 4.10 shows the current request algorithm for the Buckeye Bullet 2.

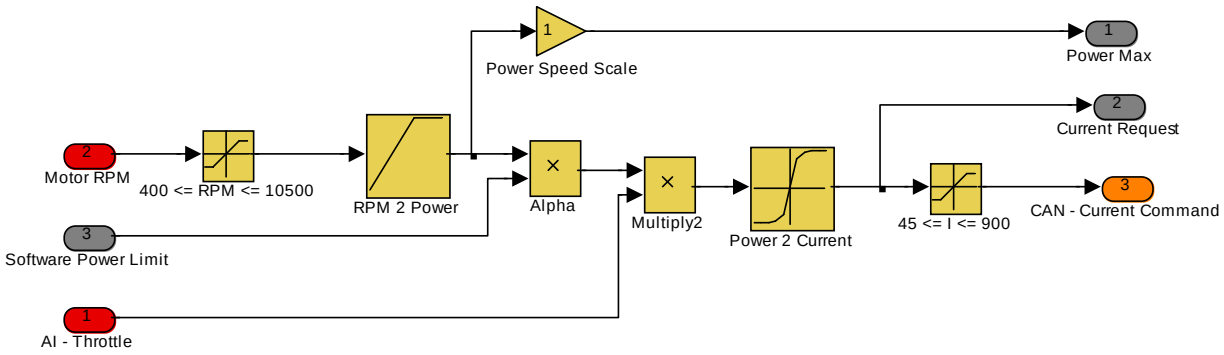

Figure 4.10: BB2 Current Request Algorithm

4.3 2008 Season Results

2008 was the second racing season for the Buckeye Bullet 2. The 2007 season proved to be a great learning experience for the team. Setting a world record in the first year and achieving the fastest recorded speed for a hydrogen fuel cell powered vehicle are great accomplishments. However, there were many issues with the vehicle that needed to be address before the 2008 season if the team hoped to reach its goals of 300 mph. The BB2 raced twice during 2008; once in August during Speedweek and once in September during a private FIA meet.

4.3.1 Speed Week 2008

The Buckeye Bullet 2's first race event in 2008 was Speedweek. The main goal for this meet was to prove the reliability of the fuel cell system. Before the first run several spin tests were performed in the pit area to ensure that all systems were functioning properly on the salt. The first run on the salt for that season occurred on August 19. This first run resulted in a blistering 338 [km/h] (210 [mph]) speed recorded by the SCTA. This was a great way to start of the week. However, during this run the vehicle was not shutdown by the driver. The vehicle shutdown due to faulty emergency power off (EPO) switch. The EPO switch is an electrical switch at the rear of the vehicle that allows a team member or safety personal to cut power to the vehicle in the event of an emergency. The switch disconnects power from the batteries to the fuel cell systems. This effectively closes the tank solenoids and stops the fuel cells.

Several more run attempts were made with the faulty EPO switch before the failure was properly identified. The EPO switch is required by SCTA rules; therefore, an improvised replacement EPO switch was installed. On the morning of August 21, the following run with the properly working EPO switch resulted in the vehicle reaching 360

[km/h] (224 [mph]) recorded by the SCTA. This run was ended by a premature deployment of the vehicle's parachutes. For ease of operation all driver controls are placed on the steering wheel. This allows the driver to keep his hands on the wheel at all times. However, during the run the driver inadvertently pushed the parachute release button rather than the upshift button.

The course was shut down due to high winds so the next run was not until August 22. The following run was the fastest run for the BB2 ever recorded. The top speed measured by the SCTA was 461.024 [km/h] (286.467 [mph]) at the exit of the 5th mile. The top speed measured by the vehicles onboard GPS system after the final timed mile was 478 [km/h] (297 [mph]). The fuel cell produced 560 kW during the run. All of the vehicle systems worked flawlessly. The vehicle's power was limited to 560 kW during the run by the inverter settings. Until this time the inverter had not been the limiting factor. The fuel cells had successfully reached over 600 kW of power during testing, therefore, it was known that the car had more to give. Now with the fuel cell systems and other vehicle systems working perfectly it was necessary to increase the inverter limits to increase the power draw from the fuel cell modules.

The inverter settings were increased from 80% torque limit to 90% torque limit. The subsequent run resulted in a vehicle shutdown due to an inverter fault. The following two runs the inverter was limited back to 85% and 83% respectively. Both runs resulted in inverter faults and shutdowns. It should be noted that throughout the week up to this point there were no fuel cell related shutdowns. The reliability and performance of the fuel cell systems had been verified. At this point the fuel cell system was no longer the limiting factor in the power production.

On second run on August 23 a low humidification pump pressure caused a fuel cell system shutdown. The third and final run on August 23 resulted in an overpressure event that

caused a leak in stack B. The failure was caused by a malfunction in MFC B that resulted in a large overshoot in mass flow rate that lead to a pressure spike. Detailed analysis of this event is discussed in chapter 3. This event ended Speedweek for BB2 team as a stack leak is not field serviceable. A summary of the runs completed during Speedweek 2008 is shown in Table 4.3. It should be noted that the peak speed presented in this table is recorded from the vehicle's GPS data and may not match the peak speed as recorded by the SCTA.

Run No.	Date	Peak Speed	Peak Power	Run end condition
1	August 19	360 km/h	553 kW	Shutdown due to faulty EPO switch
2	August 20	63 km/h	178 kW	Shutdown due to faulty EPO switch
3	August 21	365 km/h	550 kW	Early parachute deployment
4	August 22	478 km/h	560 kW	No faults
5	August 22	375 km/h	590 kW	Shutdown from inverter over-current
6	August 22	455 km/h	589 kW	Shutdown from inverter over-current
7	August 23	460 km/h	588 kW	Shutdown from inverter over-current

Table 4.3: Run Summary for 2008 Racing Season [7]

4.3.2 FIA Meet 2008

The stack leak that occurred in August could only be repaired at the Ballard facilities in Vancouver. The FIA meet began on September 22, 2008. This meant that FCM B had to be shipped to Vancouver, serviced, shipped back to Ohio and installed into the vehicle in less than one month. The task was completed with the diligence and dedication of BB2 team members and Ballard personnel. However, the absence of the FCM made testing the fuel cell system, inverter and motor almost impossible in-between the two racing events. Therefore, after the fuel cell system was repaired an installed into the vehicle it was shipped to the salt flats without testing.

Upon arrival to the salt flats during the FIA meet in 2008 it was discovered that the vehicle had a very serious failure. The custom made motor had an internal short between the rotor and stator that made the motor unusable. Disassembly of the motor at a shop in Utah revealed that the carbon fiber windings that surround part of the rotor had frayed and shorted

against the stator. Later investigation implies that this failure was caused by the motor spinning over speed during shifts. Figure 4.11 shows a plot of motor rpm during one of the runs during Speedweek 2008.

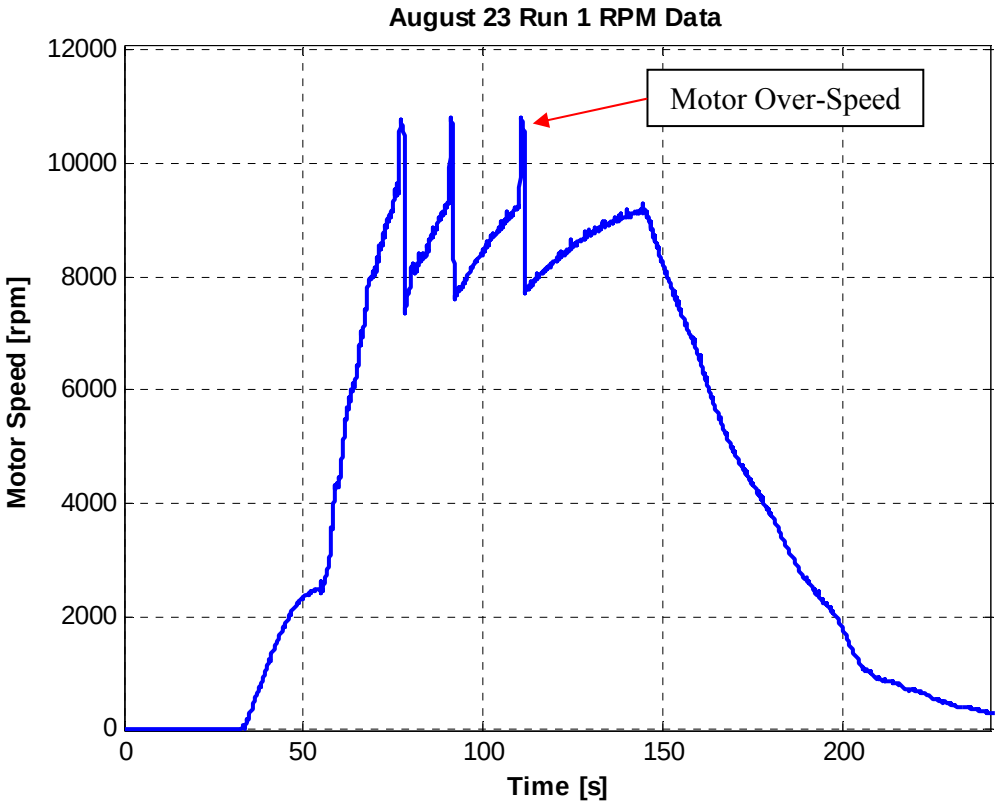

Figure 4.11: Motor Speed

The motor was rebuilt in Utah within less than a week and returned to the team on the morning of September 26 for the final day of the FIA racing event. This gave the BB2 team far less time than they had originally anticipated for tuning the vehicle and making test runs. The FIA track is longer than the SCTA sanction track. The speed recorded by the FIA is taken a mile later which means that the BB2 needed to run for 6 miles under power rather than the normal 5. This requires a change to the control code to reduce the stoichiometric ratio on the cathode to conserve heliox and ensure that the vehicle is able to complete 6 miles under power. It was anticipated that the team would have a full week on the track to test the

necessary changes and make adjustments. However, with the motor failure an entire week of testing and racing had to be compressed into one day of racing.

The team was able to complete 4 runs on August 26th. The first run on the 26th was aborted due to a control code issue that resulted in a failure to properly open the hydrogen tank solenoid. The hydrogen tank contains a safety system that will not permit high flow if the pressure difference inside the tank and the connecting line is too great. This ensures that if a significant leak occurs that hydrogen tank will restrict large flow rates. This means that the control code must pressurize the hydrogen line before significant hydrogen flow rates. A coding error caused prevented the line from properly pressurizing at the start and thus the tank solenoids did not fully open.

After fixing the coding issue, the next two runs were aborted due to individual low cell voltages. The exact cause of these low cells is not certain at this time. However, there are several possible answers. During these runs the purge solenoid is commanded to say open. This can happen for several reasons. The purge solenoid can be held open if the hydrogen pressure is too high or if the stack has some low cell. The solenoid opens for low cells in an effort to purge contaminants out of the anode and increase the hydrogen concentration. However, for the BB2 low cells are usually not caused by anode contaminants because the runs last for such a short time that there is not much time for contaminants to leak over from the cathode. For the BB2, most low cells are caused by low hydrogen pressure on the anode. Therefore opening purge makes this problem worst. The other scenario is that the purge is held open to reduce hydrogen pressure on the stack because the pressure is too high.

The final run on August 26th resulted in another overpressure event. MFC B malfunctioned and overshot the mass flow command resulting in a pressure spike on the cathode. Because the anode pressure references the cathode, the pressure on the anode

increased as well. The high pressure on the anode and cathode blew one of the stack seals on module B. The escaping heliox and hydrogen ignited and caused minor damage to the vehicle's body panels and fuel cell module panels. All other major vehicle systems and the driver were unharmed.

The fuel cell system that proved to be almost bullet proof during Speedweek showed that it clearly still has room for improvement.

Chapter Summary

This chapter describes the approach used for modeling the BB2 fuel cell stack. The fuel cell voltage at any current draw is determined to be the sum of the ideal stack voltage and the activation and ohmic losses. Empirical methods were used to determine the voltage losses and how they are affected by temperature, pressure, current draw, and reactant concentration.

Changes made to the vehicle during the 2008 season drastically improved the fuel cell system reliability. This allowed the team to achieve a top recorded speed of 461.024 [km/h] (286.467 [mph]) during Speedweek 2008. However, failures occurring both during Speedweek and the private FIA week show the need for further improvement.

Chapter 5 :

Conclusion and Future Work

This chapter provides a summary and conclusion of the work presented in this thesis. It also outlines future work to be done on the vehicle and the fuel cell systems. The majority of the future work centers around addressing the overpressure events that occurred in 2008 and redesigning the system to eliminate this failure. This section also proposes several other changes to the vehicle such as removing the fuel cell humidification system and making a new motor.

5.1 Conclusion of Work

In two short years the Buckeye Bullet 2 has become the fastest hydrogen fuel cell powered vehicle. This is an incredible feat considering that the students working on the project only do so part time and attend a full course load of classes through much of the year. Although the team receives support from industry supports, the students on the team still remain the ultimate facilitators of the project.

Tremendous progress has been made with the vehicle between 2007 and 2008. In the 2007 season the vehicle had many issues that caused it to shut down. The primary issue was hydrogen starvation at the stack. This problem was addressed by modifying the hydrogen supply system to the stack to allow for high flow. The hydrogen injectors nozzles were increased in size to accommodate 500 [amps] per module.

Another major area of improvement over the 2008 season was with vehicle weight reduction. The majority of weight was removed from the gas delivery system, cooling

system and fuel cell modules. The total weight reduction reduced the vehicle weight by roughly 8%.

The 2008 season saw a great improvement for the BB2. The fuel cell system performed very reliably during Speedweek 2008. An unfortunate motor failure and a shortened timeline for racing resulted in a disappointing FIA meet in 2008. Both events ended with an overpressure event that damaged FCM B.

The cause of this overpressure event has been identified as a malfunction of the mass flow controller for module B. Changes to the exhaust system and an overall higher stack pressure between 2007 and 2008 increased the system sensitivity to increased mass flow rate inputs. However, the following section will outline future plans to mitigate these failures.

5.2 Future Work

Although the Buckeye Bullet has come a long way in development since the project was first start in 2004, there are still areas of the vehicle design that need to be addressed. The heliox system needs to be revised to eliminate the possibility of pressure spikes that can damage the stack seals. Additionally there may be potential for further weight reduction by removal of the humidification system. Also, development of a new or modified motor might improve power delivery to the driveline.

5.2.1 Possible Heliox System Revisions

It is evident from the model results shown in Chapter 3 that if a significantly higher than designed mass flow rate of heliox enters the stack that a dangerous pressure increase can occur. There are two main avenues to address this issue. One would be to allow the system to release this pressure to eliminate the possibility of damage to the stack. The other possibility would be to eliminate that possibility of having such a high mass flow rate.

The first methodology would require the least amount of modification to the current system. This would entail installing some kind of pressure relief device on the heliox inlet of the stack to release pressure in the case of a pressure surge. The current heliox system model can be used to accurately assess the performance of such a system and determine the necessary flow capacity and pressure setting of the pressure relief device. Figure 5.1 shows one possible heliox system with a PRV at the inlet.

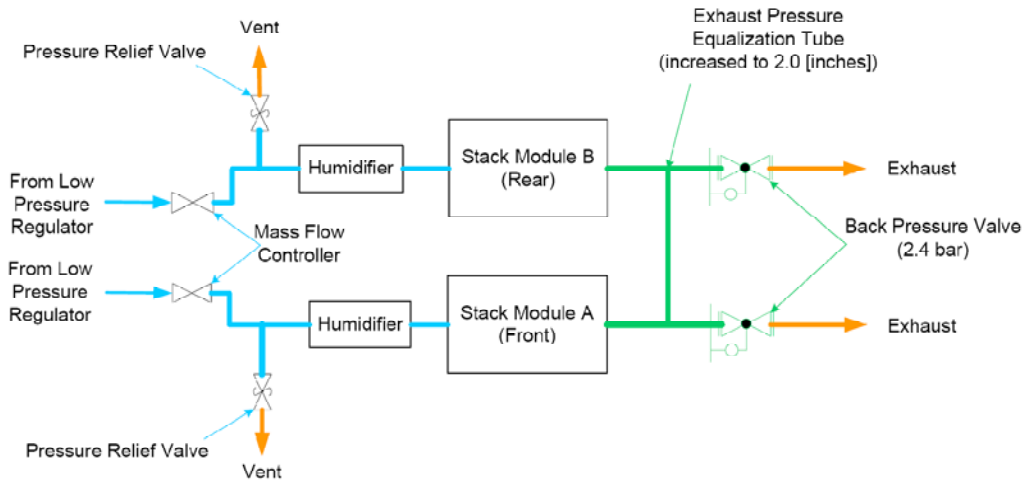

Figure 5.1: Possible Heliox System Redesign with Pressure Relief Valves

The second method for eliminating pressure spikes in the air system would be to eliminate the potential to flow above normal flow rates. It is not clear exactly what causes the MFCs to overshoot. It might be an issue with their software that causes overshoot in the control system. It has been shown in testing that the MFCs are susceptible to moisture and salt. Corrosion and water intrusion will cause undesired flow rates through the MFCs. Another possibility is that the MFCs are susceptible to the vibrations they endure during a run. Whatever the cause for the MFC failure it is not within the abilities of the BB2 team to modify or redesign the MFC to eliminate the possibility of overshoot. Therefore, the only way to eliminate the potential to have uncontrolled jumps in flow rate is to eliminate the mass flow controllers from the system altogether.

The Ford 999 used a system of metering valves under choked flow conditions to regulate the flow of heliox through the stack. The system consisted of an idle flow orifice and a high flow orifice. Solenoid valves where used to actuate the high flow orifices. A similar system could be adapted to replace the mass flow controllers. This is possible because the vehicle only spends a short period of time at low power levels. 85% of the run is spent at full power. However, this would slightly increase the overall heliox consumption because more heliox would be wasted at the beginning of the run. This is a concern because during the 2008 season the vehicle ran out of heliox just after the 5th mile which is adequate for the SCTA course but too short for the FIA course. Although the stoichiometric ratio could be adjusted to use less heliox this should only be considered as a last resort because low stoich ratios can negatively affect fuel cell performance.

One option to address heliox consumption for this type of system would be to increase the number of metering valves. A system with three different sized orifices could generate 8 discrete flow levels. This would allow the vehicle to use heliox more efficiently and makes this system more attractive. However, this system would take much more development time and testing compared to simply installing a pressure relief valve. The system currently performs well with the MFCs and changing the system entirely at this stage in the project may not be worth the additional effort. Figure 5.2 shows a potential system redesign using three metering valves.

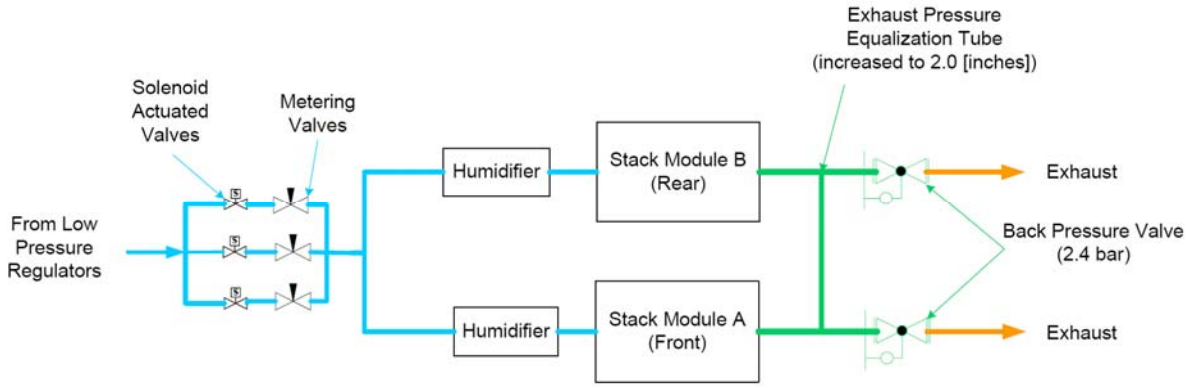

Figure 5.2: Possible Heliox System Redesign with Metering Valves

5.2.2 Removal of Fuel Cell Humidification System

Water management is very important in fuel cell systems. Water is not only a product of the reaction but also essential for the reaction to take place. Water allows the H+ ions to travel through the PEM membrane. As the water content falls, the conductivity falls in a more or less linear fashion [9]. However, if there is too much water in the stack this can cause flooding in the stack as previously discussed in chapter 3. Therefore control of the humidification system is very important in fuel cell systems to ensure that the membranes are hydrated to the appropriate amount.

One potential area for further weight reduction is the humidification system for the BB2. The Ford 999 did not use an onboard humidification system. Rather they conditioned the cells while stationary using a separate humidification system. Then during the run they relied on the product water creation to provide adequate humidification. The water produced in the reaction is directly proportional to the current draw. At 880 [Amps] the fuel cells are producing 78.9 [g/s] of water during the reaction. Removing the system would reduce weight and complexity in the system. Less complexity would mean there are less components to fail. Several failures in the 2008 testing season were linked to the humidification system. Further testing will be necessary to see if this is feasible for the BB2.

5.2.3 New Motor

The next major area of development for the BB2 will be in the motor and inverter. The motor used for the BB2 is the same one that was used in the original Buckeye Bullet. The motor was initially design for a higher voltage and lower current than what is ideal for the BB2. One of the main issues during Speedweek 2008 was that the motor was not able to draw the fuel cell's maximum amount of power. Further dynamometer testing will be necessary to determine whether the current motor and inverter are capable of drawing 600 [kW] at 680 [V] on the DC side.

If the current motor is not capable of this objective, it is possible to rewind the motor and design is such that it produces the same power at a lower voltage and higher current. This would allow the full 600 [kW] to be drawn from the fuel cells and increase power over a larger RPM range.

References

[1] *2007 Rules and Record*. Southen California Timing Association. 2007

[2] Göschel Burkhard. BMW's Drivetrain for Tomorrow. Automotive Engineering International, January 2005.

[3] Serious Wheels. [Online] www.seriouswheels.com.

[4] Ford sets land speed record with fuel cell racecar. Fuel Cells Bulletin. Volume 2007, Issue 10, October 2007.

[5] Hillstrom, Edward. Investigation of Chassis Rigidity and Vehicle Handling of an Electric Land Speed Vehicle. The Ohio State University. 2003.

[6] Sinsheimer, Benjamin. Design and Simulation of a Fuel Cell Land Speed Vehicle Propulsion System. The Ohio State University. 2008.

[7] Ponziani, Kevin. *Control System Design and Optimization for the Fuel Cell Powered Buckeye Bullet 2 Land Speed Vehicle*. The Ohio State University. 2008.

[8] Wright, Benjamin. *Development and Modeling of a Suspension for the Ohio State Buckeye Bullet 2.* The Ohio State University. 2006

[9] J. Larminie, A. Dicks. Fuel Cell Systems Explained. New York: Wiley, 2003.

[10] Future Energies. [Online] www.futureenergies.com

[11] Ballard Power System. [Online] www.ballard.com

[12] Ingimundarson, Ari. Stefanopoulou, Anna. Mckay, Denise. Model-Based Detection of Hydrogen Leaks in a Fuel Cell Stack. IEEE Transaction on Control System Technology, Vol. 16, No. 5, September 2008.

[13] Anderson, John. Modern Compressible Flow. Third Edition. McGraw-Hill. New York. 2003

[14] Valve Sizing. Technical Bulletin. Swagelok Company. December 2007

[15] J.C. Amphlett, R. M. Baumert, R.F. Mann, B.A. Peppley, P.R. Roberge. *Performance Modeling of the Ballard Mark IV Solid Polymer Electrolyte Fuel Cell.* Electrochemical Science and Technology. Vol 142, No. 1, January 2005

[16] Forrai, Alexandru. Funato, Hirohito. Yanagita, Yukihiro. Kato, Yoshitsugu. Fuel-Cell Paramter Estimation and Diagnositics. IEEE Transactions on Energy Converion, Vol. 20. No. 3. September 2005

[17] Fuel Cell Handbook. EG&G Technical Services. 7th Edition. November 2004

[18] *289 Series Spring-Loaded Relief Valves. Fisher Controls International. Bulletin 71.4:289 March 2008*

[19] Sopko, Thomas, *Dynamics and Stability Analysis of a Land Speed Record Electric Vehicle*, A Graduate School Thesis for The Ohio State University, 2001.

[20] Layman, Jennifer L. *Aerodynamic Design & Analysis of a High Speed Electric Car,* A Graduate School Thesis for The Ohio State University, 2002.

Appendix

A.1 Hydrogen Injector Calculation Code

```
%plot(tbps,BPS_MF_A01_A, tbps,BPS_MF_A01_B,tbb,MH_GasPressures_O2High)
clc;
load('LiskValvedP.mat');
I = 500;
P = 215;

F = 96485;
M_highflow = I*.92/(2*F)*2.016*960/1000
M_idlejet = I*.08/(2*F)*2.016*960/1000;
M_total = M_highflow+M_idlejet;
SLPM = (M_total)/0.08988*1000*60;
Lisk_dp =
interp1(LiskValvedP(:,1),LiskValvedP(:,2),SLPM,'linear','extrap')*6894.
75729;
Tescom_dp = 20

C = 1;
Po = (130*6894.75729+1.01325e5);
%Po = (P*6894.75729+1.01325e5-Lisk_dp-Tescom_dp); %N/m^3 absolute
D = 3.048e-3; %m
A_t = pi*D^2/4; %m^2
To = 0+273.15; %K
R = 8314/2.016;%J/kg*K
k = 1.41;
m_dot = C*Po*A_t/sqrt(To)*sqrt(k/R*(2/(k+1))^((k+1)/(k-1)))*1000

M_highflow/m_dot
%purge_SLPM = (m_dot - M_highflow)/0.08988*1000*60
```

A.2 Heliox System Modeling

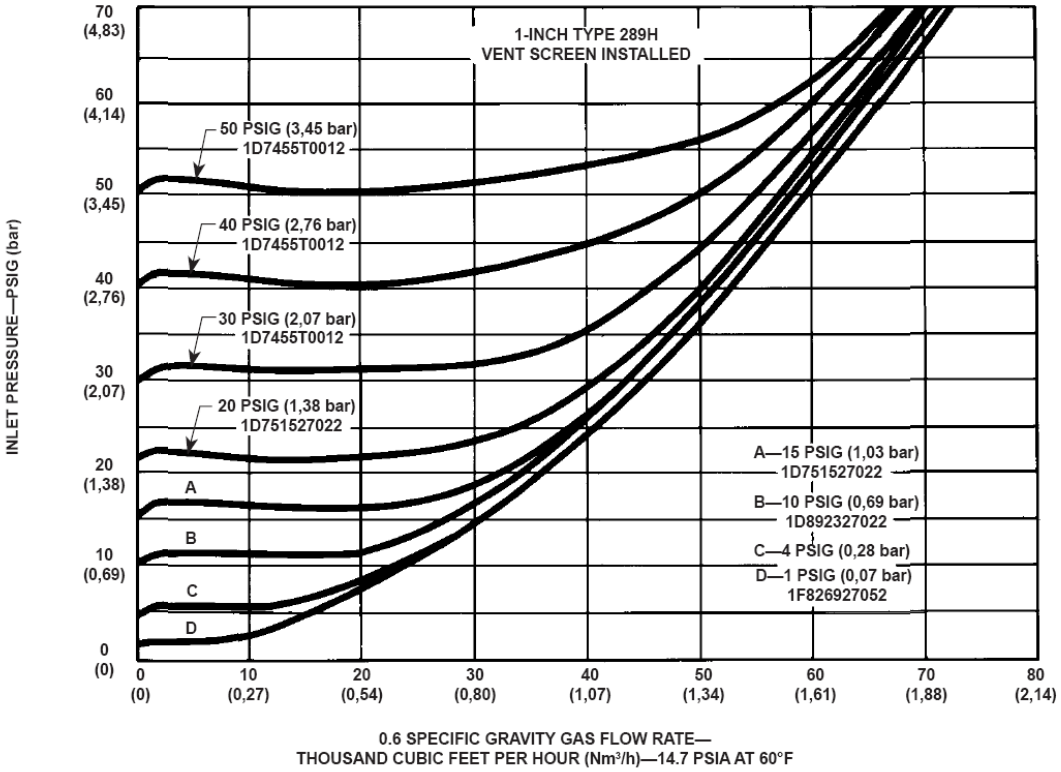

Figure A.1: Backpressure Valve Pressure Level with Varying Flowrate [18]

A.2.1 Mass Flow Controller Flow Rate Calculation

```
clear;clc
T1=20+273.15;
Kv = 6;
Cv = Kv*1.16;
P1 = 9.5; %bar
%P1 = 13.5; %bar
R = 8314/15.2018; %J/(kg*K)
rho = 1.01325e5/(8314/15.2018*293.15);
rho_air = 1.01325e5/(8314/28.97*293.15)
SG = rho/rho_air

N2 = 6950;
Q_slpm = 0.471*N2*Cv*P1*sqrt(1/(SG*T1))
Q_cftph = Q_slpm*0.0353146667*60
m_dot = Q_slpm*.001/60*rho*1000
```

A.2.2 Cross Over Tube Model

```
%clear;clc;close all
P = 3.4e5;

T = 80+273.15;
R = 8314/15.2018; %J/(kg*K)
%D = .5*0.0254;
D = 2*0.0254;
E = .0025e-3;
A = pi*D^2/4;
L = .5588;
cp_O2 = (3.626-1.878e-3*T+7.055e-6*T^2-6.764e-9*T^3+2.156e-
12*T^4)*8314/32;%J/(kg*K)
cp_He = 2.5*8314/4.003;%J/(kg*K)
cp = .4*cp_O2+.6*cp_He;
gamma = cp/(cp-R);
mu_O2 = 2.04e-5;
mu_He = 1.94e-5;
mu = .4*mu_O2+.6*1.94e-5;

M = 0.0001:.0001:1;
F = (1-
M.^2)./(gamma*M.^2)+(gamma+1)./(2*gamma).*log((gamma+1)*M.^2./(2+(gamma
-1)*M.^2));

f = 0:.00001:.1;
Re = 2.51./sqrt(f).*(10.^(-.5./sqrt(f))-E/D/3.7).^(-1);
f = f(find(Re>=0));
Re = Re(find(Re>=0));
%loglog(Re,f)

M1 = 0.01:.01:.999;
a = sqrt(gamma*R*T);
V = a*M1;
rho = P/(R*T);
Re_1 = rho*V*D/mu;
f1 = interp1(Re,f,Re_1);

for(i=1:length(M1))
    F1 = 4*f1(i)*L/D;
    F1_s = (1-
M1(i)^2)/(gamma*M1(i)^2)+(gamma+1)/(2*gamma)*log((gamma+1)*M1(i)^2/(2+(
gamma-1)*M1(i)^2));
    F2_s = F1_s-F1;
    M2 = interp1(F,M,F2_s);
    P_ratio(i) = M1(i)/M2*((2+(gamma-1)*M1(i)^2)/(2+(gamma-
1)*M2^2))^(1/2);
end

M1 = M1((not(isnan(P_ratio))));
P_ratio = P_ratio(not(isnan(P_ratio)));
m_dot = M1*P*A*sqrt(gamma/(T*R));
```

```
figure(1)
plot(P_ratio.^(-1),m_dot*1000,'r','LineWidth',2)
title('\fontsize{10}\bfCross Over Tube Flowrate (P_i_n_l_e_t = 2.4
barg)');
xlabel('\fontsize{10}\bfPressure Ratio (P_i_n_l_e_t/P_e_x_i_t)');
ylabel('\fontsize{10}\bfMass Flowrate [g/s]');
grid on;
```

A.2.3: Heliox Full 2007 System Model

```
%close all
%clear all


P_preset = 35
SG = .5247

load air_command_180

Vim = .01095
V_em = .02394
sim Cathode_System_007_2007layout

%%


figure(1)
plot(t,mdot_mfc_A,'r',t,mdot_mfc_B,'b')
xlabel('time')
ylabel('MFR g/s')
legend('MFC A','MFC B')


figure(2)
plot(t,inlet_P_A,'r',t,inlet_P_B,'b',t,BP,'g')
hold on
xlabel('time')
ylabel('Pressure (psi)')
legend('Module A inlet P','Module B inlet P','Back P')


save('results_2007_180','t','inlet_P_A','inlet_P_B','BP','mdot_mfc_A','
mdot_mfc_B','mdot_exhaust')

%V_em = .003491*2
%sim Cathode_System_007_2007layout
%
% figure(2)
% plot(t,inlet_P,'b--',t,BP,'g--')
% xlabel('time')
% ylabel('Pressure (psi)')
% %plot(tbb_cut,PT_A_07_B_cut*14.5,'r-')
```

```
% %legend('modeled inlet pressure 2007 volumes','modeled back pressure
2007 volumes',...
%    % 'modeled inlet pressure 2008 volumes','modeled back pressure
2008 volumes,')%,'PT A 07 from OPE')
% axis([0 30 20 65])
```

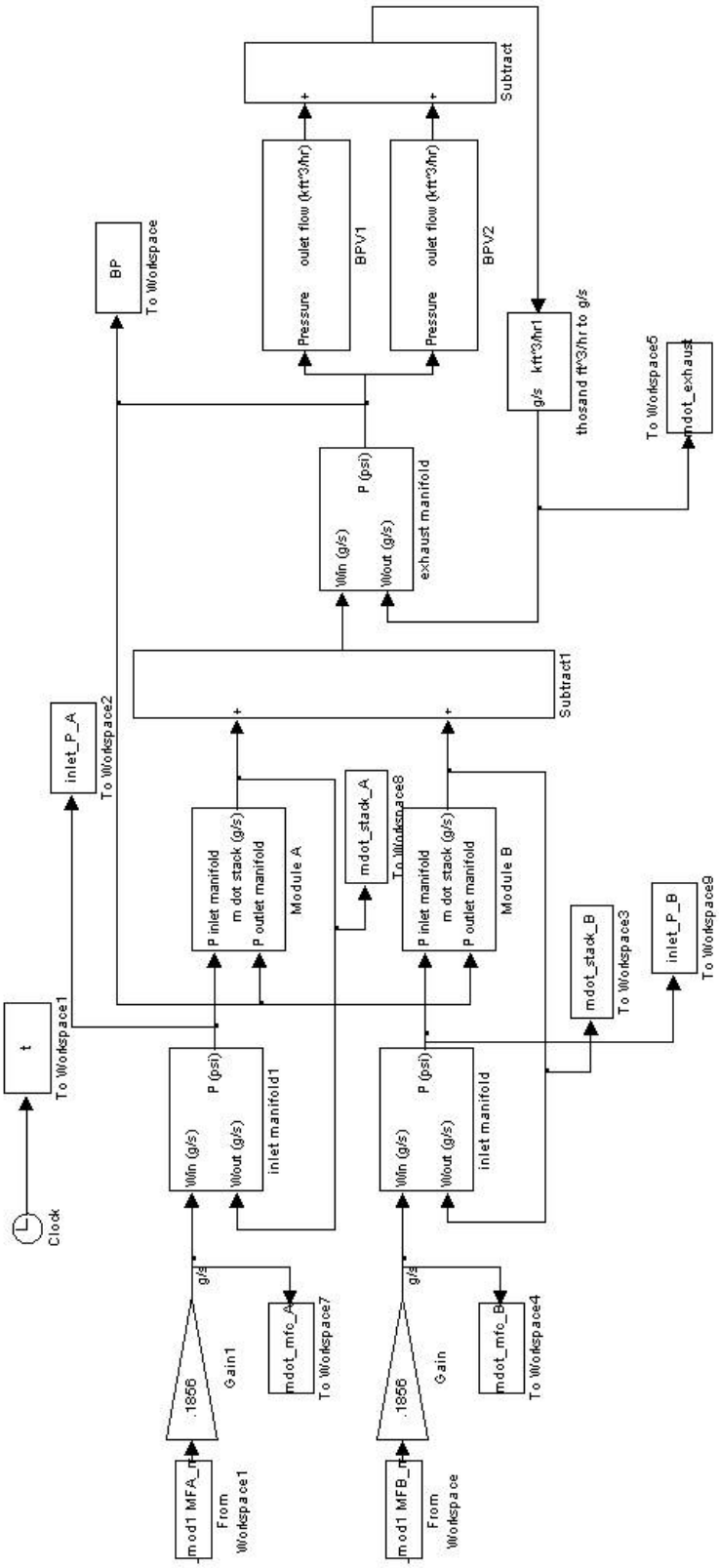
Clock
t
To Workspace1
mod1 MFA_ref
From Workspace1
mod1 MFB_ref
From Workspace
.1856
Gain1
.1856
Gain
g/s
mdot_mfc_A
To Workspace7
mdot_mfc_B
To Workspace4
Win (g/s)
Wout (g/s)
P (psi)
inlet manifold1
inlet manifold
P inlet manifold
m dot stack (g/s)
P outlet manifold
Module A
Module B
inlet_P_A
To Workspace2
mdot_stack_A
To Workspace8
mdot_stack_B
To Workspace3
inlet_P_B
To Workspace9
Subtract1
Win (g/s)
Wout (g/s)
P (psi)
exhaust manifold
BP
To Workspace
Pressure
oulet flow (kft^3/hr)
BPV1
Pressure
oulet flow (kft^3/hr)
BPV2
Subtract
g/s
kft^3/hr1
thosand ft^3/hr to g/s
To Workspace5
mdot_exhaust

Inlet Manifold Submodel

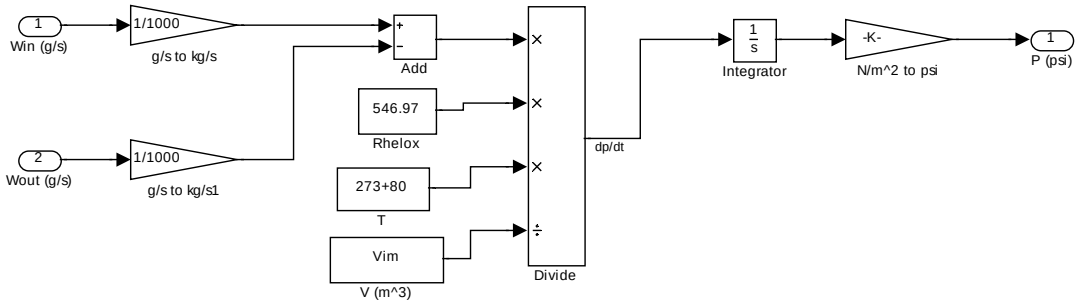

FCM Submodel

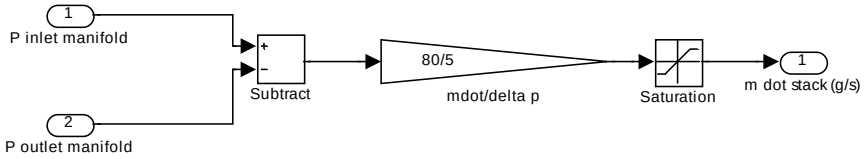

Exhaust Manifold Submodel

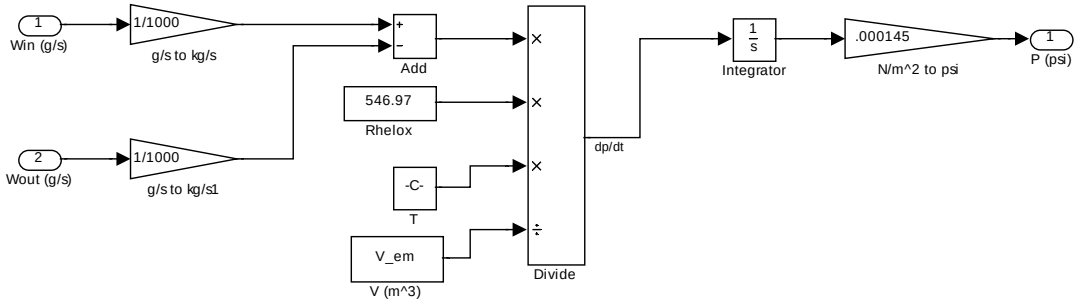

A.2.4: Heliox Full 2008 System Model

```
close all
clear all


P_preset = 35
SG = .5247

load air_command_180
load Crossover_Tube_Flow_data
PR = [wrev(P_ratio_05) P_ratio_05.^-1];
MM = [wrev(M_05) -M_05];


Vim = .01095
V_em = .003491
diam = .5*.0254; %diameter in meters




sim Cathode_System_008_2008layout2

%%


figure(1)
plot(t,mdot_mfc_A,'r',t,mdot_mfc_B,'b')
xlabel('time')
ylabel('MFR g/s')
legend('MFC A','MFC B','exhaust')
```

```
figure(2)
plot(t,inlet_P_A,'r',t,inlet_P_B,'b',t,BP_A,'m',t,BP_B,'k')
hold on
xlabel('time')
ylabel('Pressure (psi)')
legend('Module A inlet P','Module B inlet P','Back P A','Back P B')

figure(3)
plot(t,mdot_exhaust_A,'r',t,mdot_exhaust_B,'b',t,mdot_cross_over,'k')
xlabel('time')
ylabel('MFR g/s')
legend('mdot exhaust A','mdot exhaust B','cross over')

%%
figure(4)
plot(t,mdot_stack_A,'r',t,mdot_exin_A,'k',t,mdot_cross_over,'g',t,mdot_
stack_A+mdot_cross_over,'m--')

legend('stack A','exaust inlet','cross over','stack A+crossover')


%save('results_20082p0','t','inlet_P_A','inlet_P_B','BP_A','BP_B','mdot
_mfc_A','mdot_mfc_B','mdot_exhaust_A','mdot_exhaust_B')



%V_em = .003491*2
%sim Cathode_System_007_2007layout
%
% figure(2)
% plot(t,inlet_P,'b--',t,BP,'g--')
% xlabel('time')
% ylabel('Pressure (psi)')
% %plot(tbb_cut,PT_A_07_B_cut*14.5,'r-')
% %legend('modeled inlet pressure 2007 volumes','modeled back pressure
2007 volumes',...
%    % 'modeled inlet pressure 2008 volumes','modeled back pressure
2008 volumes,')%,'PT A 07 from OPE')
% axis([0 30 20 65])
```

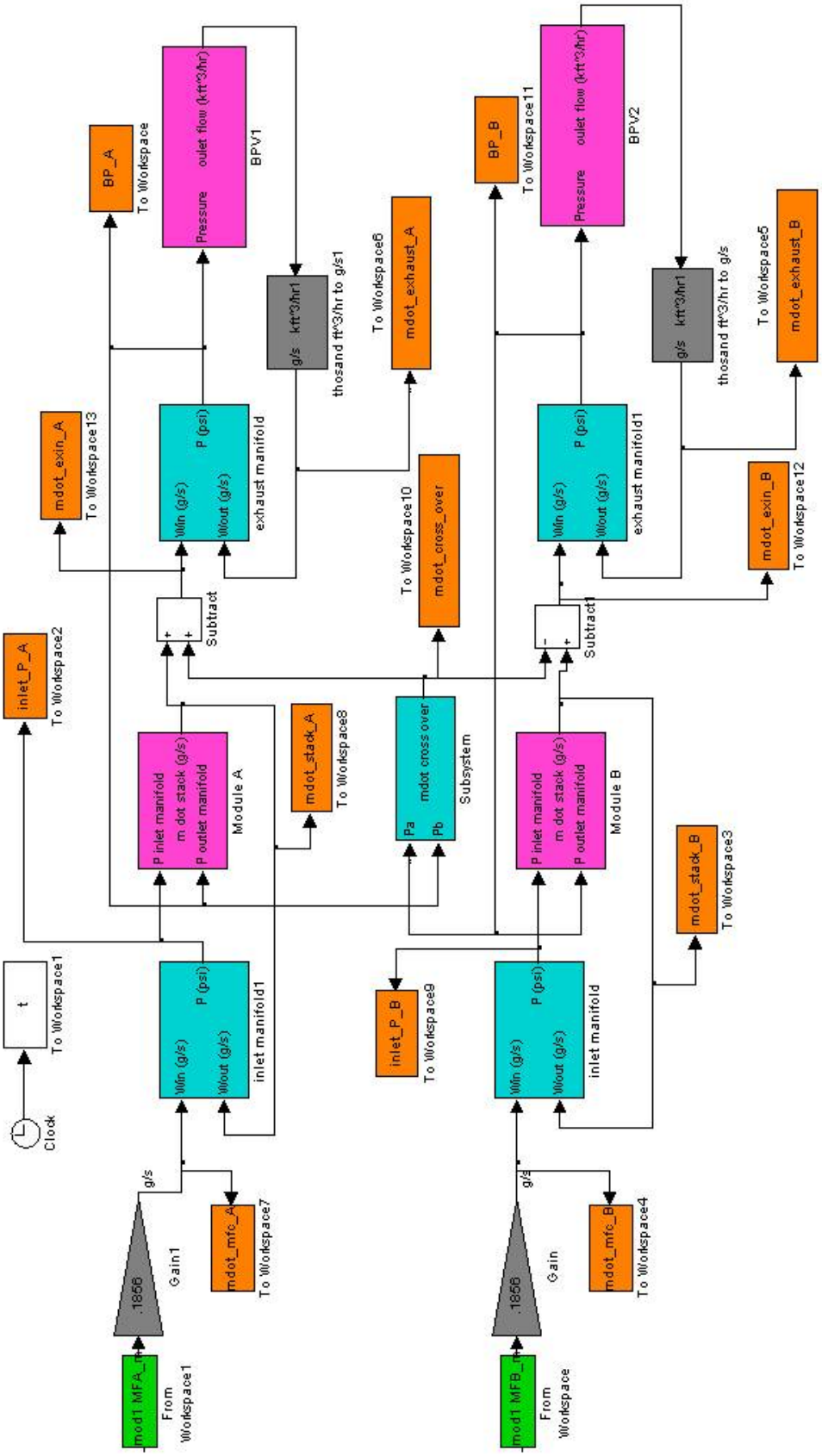
mod1 MFA_ref
From Workspace1
.1856
Gain1
g/s
mdot_mfc_A
To Workspace7
Clock
t
To Workspace1
Win (g/s)
Wout (g/s)
P (psi)
inlet manifold1
inlet_P_A
To Workspace2
P inlet manifold
m dot stack (g/s)
P outlet manifold
Module A
mdot_stack_A
To Workspace8
BP_A
To Workspace
Pressure
oulet flow (kft^3/hr)
BPV1
g/s
kft^3/hr1
thosand ft^3/hr to g/s1
mdot_exhaust_A
To Workspace6
mdot_exin_A
To Workspace13
exhaust manifold
Subtract
mdot_cross_over
To Workspace10
Pa
mdot cross over
Pb
Subsystem
inlet_P_B
To Workspace9
mod1 MFB_ref
From Workspace
.1856
Gain
g/s
mdot_mfc_B
To Workspace4
inlet manifold
Module B
mdot_stack_B
To Workspace3
BP_B
To Workspace11
BPV2
kft^3/hr1
thosand ft^3/hr to g/s
mdot_exhaust_B
To Workspace5
exhaust manifold1
Subtract1
mdot_exin_B
To Workspace12

Inlet Manifold Submodel

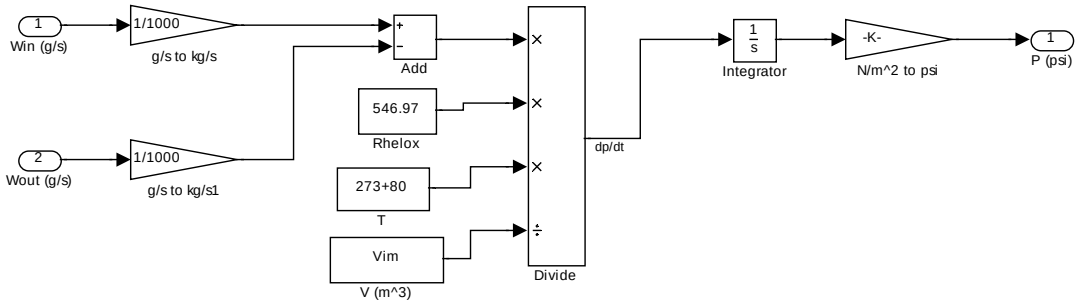

FCM submodel

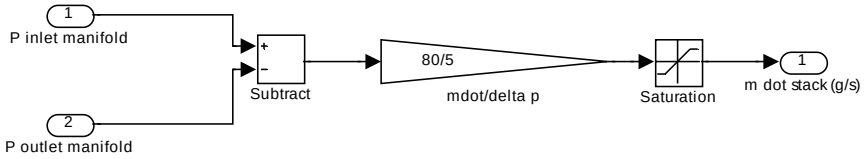

Exhaust Manifold Submodel

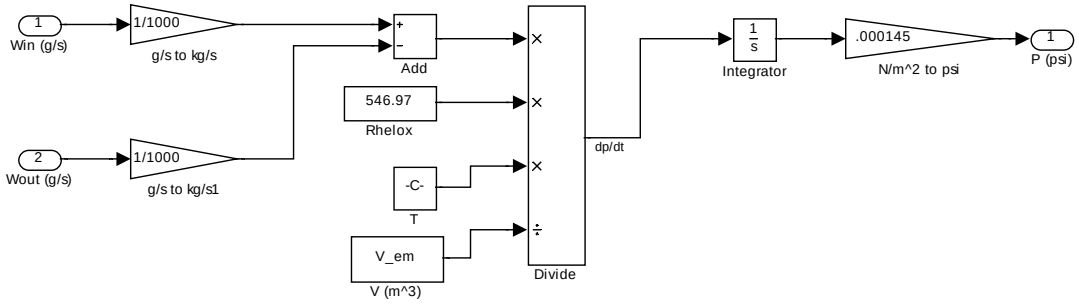

Cross Over Tube submodel

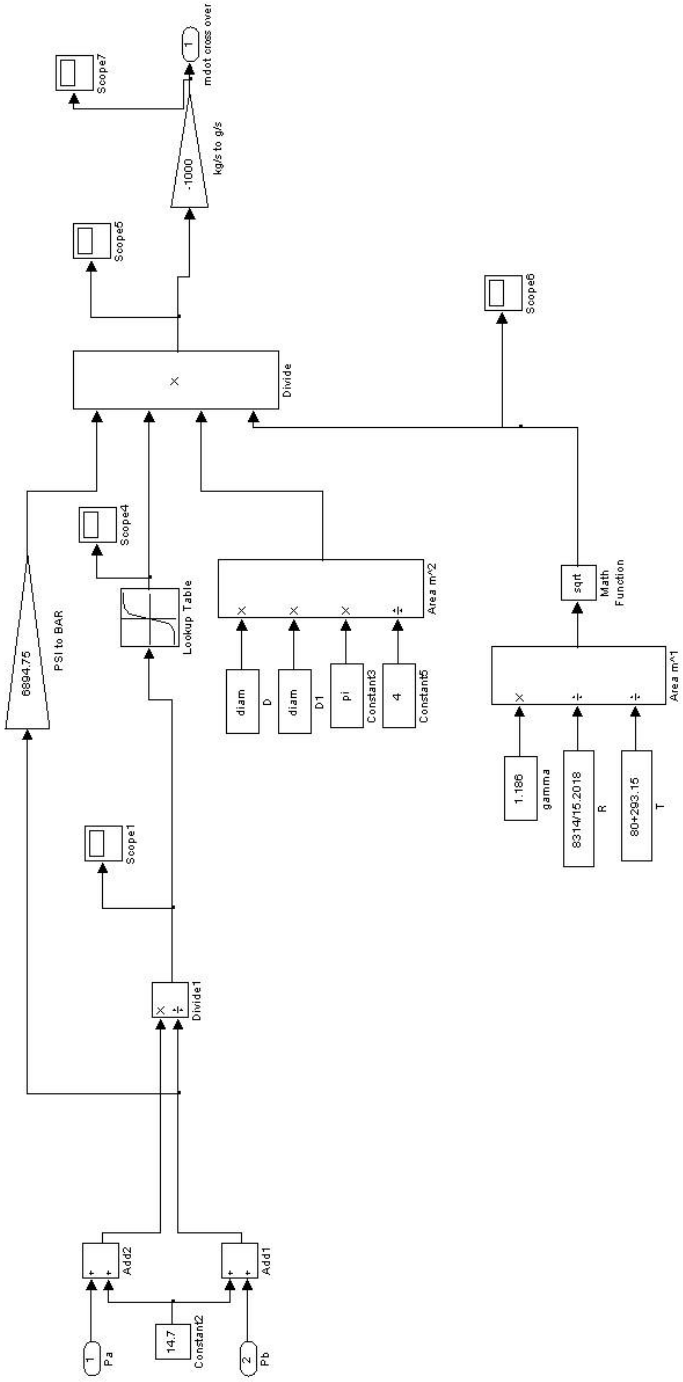

A.3: Fuel Cell Empirical Model Code

```
addpath('data');
clc;clear;%close all;
 data1 = load('June27Run2.txt');
 data2 = load('June26Run1.txt');
 data3 = load('June23Run1.txt');
 data4 = load('June19Run1.txt');
 data5 = load('June18Run1.txt');
 data6 = load('June29Run1a.txt');
 data7 = load('June29Run1b.txt');
 data8 = load('June29Run2a.txt');
 data9 = load('June29Run2b.txt');
 data10 = load('June29Run2c.txt');
data11 = load('August22Run1a.txt');
data12 = load('August22Run1b.txt');
data13 = load('August22Run1c.txt');
data14 = load('August22Run1d.txt');
data15 = load('August22Run2a.txt');
data16 = load('August22Run2b.txt');
data17 = load('August22Run2c.txt');
data18 = load('August22Run2d.txt');
data19 = load('August22Run3a.txt');
data20 = load('August22Run3b.txt');
data21 = load('August22Run3c.txt');
data22 = load('August22Run3d.txt');
data23 = load('August23Run1a.txt');
data24 = load('August23Run1b.txt');
data25 = load('August23Run1c.txt');
data26 = load('August23Run1d.txt');

data = [data1
        data2
        data3
        data6
        data7
        data8
        data9
        data10
        data11
        data12
        data13
        data14
        data15
        data16
        data17
        data18
        data19
        data20
        data21
        data22
        data23
        data24
        data25
        data26];
```

```
%data =
[data1;data2;data3;data6;data7;data8;data9;data10;data11;data12;data13;
data14;data15;data16;data17;data18];
%data = [data1;data2;data3;data6;data7;data8;data9;data10];

load('FC_polar.mat')
%%
% x = find(data(:,2)>400);
% data = data(x,:)
%%
%Raw Data
t = data(:,1);
CT_F01_A = data(:,2);
CT_F01_B = data(:,3);
PT_A07_A = data(:,4);
PT_H03_A = data(:,5);
PT_H03_B = data(:,6);
TT_A09_A = data(:,7);
TT_A09_B = data(:,8);
TT_D02_A = data(:,9);
VE_STA = data(:,10);
VE_STB = data(:,11);
VE_STC = data(:,12);
VE_STD = data(:,13);
%%
%Parameters
mm_helox = 15.201; %g/mol
mole_frac = .4;%.4*15.201/31.9880;
%R_bar = 8.314; %kJ/kmol*K
%R_O2 = R_bar/mm_helox;
%%
%Data Manipulation
V = (VE_STA + VE_STB);
T = TT_D02_A+273.15;
I = CT_F01_A;
P_O2 = mole_frac.*PT_A07_A; %partial pressure of O2

%%
%Nerst Equation
Nernst = 1.229 - 8.5e-4 * (T-298.15) + 4.3085e-5*T .* (log(PT_H03_A) +
.5.*log(P_O2));
E0 = Nernst * 960;

%%
x = find(I>250);
Vact_terms = [ones(length(I),1),T]*960;
Vohm_terms = [I, I.*T, I.*I]*960;
b = E0(x) - V(x);
A = [Vact_terms(x,:) Vohm_terms(x,:)];
c1 = inv(A'*A)*A'*b;
ohmic_c = c1(3:5)

Vohm = Vohm_terms*c1(3:5);
Vact = Vact_terms*c1(1:2);
V_theo = E0 - Vact-Vohm;
```

```
C_O2 = P_O2./(5.08e6.*exp(-498./T));
Vact_terms = [ones(length(I),1), T, T.*log(C_O2), T.*log(I)]*960;
b = E0 - V- Vohm;
A = [Vact_terms];
c2 = inv(A'*A)*A'*b;
Vact = A*c2;
V_theo = E0 - Vact - Vohm;
activation_c = c2
%%
% figure(1)
% plot(t,V,'b+',t,V_theo,'g+')
% title('Experimental Data Fit')
% xlabel('Time [s]');
% ylabel('Voltage [V]');
% legend('Experimental','Theorectical','Location','SouthEast');
% grid on;
%%
figure(2)
title('Experimental Data Fit')
plot(T-273.15,V, 'b+',T-273.15,V_theo,'g+');
xlabel('Temperature [C]');
ylabel('Voltage [V]');
legend('Experimental','Theorectical','Location','SouthEast');
grid on;
%%
% figure(3)
% plot(I,V,'b+',I,V_theo,'g+',FC_I/2,FC_V/.97,'rO');
%
% grid on;

%%
% figure(4);plot(...
%     I,Vact,'bx',...
%     I,Vohm,'b^');
% grid on;
%%
figure(5)
x1 = find(T>273.15 & T<=20+273.15);
x2 = find(T>20+273.15 & T<=40+273.15);
x3 = find(T>40+273.15 & T<=60+273.15);
x4 = find(T>60+273.15 & T<=80+273.15);
x5 = find(T>80+273.15);
hold on;
% plot(I(x1),V(x1),'b+',I(x1),V_theo(x1),'b^');
% plot(I(x2),V(x2),'c+',I(x2),V_theo(x2),'c^');
% plot(I(x3),V(x3),'g+',I(x3),V_theo(x3),'g^');
% plot(I(x4),V(x4),'r+',I(x4),V_theo(x4),'r^');
% plot(I(x5),V(x5),'m+',I(x5),V_theo(x5),'m^');
plot(I(x1),V(x1),'b+');
plot(I(x2),V(x2),'c+');
plot(I(x3),V(x3),'g+');
plot(I(x4),V(x4),'r+');
plot(I(x5),V(x5),'m+');
title('\fontsize{10}\bfExperimental Data Fit: Polarization Curve');
xlabel('\fontsize{10}\bfCurrent [amps]');
ylabel('\fontsize{10}\bfVoltage [Volts]');
legend('20^oC','40^oC','60^oC','80^oC');
```

```
grid on;
hold off;
%%
figure(6)
x1 = find(PT_A07_A<=2.0);
x2 = find(PT_A07_A>2.0 & PT_A07_A<=2.2);
x3 = find(PT_A07_A>2.2 & PT_A07_A<=2.4);
x4 = find(PT_A07_A>2.4 & PT_A07_A<=2.6);
x5 = find(PT_A07_A>2.6);
hold on;
% plot(I(x1),V(x1),'b+',I(x1),V_theo(x1),'b^');
% plot(I(x2),V(x2),'c+',I(x2),V_theo(x2),'c^');
% plot(I(x3),V(x3),'g+',I(x3),V_theo(x3),'g^');
% plot(I(x4),V(x4),'r+',I(x4),V_theo(x4),'r^');
% plot(I(x5),V(x5),'m+',I(x5),V_theo(x5),'m^');
plot(I(x1),V(x1),'b+');
plot(I(x2),V(x2),'c+');
plot(I(x3),V(x3),'g+');
plot(I(x4),V(x4),'r+');
plot(I(x5),V(x5),'m+');
title('\fontsize{10}\bfExperimental Data Fit: Polarization Curve');
xlabel('\fontsize{10}\bfCurrent [amps]');
ylabel('\fontsize{10}\bfVoltage [Volts]');
legend('P<2.0','2.2>P>2.0','2.4>P>2.2','2.6>P>2.4','2.6>P');
grid on;
hold off;
%%
%Varying Temperature Constant Pressure
clear I T Vohm Vact V_theo C_O2 P_O2 E0
I = (0:10:450)';
T = [20+273.15;40+273.15;60+273.15;80+273.15];
P_O2 = mole_frac.*2.5; %Partial Pressure of O2
figure(7)
clf;
hold on;
for(i=1:length(T))
    C_O2 = P_O2./(5.08e6.*exp(-498./T(i)));
    Vact_terms = [ones(length(I),1), T(i).*ones(length(I),1),
T(i).*log(C_O2).*ones(length(I),1), T(i).*log(I)]*960;
    Vohm_terms = [I, I.*T(i), I.*I]*960;
    Vohm = Vohm_terms*ohmic_c;
    Vact = Vact_terms*activation_c;

    switch i
        case 1
            plot(I*2,Vact,'b+',I*2,Vohm,'b^')
        case 2
            plot(I*2,Vact,'g+',I*2,Vohm,'g^')
        case 3
            plot(I*2,Vact,'r+',I*2,Vohm,'r^')
        case 4
            plot(I*2,Vact,'y+',I*2,Vohm,'y^')
    end
end
legend('Vact','Vohm','Location','SouthWest');
```

```
legend('V_a_c_t at 20^oC','V_o_h_m at 20^oC','V_a_c_t at
40^oC','V_o_h_m at 40^oC','V_a_c_t at 60^oC','V_o_h_m at
60^oC','V_a_c_t at 80^oC','V_o_h_m at 80^oC','Location','EastOutside');
xlabel('\fontsize{10}\bfCurrent [Amps]');
ylabel('\fontsize{10}\bfVoltage Loss [V]');
grid on;
hold off;
%%
figure(8)
clf;
hold on;
for(i=1:length(T))
    Nernst = 1.229 - 8.5e-4 * (T(i)-298.15) + 4.3085e-5*T(i) .* (log(3)
+ .5.*log(P_O2));
    E0 = Nernst * 960;
    C_O2 = P_O2./(5.08e6.*exp(-498./T(i)));
    Vact_terms = [ones(length(I),1), T(i).*ones(length(I),1),
T(i).*log(C_O2).*ones(length(I),1), T(i).*log(I)]*960;
    Vohm_terms = [I, I.*T(i), I.*I]*960;
    Vohm = Vohm_terms*ohmic_c;
    Vact = Vact_terms*activation_c;
    switch i
        case 1
            plot(I*2,E0-Vact-Vohm,'b+')
        case 2
            plot(I*2,E0-Vact-Vohm,'g+')
        case 3
            plot(I*2,E0-Vact-Vohm,'r+')
        case 4
            plot(I*2,E0-Vact-Vohm,'m+')
    end
end
%plot(FC_I/2,FC_V/.97,'rO');
title('\fontsize{10}\bfBB2 Polarization Curve');
xlabel('\fontsize{10}\bfCurrent [amps]');
ylabel('\fontsize{10}\bfVoltage [Volts]');
grid on;
legend('20^oC','40^oC','60^oC','80^oC');
hold off;
%%
figure(9)
clf;
hold on;
for(i=1:length(T))
    Nernst = 1.229 - 8.5e-4 * (T(i)-298.15) + 4.3085e-5*T(i) .* (log(3)
+ .5.*log(P_O2));
    E0 = Nernst * 960;
    C_O2 = P_O2./(5.08e6.*exp(-498./T(i)));
    Vact_terms = [ones(length(I),1), T(i).*ones(length(I),1),
T(i).*log(C_O2).*ones(length(I),1), T(i).*log(I)]*960;
    Vohm_terms = [I, I.*T(i), I.*I]*960;
    Vohm = Vohm_terms*ohmic_c;
    Vact = Vact_terms*activation_c;
    yunit = 1000; ylabel('\fontsize{10}\bfPower [kW]')
%     yunit = 746; ylabel('\fontsize{10}\bfPower [HP]')
    switch i
        case 1
```

```
            plot(I*2,(E0-Vact-Vohm).*I*2/yunit,'b+')
        case 2
            plot(I*2,(E0-Vact-Vohm).*I*2/yunit,'g+')
        case 3
            plot(I*2,(E0-Vact-Vohm).*I*2/yunit,'r+')
        case 4
            plot(I*2,(E0-Vact-Vohm).*I*2/yunit,'m+')
    end
end
title('\fontsize{10}\bfBB2 Power Curve');
xlabel('\fontsize{10}\bfCurrent [amps]');
grid on;
legend('20^oC','40^oC','60^oC','80^oC','Location','SE');
hold off;

%%
figure(10)
clf;
hold on;
clear I T
T = (60 + 273.15);
I = (0:500/7:500)';
Nernst = 1.229 - 8.5e-4 * (T-298.15) + 4.3085e-5*T .* (log(3) +
.5.*log(P_O2));
E0 = Nernst * 960;
C_O2 = P_O2./(5.08e6.*exp(-498/T));
Vact_terms = [ones(length(I),1), T*ones(length(I),1),
T*log(C_O2).*ones(length(I),1), T*log(I)]*960;
Vohm_terms = [I, I*T, I.*I]*960;
Vohm = Vohm_terms*ohmic_c;
Vact = Vact_terms*activation_c;
P_curve_I = 2.*I;
P_curve_V = E0-Vact-Vohm;
P_curve_V(1) = 960;
plot(P_curve_I,P_curve_V,'b+')
title('Polarization Curve');
xlabel('Current [amps]');
ylabel('Voltage [Volts]');
grid on;
hold off;

%%
%Varying Temperature Constant Pressure
figure(11)
I = (0:10:450)';
T = [80+273.15];
ohmic_c2007 = [6.417e-4 -1.813e-7 1.653e-8]';
activation_c2007 = [.8193 -3.186e-3 -7.608e-5 1.264e-4]';
clf;
hold on;
Nernst = 1.229 - 8.5e-4 * (T-298.15) + 4.3085e-5*T.*(log(3)+
.5.*log(P_O2));
    E0 = Nernst * 960;
    C_O2 = P_O2./(5.08e6.*exp(-498./T));
    Vact_terms = [ones(length(I),1), T.*ones(length(I),1),
T.*log(C_O2).*ones(length(I),1), T.*log(I)]*960;
```

```
    Vohm_terms = [I, I.*T, I.*I]*960;
    Vohm = Vohm_terms*ohmic_c;
    Vact = Vact_terms*activation_c;
    V_2008 = E0-Vact-Vohm;
    plot(I*2,V_2008,'b','LineWidth',2)
    Vohm = Vohm_terms*ohmic_c2007;
    Vact = Vact_terms*activation_c2007;
    V_2007 = E0-Vact-Vohm;
    plot(I*2,V_2007,'g','LineWidth',2)


%plot(FC_I/2,FC_V/.97,'rO');
title('\fontsize{10}\bfBB2 Polarization Curve');
xlabel('\fontsize{10}\bfCurrent [amps]');
ylabel('\fontsize{10}\bfVoltage [Volts]');
grid on;
legend('2008','2007');
hold off;

figure(12)
plot(I*2,I.*2.*V_2008/1000,'b',I*2,I.*2.*V_2007/1000,'g','LineWidth',2)
title('\fontsize{10}\bfBB2 Polarization Curve');
xlabel('\fontsize{10}\bfCurrent [amps]');
ylabel('\fontsize{10}\bfPower [kW]');
grid on;
legend('2008','2007','Location','SE');
hold off;
```